Supplementary File

Title:

Genetic risk and a primary role for cell-mediated immune mechanisms in multiple sclerosis

Authors:

The International Multiple Sclerosis Genetics Consortium (IMSGC) and the Wellcome Trust Case Control Consortium 2 (WTCCC2)

Table of Contents

Details of Association Regions 4

Background 8

Samples 10

- Case collections 10
- Clinical Information 15
- Control collections 16

Genotyping and Quality Control 18

- Genotyping 18
- Sample QC 18
  - Probe intensity outliers 19
  - Identifying outliers by clustering 21
  - Estimating relatedness via HMMs 22
  - PCA clustering 23
  - Estimating ancestry proportions 24
  - Summary of sample exclusions 26
- SNP QC 30
  - Automated cluster checking 30
  - Beta-binomial model 32

Results 36

- Controlling for population structure 36
  - Principal Components As Covariates 37
  - Clustering into Subgroups Based on Ancestry 38
  - Linear Mixed Model 39
  - Validation of the Linear Mixed Model Approach 40
  - Summary of approaches for protecting against population structure 42
- Meta Analysis 43
- Evidence at Previously Suggested Loci 45
- Analysis of signals of association 46
  - Independent signals 46
  - Defining association regions 47
  - Regional association plots 47
- Replication analysis 48
- Further Analysis 50
  - 1000 Genomes analysis 50
  - Gene Ontology analysis 50
  - Sibling recurrence risk and variance explained on the liability scale 51
  - Homogeneity of effects 52
  - Interactions 54
  - Haplotype analysis 54
  - Gender effects 55
  - X chromosome analysis 56
- Secondary phenotypes 58
  - Age at onset (AAO) 58
  - Clinical course 61
  - Rate of progression (severity) 63
  - DRB1*15:01 stratified analysis 65

Month of Birth 67
Imputation-based analysis of HLA 71
Overview 71
Detailed methods for classical HLA allele imputation 71
Validation of classical allele imputation for reported alleles 73
Details of classical HLA allele analysis 74
Genecluster analysis of secondary signals at HLA-DRB1 and HLA-A 76
Estimated coefficients for alleles in each cohort 79
References 84
Individual contributions 88
Membership of Wellcome Trust Case Control Consortium 2 91
Membership of the International Multiple Sclerosis Genetics Consortium 92
Affiliations 93
Acknowledgements 98

Details of Association Regions

Table S1. Association evidence at loci previously identified as influencing multiple sclerosis.

Chr	rsID	Position[#]	Putative gene of interest	Risk Allele	P value[+]	OR (95% CI)	Best Tag (r^2 > 0.5) previously reported SNP[$]	P value
1	rs4648356	2699024	*MMEL1*	C	3.10E-14	1.16 (1.12-1.21)	rs3748816	1.10E-13
1	rs11810217	92920965	*EVI5*	A	6.50E-12	1.15 (1.11-1.20)	rs10874727	7.90E-10
1	rs1335532	116902480	*CD58*	A	2.00E-09	1.18 (1.12-1.24)	rs1335532	1.00E-09
1	rs1323292	190807644	*RGS1*	A	8.80E-07	1.12 (1.07-1.18)	rs1323292	4.40E-07
1	rs7522462	199148218	*KIF21B*	G	9.20E-07	1.11 (1.06-1.15)	rs7522462	4.60E-07
3	rs2028597	107041527	*CBLB*	G	2.10E-04	1.13 (1.06-1.21)	rs1910499	0.00072
3	rs2293370	120702624	*TMEM39A*	G	1.10E-09	1.16 (1.11-1.22)	rs1132200	1.10E-07
3	rs2243123	161192345	*IL12A*	G	3.70E-06	1.09 (1.05-1.14)	rs2366408	2.50E-05
5	rs6897932	35910332	*IL7R*	G	2.60E-06	1.11 (1.06-1.16)	rs6897932	1.30E-06
5	rs4613763	40428485	*PTGER4*	G	6.90E-14	1.21 (1.15-1.28)	rs1373692	4.30E-10
6	rs13192841	138008907	*OLIG3*	A	2.30E-06	1.10 (1.06-1.15)	rs6938486	0.0036
8	rs1520333	79563593	*IL7*	G	6.10E-07	1.11 (1.06-1.15)		
10	rs3118470	6141719	*IL2RA*	G	2.00E-09	1.12 (1.08-1.17)		
10	rs1250550	80730323	*ZMIZ1*	A	1.40E-06	1.10 (1.06-1.14)	rs1250552	6.30E-05
11	rs650258	60588858	*CD6*	G	1.70E-09	1.12 (1.08-1.16)	rs929230	2.50E-07
12	rs1800693	6310270	*TNFRSF1A*	G	1.80E-10	1.12 (1.08-1.16)	rs1800693	9.20E-11
12	rs12368653	56419523	*CYP27B1*	A	2.00E-07	1.11 (1.06-1.15)	rs703842	2.40E-06
12	rs949143	122161116	*MPHOSPH9*	G	1.50E-04	1.08 (1.04-1.12)	rs1106240	0.00058
16	rs7200786	11085302	*CLEC16A*	A	6.30E-14	1.15 (1.11-1.20)	rs725613	4.30E-13
16	rs13333054	84568534	*IRF8*	A	7.00E-08	1.12 (1.08-1.17)		
17	rs9891119	37761506	*STAT3*	C	4.60E-07	1.10 (1.06-1.14)	rs744166	3.50E-06
19	rs8112449	10381064	*TYK2*	G	1.50E-06	1.10 (1.06-1.14)		
20	rs2425752	44135527	*CD40*	A	1.70E-06	1.10 (1.06-1.14)	rs2425752	8.50E-07

The last two columns provide the rsid and one-sided p-value, respectively, for the SNP in our dataset with the highest correlation coefficient with the previously reported SNP. No SNP is reported in these columns if the square of the maximum correlation coefficient is below 0.5 (see Supplementary Data Table C for details). Note the *TMEM39A* and *MPHOSPH9* genes are not mentioned in figure 2 of the main text as there are more logical candidates nearby (*C3orf1* and *CD80* for *TMEM39A* and *ARL6IP4* for *MPHOSPH9*). Similarly *OLIG3* is not included in figure 2 as it is not technically within the interval associated with rs13192841 although it is the closest gene.

[#] Positions are in NCBI human genome build 36 coordinates

[+] Two-sided p-value

[$] Correlation between this SNP and previously reported SNP calculated using HapMap Phase 2 CEPH haplotypes (http://www.hapmap.org/)

Table S2. Novel independent regions with replicated evidence for association and combined p-value < 5.0E-08 (upper tier) and combined p-value < 5.0E-07 (lower tier).

					Discovery		Replication		Combined
Chr	rsID	Position[#]	Gene	Risk Allele	P value	OR (95% CI)	P value[$]	OR (95% CI)	P value
Associated regions									
1	rs11581062	101180107	*VCAM1*	G	3.70E-10	1.13 (1.09-1.18)	0.042	1.07 (0.99-1.15)	2.50E-10
2	rs12466022	43212565	No gene	C	1.10E-06	1.1 (1.06-1.14)	3.00E-05	1.16 (1.08-1.24)	6.20E-10
2	rs7595037	68500599	*PLEK*	A	6.50E-07	1.1 (1.06-1.14)	3.40E-06	1.15 (1.08-1.22)	5.10E-11
2	rs17174870	112381672	*MERTK*	G	7.80E-06	1.1 (1.06-1.15)	0.00014	1.15 (1.06-1.23)	1.30E-08
2	rs10201872	230814968	*SP140*	A	9.70E-08	1.13 (1.08-1.19)	0.00022	1.15 (1.06-1.24)	1.80E-10
3	rs11129295[a]	27763784	*EOMES*	A	2.30E-08	1.11 (1.07-1.16)	0.0065	1.09 (1.02-1.16)	1.20E-09
3	rs669607	28046448	No gene	C	2.90E-11	1.13 (1.09-1.17)	5.60E-06	1.15 (1.08-1.23)	1.90E-15
3	rs9282641	123279458	*CD86*	G	1.50E-09	1.21 (1.14-1.29)	8.70E-04	1.2 (1.07-1.34)	1.00E-11
5	rs2546890	158692478	*IL12B*	A	2.70E-07	1.1 (1.06-1.14)	2.00E-06	1.15 (1.09-1.22)	1.20E-11
6	rs12212193	91053490	*BACH2*	G	9.90E-07	1.09 (1.05-1.13)	5.70E-03	1.08 (1.02-1.15)	3.80E-08
6	rs802734	128320491	*THEMIS*	A	1.60E-06	1.1 (1.06-1.14)	3.40E-04	1.13 (1.05-1.21)	5.50E-09
6	rs11154801	135781048	*MYB*	A	1.50E-12	1.15 (1.1-1.19)	3.50E-03	1.09 (1.02-1.16)	1.00E-13
6	rs17066096	137494601	*IL22RA2*	G	3.40E-10	1.14 (1.09-1.18)	2.10E-04	1.14 (1.06-1.22)	6.00E-13
6	rs1738074	159385965	*TAGAP*	G	5.30E-11	1.13 (1.09-1.17)	1.30E-05	1.14 (1.07-1.22)	6.80E-15
7	rs354033	148920397	*ZNF767*	G	6.10E-06	1.1 (1.06-1.15)	6.70E-05	1.14 (1.07-1.22)	4.70E-09
8	rs4410871	128884211	*MYC*	G	1.70E-07	1.11 (1.07-1.16)	6.40E-03	1.09 (1.02-1.17)	7.70E-09
8	rs2019960[b]	129261453	*PVT1*	G	1.40E-05	1.1 (1.05-1.15)	1.90E-05	1.16 (1.08-1.24)	5.20E-09
10	rs7923837	94471897	*HHEX*	G	3.00E-07	1.1 (1.06-1.14)	2.30E-03	1.09 (1.03-1.16)	4.90E-09
12	rs10466829	9767358	*CLECL1*	A	1.10E-05	1.09 (1.05-1.13)	1.20E-04	1.12 (1.05-1.19)	1.40E-08
14	rs4902647	68323944	*ZFP36L1*	G	3.80E-08	1.11 (1.07-1.15)	2.40E-05	1.13 (1.07-1.2)	9.30E-12
14	rs2300603	75075310	*BATF*	A	1.90E-07	1.11 (1.07-1.16)	1.50E-02	1.08 (1.01-1.16)	2.00E-08
14	rs2119704	87557442	*GALC*	C	3.50E-10	1.26 (1.17-1.36)	2.50E-02	1.12 (1-1.26)	2.20E-10
18	rs7238078	54535172	*MALT1*	A	2.20E-06	1.11 (1.06-1.16)	1.20E-04	1.14 (1.06-1.23)	2.50E-09
19	rs1077667	6619972	*TNFSF14*	G	2.10E-12	1.16 (1.11-1.21)	6.40E-03	1.14 (1.03-1.27)	9.40E-14
19	rs874628	18165700	*MPV17L2*	A	4.30E-08	1.12 (1.08-1.17)	2.80E-02	1.07 (1-1.14)	1.30E-08
19	rs2303759	54560863	*DKKL1*	C	3.80E-07	1.11 (1.07-1.15)	2.00E-03	1.11 (1.03-1.19)	5.20E-09
20	rs2248359	52224925	*CYP24A1*	G	5.10E-09	1.12 (1.08-1.16)	6.30E-04	1.11 (1.04-1.19)	2.50E-11
22	rs2283792	20461125	*MAPK1*	C	4.00E-06	1.09 (1.05-1.13)	1.30E-04	1.12 (1.05-1.18)	4.70E-09
22	rs140522	49318132	*SCO2*	A	3.90E-06	1.09 (1.05-1.14)	4.90E-04	1.12 (1.05-1.2)	1.70E-08
Regions with strong evidence for association									
4	rs228614	103797685	*NFKB1*	G	9.10E-06	1.09 (1.05-1.13)	2.40E-03	1.09 (1.03-1.16)	1.40E-07

11	rs630923	118259563	*CXCR5*	C	6.90E-06	1.11 (1.06-1.17)	6.40E-03	1.13 (1.03-1.24)	2.80E-07
16	rs2744148	1013553	*SOX8*	G	2.80E-06	1.12 (1.07-1.17)	4.70E-03	1.12 (1.03-1.22)	8.40E-08
17	rs180515	55379057	*RPS6KB1*	G	1.40E-07	1.11 (1.07-1.15)	5.00E-02	1.05 (0.99-1.12)	8.80E-08
20	rs6062314	61880157	*TNFRSF6B*	A	8.30E-07	1.17 (1.1-1.25)	2.50E-02	1.14 (1-1.29)	1.30E-07

[a] The p-value and OR values provided are after conditioning on SNPs rs669607.
[b] The p-value and OR values provided are after conditioning on SNPs rs4410871.
[#] Positions are in NCBI human genome build 36 coordinates
[$] One sided p-value.
The explicit criteria for inclusion on the table are indicated below
SNPs in the upper tier have $p_{GWAS} < 1x10^{-4.5}$, one-sided $p_{Replication} < 0.05$, and $p_{Combined} < 5x10^{-8}$
SNPs in the lower tier have $p_{GWAS} < 1x10^{-4.5}$, one sided $p_{Replication} < 0.05$, and $p_{Combined} < 5x10^{-7}$

Table S3. Secondary signals of association at loci previously identified as influencing multiple sclerosis (top tier) and novel regions with $p_{GWAS} < 1x10^{-4}$, one sided $p_{Replication} < 0.05$, and $p_{Combined} < 5x10^{-6}$ (lower tier).

Chr	rsID	Position[#]	SNP(s) conditioned on	Gene	Risk Allele	Discovery P value	Discovery OR (95% CI)	Replication P value[$]	Replication OR (95% CI)	Combined P value
Previously identified secondary signal of association										
10	rs7090512[a]	6150835	rs3118470	*IL2RA*	G	2.60E-14	1.19 (1.13-1.24)	1.40E-07	1.21 (1.13-1.31)	4.60E-20
Novel secondary signals of association										
1	rs12048904	101104124	rs11581062	*VCAM1*	A	3.70E-07	1.1 (1.06-1.14)	0.017	1.08 (1.01-1.15)	4.00E-08
3	rs4285028	123143354	rs9282641	*CD86*	A	3.40E-07	1.11 (1.07-1.16)	7.40E-03	1.09 (1.02-1.16)	1.80E-08
3	rs4308217	123275877	rs4285028, rs9282641	*CD86*	C	2.20E-06	1.1 (1.06-1.14)	3.80E-03	1.09 (1.02-1.17)	5.70E-08

[a] SNP rs7090512 replicates SNP rs11594656 previously identified in Maier et al[1].

Background

To date six moderately powered[2-7] and three smaller[8-10] multiple sclerosis GWAS have been reported (as listed in Table S4); seven of these were completed by members of our consortium. These GWAS, and subsequent follow up of interesting markers in additional samples, have identified 16 multiple sclerosis susceptibility alleles with association p-value $<5x10^{-8}$, and a further 10 alleles with p-values just slightly above this threshold.

Table S4. Multiple sclerosis GWAS reported to date

GWAS	Cases	Controls	SNPs
IMSGC	931	parents	334,923
WTCCC1	975	1,466	12,374
GeneMSA	978	883	551,642
BWH	860	1,720	709,690
ANZgene	1,618	3,413	302,098
Sardinian	882	872	555,335
Dutch Isolate	45	195	250,000
Finnish Isolate	68	136	297,343
German	592	825	300,000

GWAS = Genome-Wide Association Study, IMSGC = International Multiple Sclerosis Genetics Consortium,[2] WTCCC1 = Wellcome Trust Case Control Consortium phase 1,[3] GeneMSA = Genetic Multiple Sclerosis Asociations,[4] BWH = Brigham and Women's Hospital Partners Study,[5] ANZgene = Australia and New Zealand Multiple Sclerosis Genetics Consortium,[6] German,[10] Sardinian,[7] Dutch[8] and Finnish.[9]

The results for the 26 non-MHC risk loci that have been suggested through follow up of the six reasonably well powered GWAS are summarised in Table S5.

Table S5. Previously identified non-MHC multiple sclerosis susceptibility alleles.

SNP Allele	Freq / %	OR	Locus λs	Gene
rs6897932_C	72	1.18	1.0051	*IL7Rα*
rs2104286_T	75	1.19	1.0052	*IL2Rα*
rs12708716_A	69	1.18	1.0055	*CLEC16A*
rs2300747_A	88	1.30	1.0060	*CD58*
rs12122721_G	72	1.22	1.0073	*KIF21B*
rs1132200_C	84	1.24	1.0054	*TMEM39A*
rs10735781_G	38	1.11	1.0026	*EVI5*
rs2587156_G	93	1.59	1.0095	*IL7*
rs34536443_G	97	1.32	1.0017	*TYK2*
rs3748816_T	66	1.16	1.0047	*MMEL1*
rs9523762_A	35	1.36	1.0234	*GPC5*
rs1800693_G	45	1.20	1.0083	*TNFRSF1A*
rs17445836_G	81	1.25	1.0067	*IRF8*
rs17824933_G	25	1.18	1.0056	*CD6*
rs744166_G	42	1.15	1.0048	*STAT3*
rs1790100_G	22	1.10	1.0016	*MPHOSPH9*
rs4680534_C	34	1.11	1.0025	*IL12A*
rs2760524_G	83	1.15	1.0025	*RGS1*
rs6896969_C	61	1.10	1.0021	*PTGER4*
rs882300_C	55	1.19	1.0073	*CXCR4*
rs1250540_G	38	1.12	1.0031	*ZMIZ1*
rs9321619_A	54	1.12	1.0032	*OLIG3*
rs703842_A	71	1.23	1.0081	*CYP27B1*
rs6074022_G	28	1.20	1.0072	*CD40*
rs9657904_A	83	1.40	1.0128	*CBLB*
rs763361_A	47	1.13	1.0037	*CD226*

SNP Allele = the associated SNP and risk allele (the 16 loci in bold have achieved $p < 5x10^{-8}$ in at least one well powered study), Freq = Frequency of the risk allele in the general population, OR = Odds Ratio, Locus λs = the locus specific λs (the increased relative risk in the siblings of an affected individual attributable to this allele), Gene = the nearest gene (it is not necessarily established that this is the relevant gene).

Samples

All individuals involved in this study (cases and controls) gave valid informed consent in accordance with approval from the relevant local Ethical Committees or Institutional Review Boards (IRBs). Apart from the small number of African-Americans included in the USA twins cohort, all individuals self-reported as being of European ancestry.

Case collections

As there are no diagnostic laboratory tests for multiple sclerosis, the diagnosis depends on meeting established and well-validated criteria that combine clinical and para-clinical laboratory-based information, introduced in 1983 and revised and updated between 2001 and 2005.[11-13] The principle of these criteria is to establish that focal areas consistent with inflammatory demyelination have occurred in more than one part of the brain and spinal cord and on more than one occasion, and for which there is no better explanation than the diagnosis of multiple sclerosis. In the majority of centres disease severity has been documented using the Expanded Disability Status Score (EDSS)[14] and its dependent derivative the Multiple Sclerosis Severity Score (MSSS).[15] Clinical course, relapse and progression are defined in accordance with consensus criteria.[12,16-18] The clinical characteristics of the samples included in the study were typical (see below).

In most centres, DNA was extracted from samples of venous blood using standard methods. In some, DNA was extracted from cell lines or from saliva. Quantification, normalisation and storage methods varied between centres, however prior to screening all samples were quantified and normalised at the Sanger Institute, Cambridge, UK. Across centres DNA extraction rates were high (>98%) and in most centres samples were not subject to any additional purification. Population specific details regarding the samples recruited at each centre are provided below along with the three digit code for each group.

Australia (ANZ)
All cases were self-identified volunteers recruited at centres located in Adelaide, Brisbane, Gold Coast, Hobart, Melbourne, Newcastle, Perth and Sydney.

Belgium (BEL)
Cases were recruited between 2000 and 2008 amongst out-patients and hospitalized patients with definite MS attending the Neurology Department of the University Hospital of Leuven or the "National MS Center" in Melsbroek. Both centres are located 28 km apart in the centre of Belgium and recruited mainly amongst patients from the northern Dutch-speaking part of Belgium. Participation rate of patients attending these clinics is virtually 100%. At both centres, the majority of patients are followed-up longitudinally by neurologists specialized in MS with at least yearly visits. Approximately 40% of patients are being treated with an immunomodulatory therapy. The average EDSS/MSSS score is relatively high because the National MS Center tends to be visited by the more severely affected patients.

Denmark (DEN)
Patients were recruited by neurologists at multiple sclerosis centres from across the whole of Denmark, although the majority of patients originate from the Copenhagen area. This clinic based approach means that the proportion of patients with relapse remitting multiple sclerosis (RRMS) is higher than is seen in the general population.

Finland (FIN)
Cases were recruited from seven centres (Helsinki University Central Hospital, Tampere University Hospital, Kuopio University hospital, Oulu University Hospital, Seinäjoki Central Hospital, Satakunta Central Hospital and Rovaniemi Central Hospital) and thus come from many different regions of Finland. All were identified in hospital clinics by experienced neurologists. Twelve percent were recruited before 1998 as part of an effort to collect either multiplex families (at least two cases in a family) or trio/nuclear families (an affected individual with both parents and if not available with one parent and siblings), and the rest were recruited between 2000 and 2006 as trio/nuclear families by neurologists of the MGEN consortium. Thirteen percent of the trio cases and 95 percent of cases of multiplex families originate from the MS high-risk isolate of Southern Ostrobothnia, with increased prevalence and familial occurrence of the disease.

France (FRA)
The French MS Genetics group (REFGENSEP) has been collecting samples since 1992. Three main centres are involved in the recruitment of the patients and their families (Toulouse, Rennes and Paris) with an experienced physician based at each centre. Some patients self-refer in response to advertising campaigns run all over France through patient associations. All volunteers are examined by a REFGENSEP physician to confirm the diagnosis. Only individuals from trio (an affected and his two parents) or multiplex families (at least two affected sibs and their parents if possible) were included in this study. REFGENSEP physicians hold two annual meetings in order to review the diagnosis and clinical features of included patients.

Germany
Three centres contributed cases.

a) Berlin (GEB)
The samples have been collected from outpatients and inpatients of the Cecilie Vogt Klinik at the University Medicine Berlin. Individuals originally came from multiple sites in Germany.
b) Munich(GEM)
The samples from Munich can be stratified mainly in two cohorts regarding the origin and acquisition strategy. The first cohort comprises patients with multiple sclerosis from central Germany. The second cohort was recruited from across multiple sites and includes individuals treated with interferon-beta for at least 6 months.
c) Hamburg (GEH)

Samples were collected from Hamburg and the Northern part of Germany with the majority recruited through out-patient-clinics (ambulatory) and a minority recruited from the neurological wards.

Ireland (IRE)
The samples are regional from a clinic based population, ascertained through hospital based neurology clinics. The cohort has no specifically unusual attributes.

Italy
Two centres contributed cases.

a) Piedmont (ITP)
Patients were collected from Continental Italy (excluding Sardinia) as part of the PROGEMUS (PROgnostic GEnetic factors in MUltiple Sclerosis) project, 87% of cases were collected in North-West Italy (Novara, Torino, Milano, Pavia) and 13% in Central Italy (Rome). These patients were all recruited from hospital based clinics; mean participation rate was approximately 60% (range 20%-90%).
b) San Raffaele, Milan (ITM)

Patients have been consecutively recruited from two main projects: the Italian Network of Primary Progressive Multiple Sclerosis (PROGRESSO consortium), and from the inpatients and outpatient clinics of the Scientific Institute San Raffaele in Milan. Most of the patients are from the North of Italy (65%).

New Zealand (ANZ)
Patients were recruited across the country as part of a recent national prevalence survey. Genomic DNA was isolated from saliva self-collected into Oragene DNA tubes according to the manufacturer's instructions (DNAgenotek). Because of possible bacterial contamination and difficulty in obtaining reliable pico green and spectrophotometry measurements, all saliva DNA samples were assessed for their integrity by agarose gel electrophoresis and at least one other method.

Norway (NOR)
The Norwegian samples were derived from two sources; the Oslo MS DNA biobank and the Norwegian Multiple Sclerosis Registry and Biobank held in Bergen. In the Oslo MS DNA biobank the majority of patients are recruited by the neurologists at Oslo University Hospital, Ullevål with the remainder coming from local MS Societies and other neurological departments serving the suburban Oslo areas. Samples in the Norwegian Multiple Sclerosis Registry and Biobank were recruited from all other parts of Norway. This collection started in 2007, and currently includes approximately 1/5 of the prevalent MS patients in Norway.

Poland (POL)
All Polish patients were recruited from amongst those treated in the Department of Neurology, Medical University of Lodz. The patients were white and Polish. None of the patients selected in the study have a family history of the disease.

Spain (SPN)
Patients were recruited from amongst those attending the neurology outpatient clinic in the Unitat de Neuroimmunologia Clínica - Hospital Universitari Vall d'Hebron (http://www.vhebron.net/), the Hospital Clinic of Barcelona (http://www.hospitalclinic.org/), and the MS centre at the University of Navarra (http://www.unav.es/).

Sweden (SWE)
Swedish samples were derived from three sources (overlaps between these were prevented using the national personal identification numbers): An ongoing population based case-control study called EIMS (Epidemiological Investigations in Multiple Sclerosis)[19] in which diagnosis was established at neurological clinics throughout Sweden, a set of local patients from Stockholm County (recruited and diagnosed at Karolinska University Hospital and Danderyds Hospital) and a set of patients being treated with Natalizumab (recruited and diagnosed throughout Sweden in conjunction with the start of treatment). Sample handling and DNA extraction for first and third sources was performed at the Karolinska Insitutet Biobank, while it was performed at the Department of Clinical Neurosciences, Karolinska Insitutet for the second cohort.

Control individuals were also recruited from the EIMS study matched to the EIMS patients for age, sex, and geographic location. As these samples were processed alongside the case samples that are described here.

United Kingdom
Five centres contributed cases.

a) University of Cambridge (UKC)
Cases were recruited from across the British Isles with the majority coming from South East England (56% living within 100 miles of Cambridge). All were identified and referred by Members of the Association of British Neurologists and recruited between 2002 and 2009;

10% have a family history of the disease. Sixteen percent were recruited as part of an effort to collect trio families (an affected individual and both his / her parents), and as a result have a slightly lower than average age for prevalent people with multiple sclerosis. Other than steroids only a minority of patients have received immunomodulatory therapy such as beta-Interferon (9%), Glatiramer Acetate (3%), Campath-1H (4%) or other cytotoxics (e.g. Mitoxantron) (3%).

b) University of Cardiff (UKW)

The University Hospital of Wales serves a local population of 1.2 million and provides a network of MS clinics across the South Eastern part of the country. Cases were recruited from these clinics.

c) University of Keele, Greater Manchester (UKN)

Cases were recruited from the North Staffordshire Hospital in Stoke-on-Trent, Hope Hospital in Manchester and Walton Centre in Liverpool during the period from 2000 to 2008. Together these centres cover a significant part of north of England (Merseyside, Greater Manchester, Cheshire, Staffordshire and Derbyshire). Participation rate from neurology clinics recruitment is currently approximately 60%. Patients were recruited from general neurology outpatient clinics, Disease Modifying Treatment Clinics and newly diagnosed MS patients' clinics.

d) University of Plymouth (UKP)

Samples were obtained from recruits to the Cannabinoid Use in Progressive Inflammatory brain Disease (CUPID). This 30 centre UK-wide placebo controlled trial randomised individuals with primary or secondary progressive disease with EDSS between 4.0 and 6.5.

e) Imperial College MS Tissue Bank (UKC)

All post-mortem tissues were obtained via a UK prospective donor scheme. In these individuals the diagnosis of multiple sclerosis has been confirmed neuropathologically according to the ICDNS criteria (www.ICDNS.org). Tissue blocks for DNA extraction were removed from the cerebellum of the fresh brain, snap frozen in isopentane on dry ice and stored at -80°C.

United States of America

Four centres contributed cases.

a) Boston (USB)

Patients were recruited from three different sources: the Brigham & Women's Hospital, the Accelerated Cure Project (http://www.acceleratedcure.org/repository/index.php) and Washington University St Louis. Each subject was recruited through an MS Centre at an academic institution.

b) San Francisco (USC)

Patients were recruited from the UCSF MS clinic and from other sites in the US via referral from physicians or self-referral in response to advertisements in MS newsletters and at MS functions. To minimize inter-observer variability and guarantee cohesive and thorough training of all collaborators, detailed instructional sessions on ascertainment procedures are performed at each site by UCSF personnel. Phlebotomy is performed at the individual's preferred clinic, or at the subject's home by a nationwide phlebotomy service. Blood specimens (4 x 7.5 ml tubes) are transferred or mailed by courier to the UCSF laboratory for processing. For this study, blood samples were collected between 1987 and 2007.

c) Berkley (USL)

Patients from the University of California Berkeley/ Kaiser Permanente Division of Research were recruited from Northern California between 2006 and 2008. All cases were current members of the Kaiser Permanente Northern California Region (KPNCR) and were identified through the KPNCR clinical database. All were between 18-60 years of age and were unrelated to anyone else already recruited. Participation rate among the initially identified cases was 64%. DNA was extracted from the blood using Purgene(Gentra). Quantification was performed with either Nanodrop or Tecan spectrophotometer.

d) Twins (UST)

Twins with MS were sought by advertisements in North American newspapers and other periodicals from 1980 through 1992. Ascertainment was designed to capture pairs of twins in whom at least one member had physician-diagnosed MS. No concordant pairs were doubly ascertained. Pairs identified as discordant for the disease were verified based on the neurological health of the unaffected co-twin, most often by direct contact. Zygosity was initially assigned according to the twins' own perception. We have estimated that approximately 27% of the North American twin cases prevalent at any time during the period were identified. The characteristics of the twin respondents have been described previously.[20,21]

Clinical Information

Data regarding age at onset, age (at EDSS assessment), EDSS, MSSS and clinical course (primary progressive or relapsing onset) were available in 89%, 78%, 74%, 72% and 86% of the 9,772 cases. Across these samples the mean age at onset, age (at EDSS assessment), EDSS and MSSS were 32.3 years, 44.8 years, 3.9 and 4.9 respectively. In terms of clinical course 11% of cases had primary progressive disease. The clinical characteristics of each group are shown in Table S6.

Table S6. Clinical characteristics by group.

Group	AAO / y	AGE* / y	EDSS	MSSS	PPMS / %
ANZ	33.5	47.6	3.6	4.2	1
BEL	33.1	48.6	5.0	5.9	12
DEN	30.7	39.6	3.6	5.5	4
FIN	29.8	44.1	4.1	4.7	8
FRA	26.8	37.2	3.6	4.7	0
GEB	28.4	35.7	2.3	3.6	0
GEM	32.5	40.2	3.3	4.8	7
GEH	33.2	42.9	3.2	4.5	21
ITP	31.3	42.3	3.2	4.2	8
ITM	33.5	45.0	3.9	4.8	41
NOR	33.7	48.5	3.8	4.4	13
POL	31.2	39.9	2.8	1.5	11
SPN	30.7	46.1	4.7	5.2	23
SWE	33.3	39.2	1.4	3.7	5
UKC	32.9	48.4	5.0	5.7	15
UKN	32.6	44.6	4.8	6.1	12
UKP	37.8	51.9	5.8	6.7	41
UKW	31.3	44.5	4.5	5.7	9
USB	32.1	45.5	3.2	3.9	9
USC	32.2	45.8	4.1	5.1	7
USL	30.6	49.5	2.9	2.7	0
UST	30.3	55.9	3.8	5.2	0
All	32.3	44.8	3.9	4.9	11

* The age at which the EDSS was recorded. No clinical data were available for the Irish cases.

Control collections

In this study we used the common control data sets generated as part of WTCCC2 (2,737 from the National Blood Service (NBS) and 2,930 from the 1958 Birth Cohort). We also generated control data from 665 healthy subjects from the Swedish EIMS study (as described above). To supplement these internally generated control data and provide more appropriate controls for the non-UK populations we collated data from existing Illumina typed control samples obtained from independent sources (external control data). The Swedish EIMS samples are described above alongside the Swedish cases.

National Blood Service (NBS)
These samples were obtained from the UK blood transfusions services repository of anonymised DNA samples that was originally established to support WTCCC1.[22]

1958 Birth Cohort (58C)
These samples were obtained from the National Child Development Study an epidemiological survey based on all individuals born in England, Wales and Scotland during one week in 1958 (www.b58cgene.sgul.ac.uk/followup.php). DNA was obtained from EBV-transformed cell lines. These internal control samples were subjected to the same DNA QC process outlined for the case samples.

CAHRES (Cancer Hormone Replacement Epidemiology in Sweden)
These data were obtained as part of a population-based case-control study of postmenopausal breast cancer in women born in Sweden aged 50-74 years at the time of enrolment which was between October 1, 1993 and March 31, 1995. The control subjects were randomly selected from the Swedish Registry of the Total Population and frequency matched to the expected age distribution of the cases. Details on data collection and subjects have been described previously.[23]

CHOP (Children's Hospital of Philadelphia)
These data were obtained from healthy controls recruited through the CHOP Health Care Network, including various primary care clinics and well child clinics. The control subjects were screened for any neurological or chronic medical conditions by a questionnaire and this was further confirmed by review of electronic medical records. The subjects included here were all of European ancestry (detailed self-reported assessment and genetic based analysis).

EGEA (Epidemiological study of Genetics and Environment of Asthma)
These data were obtained from the control subjects involved in the Epidemiological study on the Genetics and Environment of Asthma (EGEA).[24,25] EGEA is a 12-year longitudinal survey where all individuals were of European ancestry and were born in France. Controls were a combination of population-based and unaffected family members of probands. Genotyping was carried out using the Illumina Human610 quad array at the Commissariat à L'Energie Atomique, Institut de Génomique, Centre National de Génotypage, Evry, France. Raw data was analyzed using GTS Image and extracted for statistical analysis. Only two of eight Asthma associated SNPs (rs1342326, rs3771166, rs744910, rs3894194, rs2284033, rs2786098, rs1588265, rs7216389) listed in the GWAS catalogue (http://www.genome.gov/26525384) showed nominally significant evidence of association with multiple sclerosis - rs1588265 (p=0.037) and rs7216389 (p=0.019).

GAS (Gabriel Advanced Survey)
These data were obtained from the control subjects involved in the GABRIEL ADVANCED SURVEY a cross-sectional population-based survey conducted in rural areas of Austria, Germany, and Switzerland. In total, 135,359 children aged 6-12 years were addressed through schools. Genomic DNA was purified from blood samples using the Puregene chemistry

(QIAGEN, Hilden, Germany) on an Autopure LS instrument (QIAGEN, Hilden, Germany). Genotyping was carried out using the Illumina Human610 quad array at the Commissariat à L'Energie Atomique, Institut de Génomique, Centre National de Génotypage, Evry, France. Raw data was analyzed using GTS Image and extracted for statistical analysis.

HealthMet 2000
These data were provided from the controls involved in the GenMetS subset of the Health 2000 project. All individuals are aged 30 and were collected from all across Finland.

KORA
The KORA S4 survey (4,261 participants), an independent population-based sample from the general population living in the region of Augsburg, Southern Germany, was conducted in 1999/2001. A total of 3,080 subjects participated in a follow-up examination of S4 in 2006-08 (KORA F4), comprising individuals who, at that time, were aged 32–81 years.[26] Genotyping was done in 488 selected individuals using the Illumina 550K GeneChip array.

POPGEN
These data were provided from the PopGen project.[27] A collection of individuals recruited from Northern Germany for the express purpose of providing control genotypes and extensive phenotypic details to aid the analysis of studies in complex genetics. Genotyping was performed as a service by Illumina.

HYPERGENES
These control data were collected as part of the HYPERGENES (European Network for Genetic-Epidemiological Studies) project (HEALTH-F4-2007-201550). The individuals involved were recruited after 2000 from across Continental Italy (excluding Sardinia), mainly in the area surrounding Milan. All individuals self-reported as being exclusively of European ancestry, in particular Italian origin for more than two generations. All individuals were more than 55 years of age. Each DNA sample was quantified and normalized to 50ngul^{-1} prior to genotyping. The genotyping was performed in the Genomic Laboratory of the Genomic and Bioinformatic platform at the University of Milan. Each sample was genotyped using Illumina Infinium II 1M duo BeadChips (Illumina, San Diego, CA, USA).

MG_GWAS (Myaesthenia Gravis GWAS)
These genome-wide data were obtained from healthy Norwegian individuals recruited through the Norwegian Bone Marrow Donor Registry held at the Institute of Immunology, Oslo University Hospital, Norway (http://www.nordonor.org/). These samples were genotyped on the IIlumina 550 chip by the Myasthenia Gravis Genetic Consortium (MGGC) who generously provided these data as external controls.

PROCARDIS
A total of 340 men and 340 women, free of coronary artery disease, were recruited at random from the general population of the greater Stockholm area for inclusion as controls in the PROCARDIS program.[28,29]

Genotyping and Quality Control

Genotyping

Case samples (along with the Swedish EIMS controls and co-twins) were genotyped on the Human660-Quad chip; a custom designed array based on the Human550 supplemented with 60,000 additional probes that were intended to allow the genotyping of common CNVs as identified by the Structural Variation Consortium.[30] The WTCCC2 common controls were genotyped on the Human1.2M-Duo chip (a second custom array based on the Human1M-Duo supplemented with the same 60,000 CNV probes). All genotyping was performed on the Illumina Infinium platform at the Wellcome Trust Sanger Institute (WTSI).

All genotypes used for analysis were called using the program Illuminus,[31] run at the WTSI, by processing each of the two shared control collections, the WTCCC2 funded MS study samples and each external control collection as separate batches.

Sample QC

We describe below the quality control (QC) of the case samples collected as part of the WTCCC2 MS analysis; where appropriate similar approaches were used for both internal and external controls. A summary of the total numbers of exclusions are given at the end of this section.

Collectively the 23 research groups contributing cases to this study provided a total of 20,526 DNA samples. Most of these (14,730) were first sent to the Centre for Integrated Genomic Medical Research (CIGMR) in Manchester (UK) where they were set on to 96 well plates prior to shipment to the Wellcome Trust Sanger Institute in Cambridge (UK). The remainder were shipped directly to the Sanger Institute on 96 well plates. The 20,526 samples included 665 unaffected Swedish controls and 236 US affected twin pairs (472 samples); 115 monozygotic pairs (31 concordant for disease) and 121 dizygotic pairs (11 concordant for disease); 11 of the twin pairs are of African American origin all other pairs are white. Counting only the index affected individual from each white twin pair (n=225) there were 19,614 independent white cases in total.

At the Sanger Institute each sample was finger printed with a panel of Sequenom markers (either 30 or 31 in total); 609 samples (3.0%) either failed to genotype on Sequenom or gave data of inadequate quality. These samples were therefore excluded. Amongst the 20,526 individuals, gender was specified by the provider as female in 14,470, male in 5,971 (2.4F:1M) and was unspecified in the remaining 85. Sequenom X-linked markers were un-interpretable in 502 of the 20,441 gender known individuals. Amongst the 19,939 testable individuals the specified gender was confirmed in 98.4% (19,626). The 313 (1.6%) individuals with mis-specified gender were excluded. DNA concentration was measured in duplicate with picogreen. The average concentration in our samples was 155ngμl^{-1} (ranging from 0 to 991). Samples were considered unsuitable for screening if the concentration was below 50ngμl^{-1} or if there was more than 10% difference in the two measurements. A total of 17,085 samples passed Pico QC from which 17,055 were normalised to 50ngμl^{-1}. Running DNA from the 17,055 normalised samples on an agarose gel revealed 165 samples with degraded DNA and 191 samples with a weak or absent band. In total 16,133 (78.6%) samples passed all aspects of the DNA QC process.

For each group samples were prioritised for screening according to the availability of phenotypic information and appropriate population specific controls. As a result the

proportion of samples from each group selected for screening varies. In total 11,527 samples were selected and typed, and of these 10,908 (94.6%) gave call rates of > 92.5% in Beadstudio analysis (the Illumina genotyping program). Typing was re-attempted in the 619 that failed to reach this threshold and 540 (87.2%) of these repeats gave call rates of >92.5%. Typing was attempted a third time in the 79 samples that had failed both previous attempts but only 13 (16.5%) of these passed the minimum 92.5% call rate threshold. As part of the QC and DNA tracking process 228 samples were genotyped in duplicate. (Note that all samples were subsequently recalled using Illuminus.)

The same QC process applied to the case samples was also applied to the internal control data (see below). For the external control samples there was no Sequenom finger printing available, but all other sample related QC checks were performed.

Probe intensity outliers

First pass analysis of these data revealed an unexpectedly large number of SNPs showing apparent evidence of association in the absence of any corresponding evidence in correlated flanking SNPs. Inspection of the cluster plots from these isolated SNPs suggested that these aberrant associations resulted from deviation in the measured signal intensities from a subset of samples (see Figure S1).

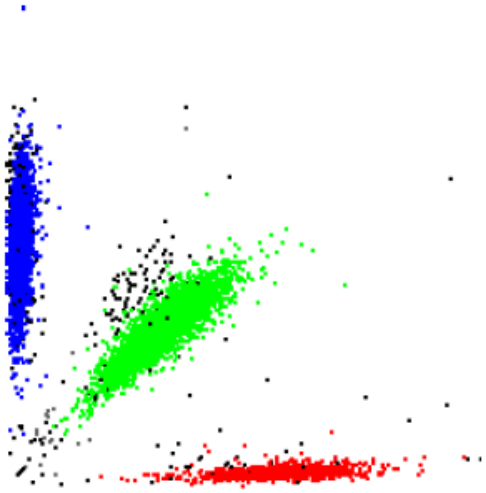

Figure S1. An example of a cluster plot (rs272516) distorted by inclusion of intensity difference outlier samples. The outliers are coloured black to highlight them from the main clusters.

In an attempt to identify those samples with a systematic difference in the signal intensity between the two channels used to indicate the presence of the alternate alleles at a SNP (channels x and y), we calculated and compared the mean relative intensity difference between the channels across a set of 10,000 randomly selected SNPs from across the 22 autosomal chromosomes in each of the samples (i.e. the mean of y-x over these markers). The resulting distribution revealed a significant number of outliers. Moreover, plotting this mean difference with respect to the time at which each sample was processed (see Figure S2) showed that many of these outlying samples were clustered on particular 96 well plates, raising concerns about the measured intensities in the other samples from these plates.

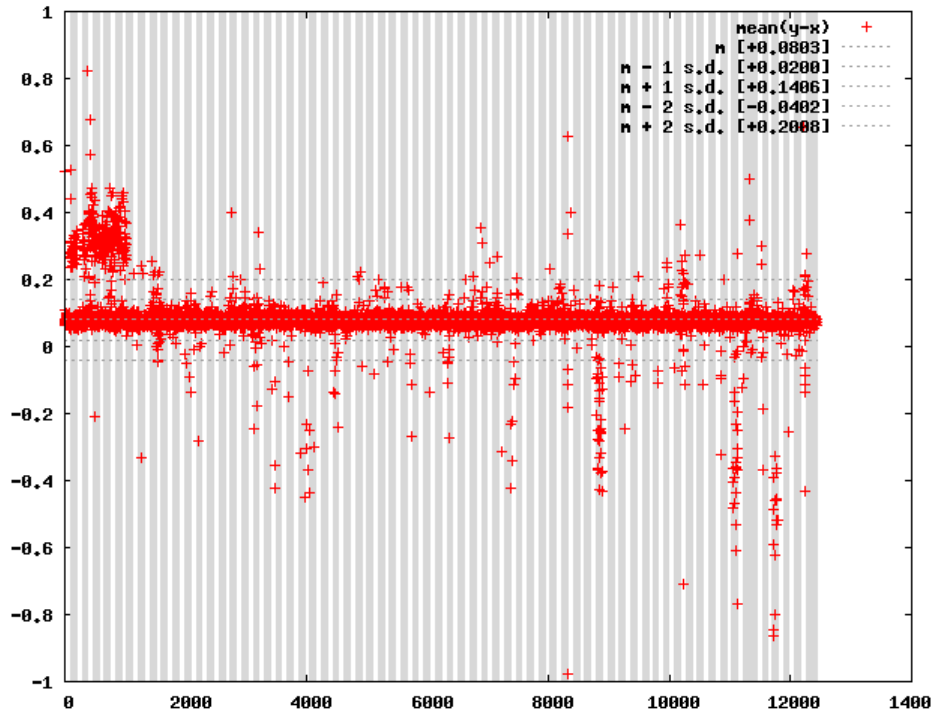

Figure S2. The mean difference in intensity for each sample plotted with respect to the chronological order in which they were processed. The vertical gray and white bars indicate individual 96 well plates. The X-axis shows the cumulative number of wells (Note not all plates were full). The plot also shows some data related to control samples and samples from other WTCCC2 trait samples analysed alongside multiple sclerosis samples on these particular plates.

To correct for this unexpected effect we excluded all data sets that gave mean differences that were outliers and all data sets from plates where more than 50% of the samples were outliers regardless of the mean difference calculated. Repeat typing was completed in 970 samples. After this additional typing genome-wide datasets passing the minimum Beadstudio call rate threshold of 92.5% were available from 11,370 samples. Six of these samples were typed in duplicate - two from Finland, one from France, one twin and two Swedish controls - so that in total 11,376 data sets were potentially available for analysis and were transferred to the Wellcome Trust Centre for Human Genetics in Oxford. Re-plotting the mean difference in relative intensities showed that just five of these data sets were modest outliers (see Figure S3) and these were excluded in subsequent analysis. Inspection also showed that 27 samples had <90% concordance in the genotype calls that were defined in the Sequenom finger printing at the start of the DNA handling process. These samples were also subsequently excluded.

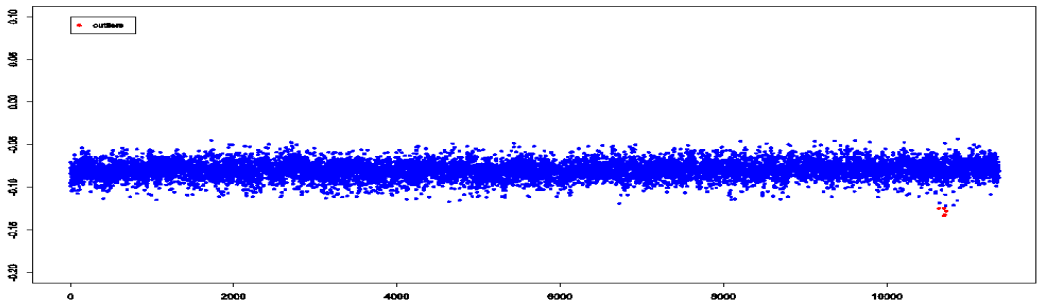

Figure S3. The mean difference in intensity for each sample plotted with respect to the chronological order in which they were processed after excluding outlying samples and plates and repeat typing in the excluded samples. The five outlier samples are shown in red.

Identifying outliers by clustering

Rather than applying arbitrary thresholds to standard measures of genotyping QC we modelled the distribution of relevant variables over the collection as a whole and used Bayesian clustering approaches to identify and exclude samples inferred to be outliers.[32] Considering the call rate and mean heterozygosity for each sample we established that 471 samples deviated from the inferred distribution of these variables and were therefore excluded from analysis (see Figure S4).

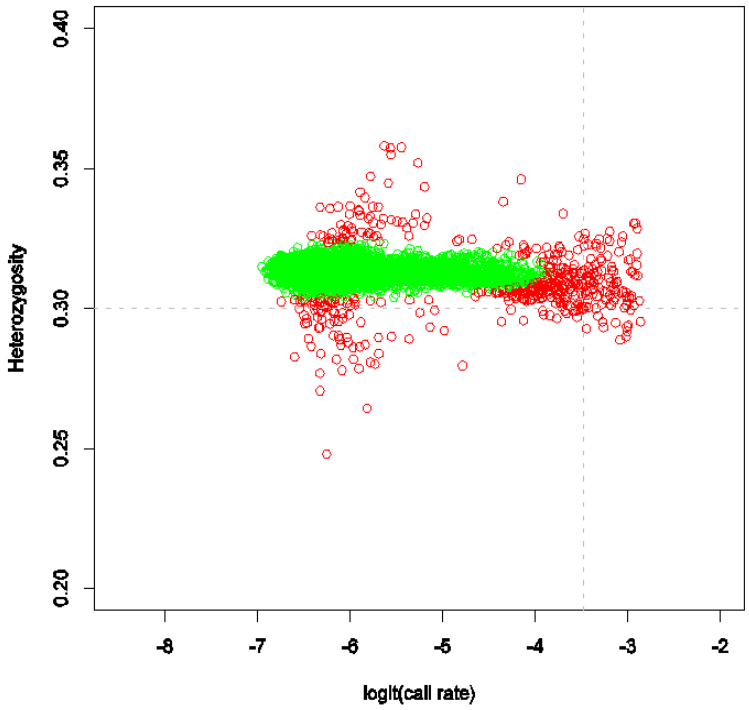

Figure S4. Plot of mean heterozygosity against logit(call rate). Samples considered to be significant outliers (n=471) are shown as red circles and those consistent with the main distribution are shown as green circles.

We then used the mean intensity in a single channel from the SNPs in the non-pseudo autosomal part of the X chromosome to consider gender, anticipating a significantly lower mean intensity in males than in females (see Figure S5). Four samples gave mean intensity values that differed from their nearest gender specific distribution, 16 samples gave mean levels that were inconsistent with the gender reported by the sample supplier and 35 samples had no gender information supplied. All 55 of these samples were also excluded.

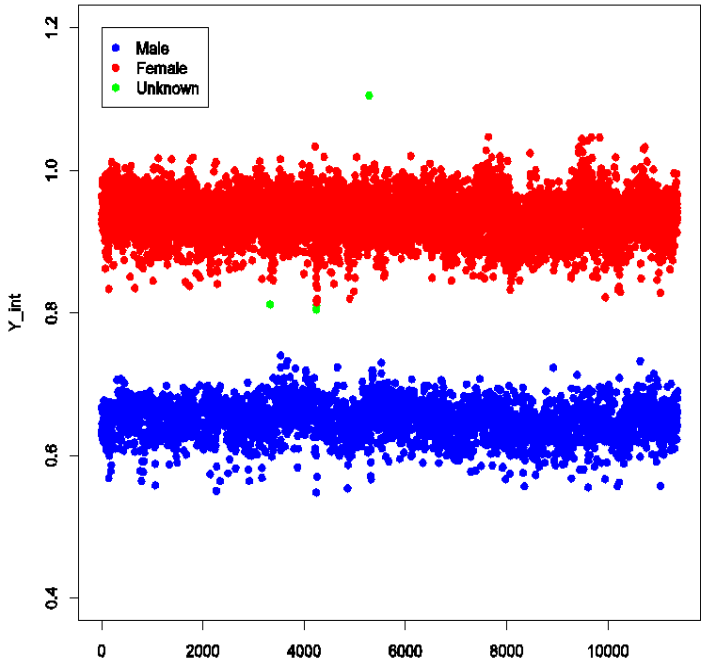

Figure S5. Mean intensity of one channel in SNPs from the non-pseudo autosomal part of the X chromosome. Male samples give clearly lower mean values than female samples (as they less often carry alleles measured by the tested channel). Bayesian cluster analysis shows that four samples gave mean values that were significant outliers in comparison to either gender specific group.

Estimating relatedness via HMMs

To investigate recent shared ancestry between samples we used a hidden Markov model (HMM) to estimate the identity by descent (IBD) across the genome between each pair of individuals. Theoretically the concept of IBD is defined with respect to some time-point in the past which in our HMM should be reflected by the allele frequencies of the ancestral population at that time. In this analysis we have simply used the allele frequencies of the current population which should work well when the goal is to identify relatedness just a few generations back in time. This analysis was based on a genome-wide subset of 11,547 SNPs which should be enough for identifying close relatedness, although may not be enough to accurately estimate more distant relatedness. For each pair of individuals with >5% of the genome IBD for at least one allele we iteratively removed the individual with the lowest call rate until all pairs of individuals had <5% IBD (in this process we allowed for the expected relationships between the twin samples and preferentially kept the affected index twin even if the unaffected co-twin had a higher call rate). In total 289 individuals were excluded in this process and a large majority of them belonged either to a duplicate or a first-degree relative pair (see Figure S6).

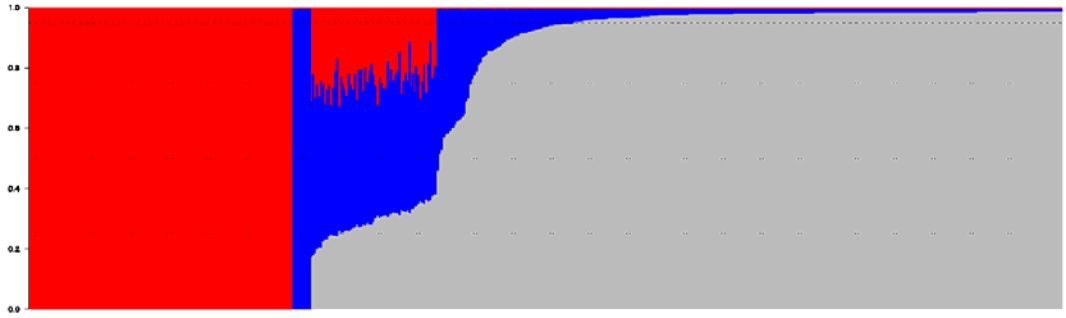

Figure S6. Identity by descent (IBD) across the genome for the 1000 most related sample pairs (ranked from the most related on the left to the least related on the right). The genome in

each pairwise comparison is represented by a vertical line. Grey colouration indicates zero alleles IBD, blue indicates 1 allele IBD and red indicates 2 alleles IBD. Those pairs where the line is entirely red are monozygotic twins or duplicate samples (intentional or unintentional). Those where the line is entirely blue are parent-child pairs and those where the sharing is approximately one quarter red (2 sharing), one half blue (1 sharing) and one quarter gray (zero sharing) are siblings or dizygotic twins. Other samples with inflated IBD sharing represent less related individuals, i.e. grandparents, aunts, uncles, cousins etc. The upper most horizontal dotted line indicates the 5% IBD cut-off threshold and the other dotted horizontal lines 25% centiles.

PCA clustering

In order to begin to correct for the structure in this complex data set we used principal components analysis (PCA) using the program SHELLFISH (www.stats.ox.ac.uk/~davison/software/shellfish/shellfish.php) to identify and exclude samples with significant non-European ancestry. To do this we selected SNPs from among our post-QC set with non-complementary alleles and minor allele frequency (MAF) > 0.05 in each HapMap Phase 2 population. We then filtered this set of SNPs to minimize the correlation between markers due to linkage disequilibrium (LD). This established a subset of 206,508 SNPs for the internal samples (198,992 SNPs for the external samples) that covered the genome (excluding the MHC region, a set of highly differentiated SNPs identified in WTCCC1, and all SNPs in regions with unusually high loadings based on visual inspection of the first 20 axes of a PCA applied to control samples only). Using the data from this subset of SNPs we projected our samples onto the first two principal components from the PCA of the Hapmap data. Through Bayesian clustering analysis we excluded 180 samples with non-European ancestry (see Figure S7 and Figure S8).

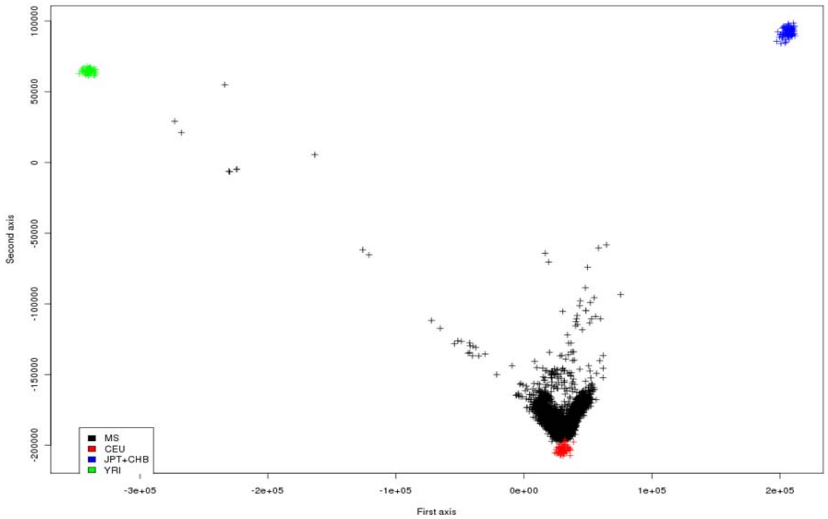

Figure S7. The projection of samples onto the first two principal components of the Hapmap data. Our samples are labelled in black, while the European (CEU) samples are red, the Asian (JPT + CHB) samples are blue and the African (YRI) samples are labelled in green.

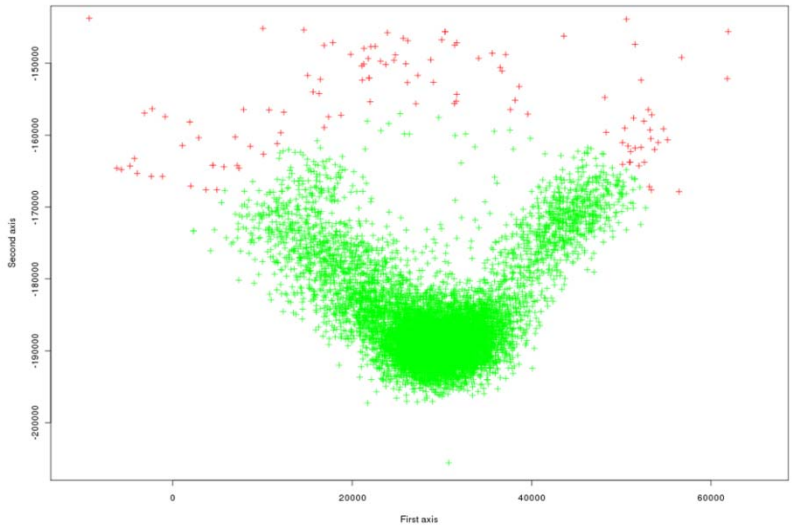

Figure S8. A close-up view of the main cluster of our samples with those showing evidence of being outliers from the main distribution coloured in red and those being part of the main distribution being coloured in green.

After visual inspection of a PCA plot applied to the UK samples only, 21 additional outlying UK cases were also excluded (see Figure S9).

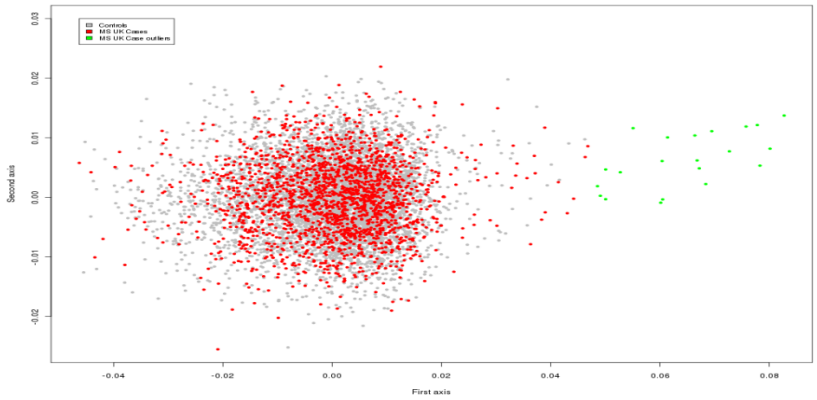

Figure S9. First two eigenvectors of PCA analysis applied to the UK cases and controls only. The removed outlying case subjects are shown in green. The remaining cases are shown in red and the controls in grey.

Estimating ancestry proportions

To further refine our correction for ancestry, we estimated the proportion of each individual's genome that is most closely related ancestrally to each of the 10 Hapmap Phase 3 populations, allowing for a "Null" group to allow for potential genotyping errors (see Figure S10). Specifically for each individual we used a beta-binomial model to describe the probability of the individual's observed genotypes conditional on the allele counts of each HapMap population at each SNP. We then calculated the expected posterior proportion of the individual's SNPs genome-wide that are most closely related to each HapMap population under this model, assuming *a priori* that each population is equally likely to be most related. Further refinements were implemented to account for ancestry proportions of the HapMap populations. We used the phased build 36 (release 2) HapMap Phase 3 data downloaded from http://hapmap.ncbi.nlm.nih.gov/downloads/phasing/2009-02_phaseIII/HapMap3_r2/, using the combined set of all phased haplotypes across the trio, duo, and unrelated samples for each population. The 10 populations represented samples of (1) African ancestry in Southwest

USA (ASW), (2) Utah residents with Northern and Western European ancestry (CEU), (3) Han Chinese in Beijing, China plus Japanese in Tokyo, Japan (CHB+JPT), (4) Chinese in Metropolitan Denver, Colorado (CHD), (5) Gujarati Indian in Houston, Texas (GIH), (6) Luhya in Webuye, Kenya (LWK), (7) Mexican ancestry in Los Angeles, California (MEX), (8) Maasai in Kinyawa, Kenya (MKK), (9) Toscans in Italy (TSI), and (10) Yoruba in Ibadan, Nigeria (YRI). To determine proportions of ancestry, we used the 188,110 SNPs corresponding to the overlapping set between the SNPs selected for PCA and the SNPs contained in our HapMap3 samples. Based on this analysis, we excluded 37 individuals with a significantly different ancestry profile relative to the others, defined as having either (a) a total proportion of "Null" SNPs > 0.05, or (b) a combined non-Null proportion from the four HapMap populations with African ancestry (i.e. ASW, LWK, MKK, YRI) > 0.05.

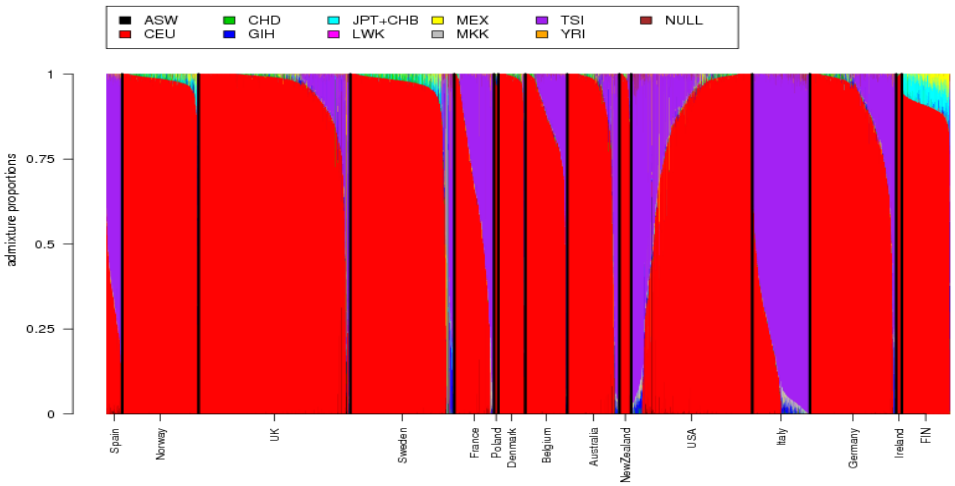

Figure S10. Admixture plot. Each individual's genome is represented by a vertical line divided into differently coloured sections corresponding to the proportion of their genome most closely related to each of the 10 Hapmap 3 populations, allowing for an uninformative "Null" group (see colour key). Within each country specific set of samples, individuals are ordered according to their ranking along the first axis of a PCA applied to their estimated admixture proportions. As expected almost all individuals are best represented as some mixture of northern (CEU) and southern (TSI) European Hapmap populations. A degree of Asian ancestry is seen in the Scandinavian groups, especially the Finnish.

Summary of sample exclusions

After comparing the genotype data generated in this study with that generated for the same samples in previous studies we excluded 25 samples due to inconsistencies, along with a further 13 for which the clinical diagnosis was considered to fall outside the research definitions. Non-white and unaffected twins (n=90) were also excluded. At the end of the QC process 1075 of the samples (8.9%) were excluded, approximately 20% of these for more than one reason. This left 9,772 cases and 527 controls (Swedish) for inclusion in the analysis. Table S7 shows the population specific breakdown for the exclusions while Table S8 shows the group specific breakdown of the samples processed through to inclusion.
The same QC process applied to the case samples was also applied to the Internal control data. For the external control samples there was no Sequenom finger printing to check but all other sample related QC checks were performed (for additional SNP QC checks performed on these data see below). Table S9 shows the population specific breakdown for the exclusions in the control data sets while Table S10 shows the group specific breakdown of the control samples processed through to inclusion.

Table S7. Country specific breakdown of exclusions

Country	I	S	CR/H	G	R	PC	A	O
Australia	0	3	24	5	13	9	6	0
Belgium	0	0	14	0	5	2	0	2
Denmark	0	0	18	2	3	8	0	0
Finland	0	1	29	0	24	19	0	2
France	0	14	23	4	11	17	2	1
Germany	0	1	29	9	5	21	1	2
Ireland	0	0	11	0	1	0	0	0
Italy	0	0	19	7	3	1	2	0
New Zealand	0	0	5	2	1	0	2	0
Norway	0	2	42	1	25	9	0	0
Poland	0	0	1	0	0	0	0	0
Spain	0	0	4	0	1	1	0	0
Sweden	0	0	103	4	14	63	4	6
UK	4	4	80	20	60	15	0	32
USA	1	2	69	1	123	15	20	104
Total	5	27	471	55	289	180	37	149

I = Intensity outliers, S = Sequenom check, CR/H = Call Rate and Heterozygosity, G = Gender check, R = Relatedness check, PC = Hapmap Principal Component Analysis, A = Ancestry/Admixture analysis (includes UK outliers), O = Other exclusions - inconsistency with previous genotypes (25), UK only PCA analysis outliers (21), doubt over diagnosis (13), non-white and unaffected twins (90).

Table S8. Sample disposition by group.

PreFix	Collected	Passed DNA QC	Screening Attempted	Screening Successful	Analysed
ANZ	1,225	1,043	868	861	793
BEL	719	625	577	566	544
DEN	802	687	366	363	332
FIN	894	674	655	650	581
FRA	751	658	535	535	479
GEB	339	194	64	63	53
GEM	1,952	1,697	1,059	1,053	1,000
GEH	665	603	50	50	47
IRE	465	288	76	73	61
ITP	832	515	385	382	366
ITM	528	419	395	394	379
NOR	2,072	1,967	1040	1,030	953
POL	95	63	59	59	58
SPN	768	700	214	211	205
SWE[a]	1,812/665	729/602	777/630[c]	773/626	685/527
UKC	1,248	1,078	894	848	762
UKN	822	414	410	379	324
UKW	567	521	510	509	481
UKP	454	384	313	312	287
USB	1,274	1010	624	616	563
USC	541	489	419	417	382
UST[b]	225/247	133/115	133/107	130/104	102/0
USL	564	525	367	366	335
Total	20,526	16,133	11,527	11,370	10,299

[a] For the Swedish samples cases and controls are shown separately (cases/controls)

[b] For the twins the first number indicates the number of unrelated white affected individuals while the second number indicates the number of all additional individuals, i.e. affected and unaffected co-twins. Twin based analysis will be reported elsewhere and in this report only the unrelated white affected index twins were considered.

[c] These numbers include 251 samples (223 cases and 28 controls) that failed one or more aspects of DNA QC but had rich phenotypic data and were therefore included in preference to samples with less detailed phenotypic data that had passed QC. The results of analysis with respect to these detailed phenotypic data will be published elsewhere. In total 216 (86%) of these lower quality samples (192 cases and 24 controls) were ultimately included in the analysis presented here.

Table S9. Study specific breakdown of control exclusions

Study	S	I	CR/H	G	R	PC	A
Internal							
NBS	8	23	111	14	52	51	0
58C	1	32	163	11	19	57	0
External							
CAHRES	-	0	12	2	4	0	0
CHOP_1	-	11	133	25	45	34	16
CHOP_2	-	13	250	74	115	87	71
CHOP_3	-	0	178	0	79	109	56
EGEA	-	0	4	1	0	1	4
GAS	-	0	7	4	2	0	0
HealthMet2000	-	1	154	20	42	6	1
HYPHSR	-	4	20	15	10	0	5
KORA	-	7	16	1	3	0	1
MGGWAS	-	0	3	0	2	0	0
POPGEN	-	1	0	0	1	0	1
PROCARDIS	-	1	11	5	4	2	2
		38	788	147	307	239	157

S = Sequenom check, I = Intensity outliers, CR/H = Call Rate and Heterozygosity, G = Gender check, R = Relatedness check, PC = Hapmap Principal Component Analysis, A = Ancestry/Admixture analysis.

Table S10. Control Data sets

Study	Population	Illumina Chip	Samples - pre QC	Samples - post QC
Internal				
NBS	UK	1.2M	2737	2501
58C	UK	1.2M	2930	2674
External				
CAHRES	Sweden	550v3	764	746
CHOP_1	USA	555v1	991	746
CHOP_2	USA	561v3	3,024	2,464
CHOP_3	USA	610	2,554	2,160
EGEA	France	610	357	347
GAS	Germany	610	784	771
HealthMet2000	Finland	610v1	2,355	2,165
HYPERGENES	Italy	1M	619	571
KORA	Germany	550v3	486	463
MG_GWAS	Norway	550v3	125	121
POPGEN	Germany	550v3	468	465
PROCARDIS	Sweden	1M	678	655
Total		533,595*	18,872	16,849

* The number of SNPs common to all data sets.

SNP QC

In order to remove SNPs for which incorrect genotype calling could lead to differences in allele frequencies between collections we developed and applied two novel approaches. These new tools were used in conjunction with more standard filters on genotype summary statistics. Filters on SNP metrics were applied as shown in Table S11:

Table S11. SNP metric filters

	Minor allele frequency	Statistical Information	Call rate	Hardy-Weinberg p-value	Plate association p-value	Additional filters
Shared control data*	> 0.1%	>0.9	NA	$> 10^{-50}$	$> 10^{-50}$	Automated cluster checks
Internal MS data	> 0.1%	>0.9	NA	$> 10^{-50}$	$> 10^{-50}$	Automated cluster checks
External control data	> 0.1%	>0.975	>98%	$> 10^{-20}$	NA	Beta-binomial modelling

*These filters were applied separately to the 1958BC and UKBS control set. SNPs were removed if they failed to meet the above criteria in either group.

Most of these filters are based on metrics which are routinely used for GWAS QC. The plate association P-value is an n-degrees of freedom test looking for significant differences in allele frequency between the 96-well plates on which samples were genotyped. The statistical information filter is a measure which offsets the degree of uncertainty about the allele frequency of the SNP against how much would be expected if the SNP was genotyped perfectly (with the same expected allele frequency). See www.stats.ox.ac.uk/~marchini/software/gwas/snptest.html and [33] for more details. In practice this filter has the effect of requiring higher call rates for rarer SNPs (see for example [32]).

In total these measures reduced the number of available SNPs by 15% from 533,595 to 475,806. A further 94 SNPs were removed after visual inspection of their cluster plots.

Automated cluster checking

The first of the novel SNP QC approaches was applied to data generated by the genotyping funded as part of the WTCCC2: the two shared control groups and the samples (largely cases) collected for the MS study. Each of these three collections went through the WTSI genotyping and calling pipeline as separate experimental batches. As a result, slight differences in genotyping performance or sporadic errors of the clustering algorithm can give rise to incorrect genotype calls, which can in turn lead to false positive signals of association.

Errors of this kind often become clear when the raw intensities (from which the genotypes are called) are plotted and coloured by the inferred genotypes (so-called cluster plots), with individuals in the same location in 2-dimensional space being called differentially across batches or collections. In the large majority of cases these errors can be detected using standard metrics, as one or more batches will either have a decreased call rate or deviate strongly from Hardy-Weinberg equilibrium. However, this is not always the case and problematic SNPs can be missed. In order to further protect against differential calling

between batches, we implemented an automated approach that checks that the positions of the inferred genotype clusters are consistent.

The approach is applied at each SNP as follows, assuming there are three batches:

- For each batch fit a bi-variate normal distribution to each of the genotype clusters using the calls provided. We now have three sets of fitted clusters, one for each batch.
- Recall the genotypes in each batch using the clusters fitted both to the batch from which the clusters were inferred and from the two other batches.
- For each cluster there are now four sets of calls:
  - The original calls
  - The calls obtained by fitting clusters to the same batch
  - The calls obtained by using the clusters fitted to each of the other two batches.
- For each batch do a chi-squared test for an allele frequency difference between the original calls and the 3 sets of calls obtained by fitting the inferred cluster.
- Exclude SNPs where any of the nine p-values is $< 10^{-10}$.

The consequence of applying the above procedure is to remove SNPs where either the clusters are not well described by refitting a bi-variate normal distribution, or where the difference in the position or size of the clusters between batches is sufficient to significantly change the estimated allele frequency.

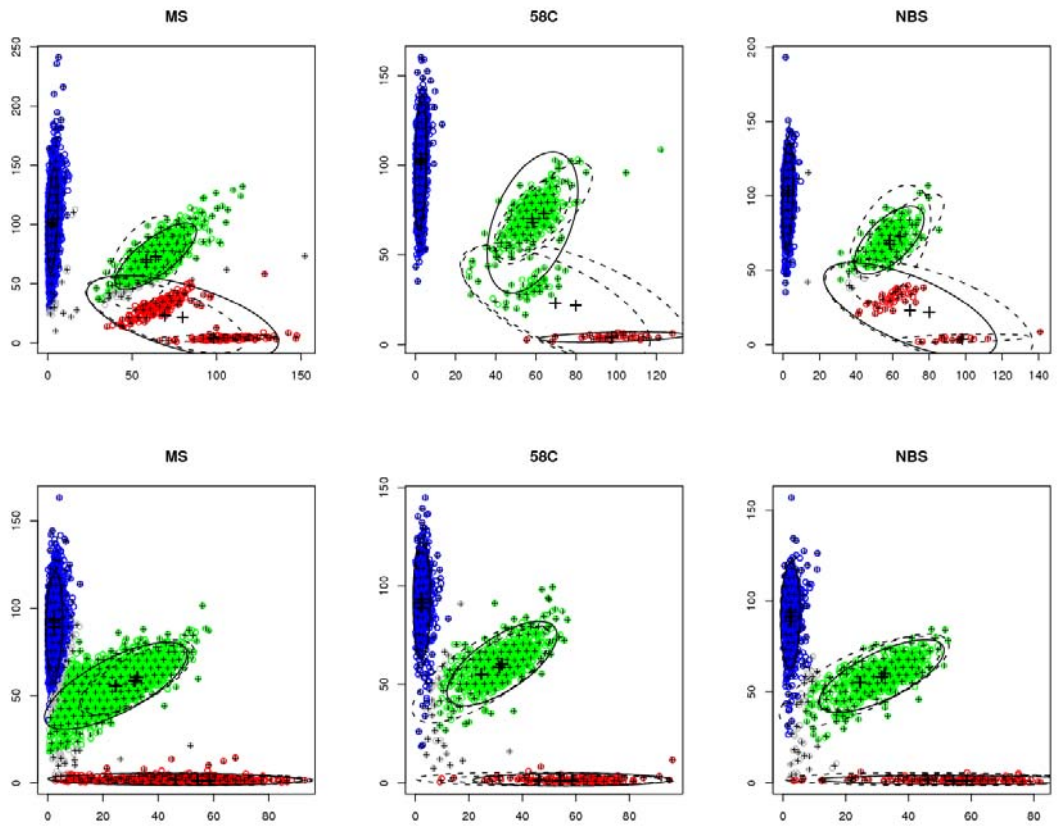

Figure S11. Cluster plots at two SNPs removed by the automated checking. Each individual is represented by a point plotting the intensity of the probes targeting the two alleles at each SNP, and coloured by the inferred genotypes. Superimposed on the plots are cluster positions inferred from the calls in that batch (solid black lines) and from the other two batches (dotted black lines).

Two examples of SNPs which failed the automated cluster plot check are shown above in Figure S11. In the first example the calling algorithm has labelled an outlying cluster as being

heterozygote (green) in the 58C collection and homozygote (red) in the MS and NBS collections. When the cluster positions of these two collections are applied to the 58C data, these individuals will get reassigned new genotypes and will generate a significant difference in allele frequency with respect to the original call. The second example above illustrates the sensitivity of the check to subtle differences between the collections in the position of the clusters. In the MS collection the increased sample size and experimental noise expands the scope of the heterozygote cluster into space in which individuals are called homozygotes (blue) in the other two collections. Both examples lead to differences in allele frequencies between cases and controls and are not identified by simple summaries of the genotype data.

Beta-binomial model

In an attempt to identify SNPs with potentially misspecified genotypes in one or more of our control datasets, we compared observed allele frequencies across datasets with that expected under a simple population genetic model. Following the approach suggested by Balding and Nichols[34] we assumed that the populations represented by our control datasets are all related to a single ancestral population via a star-shaped phylogeny. At each SNP, we assume that the frequency of a particular allele in a dataset follows a beta distribution with mean representing the allele frequency of the ancestral population common to all datasets and variance proportional to the level of "drift" in that dataset. We then assume that a dataset's observed genotype counts at a SNP follow a binomial distribution with the mean equal to this ancestral allele frequency. The level of "drift" in a dataset is estimated using joint information across all SNPs (see Figure S12), and SNPs for which any dataset does not follow this beta-binomial model are flagged as "errors". We used a Markov Chain Monte Carlo (MCMC) procedure (somewhat analogous to that in [35]) to estimate drift, ancestral allele frequencies at each SNP, and the probability that each SNP is an "error", using genotype counts from each of the external datasets, 58BC and NBS datasets to define separate "populations." SNPs were flagged if the posterior probability of being an "error" was ≥ 0.1 in any population, resulting in 36,424 SNP exclusions across all chromosomes. Examples of excluded SNPs are shown in Figure S13 and Figure S14.

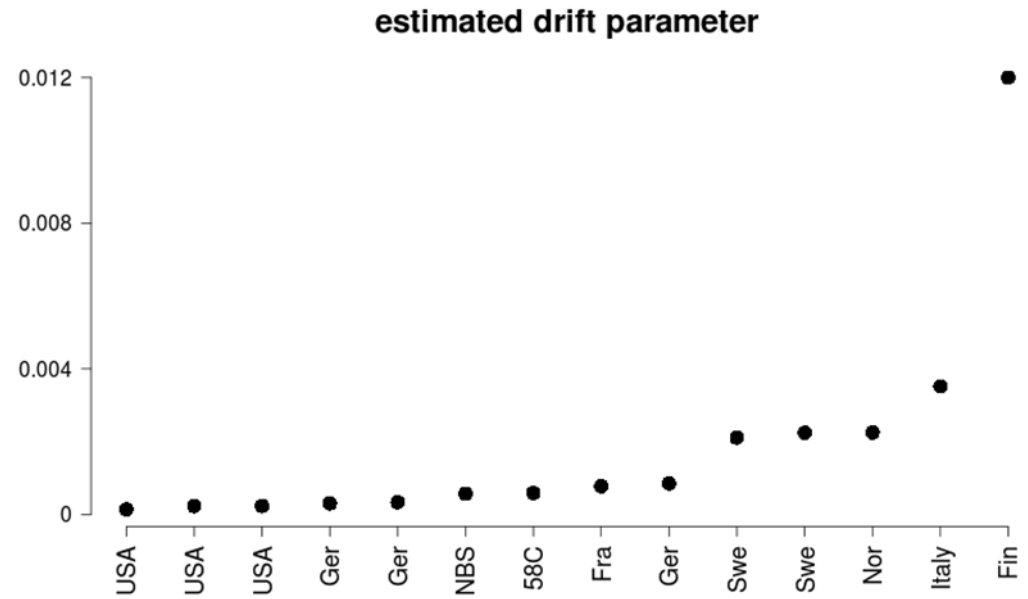

Figure S12. Estimated deviations ("drift") from average allele frequencies across all SNPs in the different control datasets. From left to right, these datasets are (corresponding to the labels in Table S9): CHOP_3, CHOP_2, CHOP_1, KORA, GAS, NBS, 58C, EGEA, POPGEN, PROCARDIS, CAHRES, MGGWAS, HYPHSR, and HealthMet2000. As average allele frequency estimates at each SNP are based on sample allele frequencies, they are heavily

influenced by sample size; hence the estimated drift for USA samples (for which we have many samples relative to the other datasets) are low. As expected, however, estimated drift increases in the northern and southern European populations relative to the central European populations.

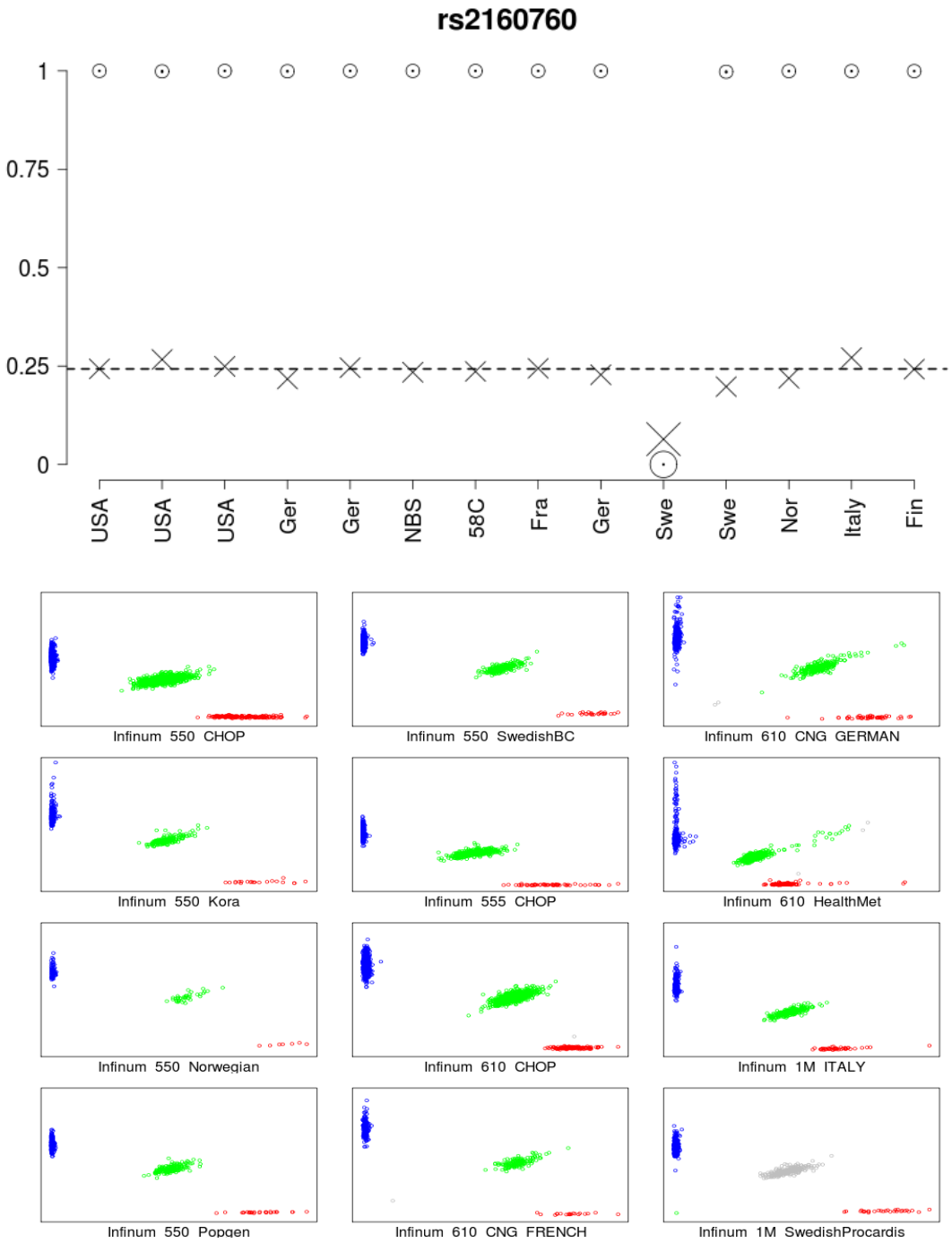

Figure S13. (top) Example of SNP rs2160760, depicting the probability that the SNP is a "non-error" (open circles, with 95% credible intervals in horizontal lines through the circle) and the sample allele frequency (crosses) for each population. The dashed line gives the estimated ancestral allele frequency under the model. Here, the first Swedish population corresponding to the Infinum_1M_SwedishProcardis dataset, has an outlying sample allele frequency and is flagged by the model as an "error". (bottom) Visual inspection of the intensity cluster plots at this SNP suggests that this dataset has questionable calls, as all SNPs that appear to be heterozygous (grey cloud) were classified as missing.

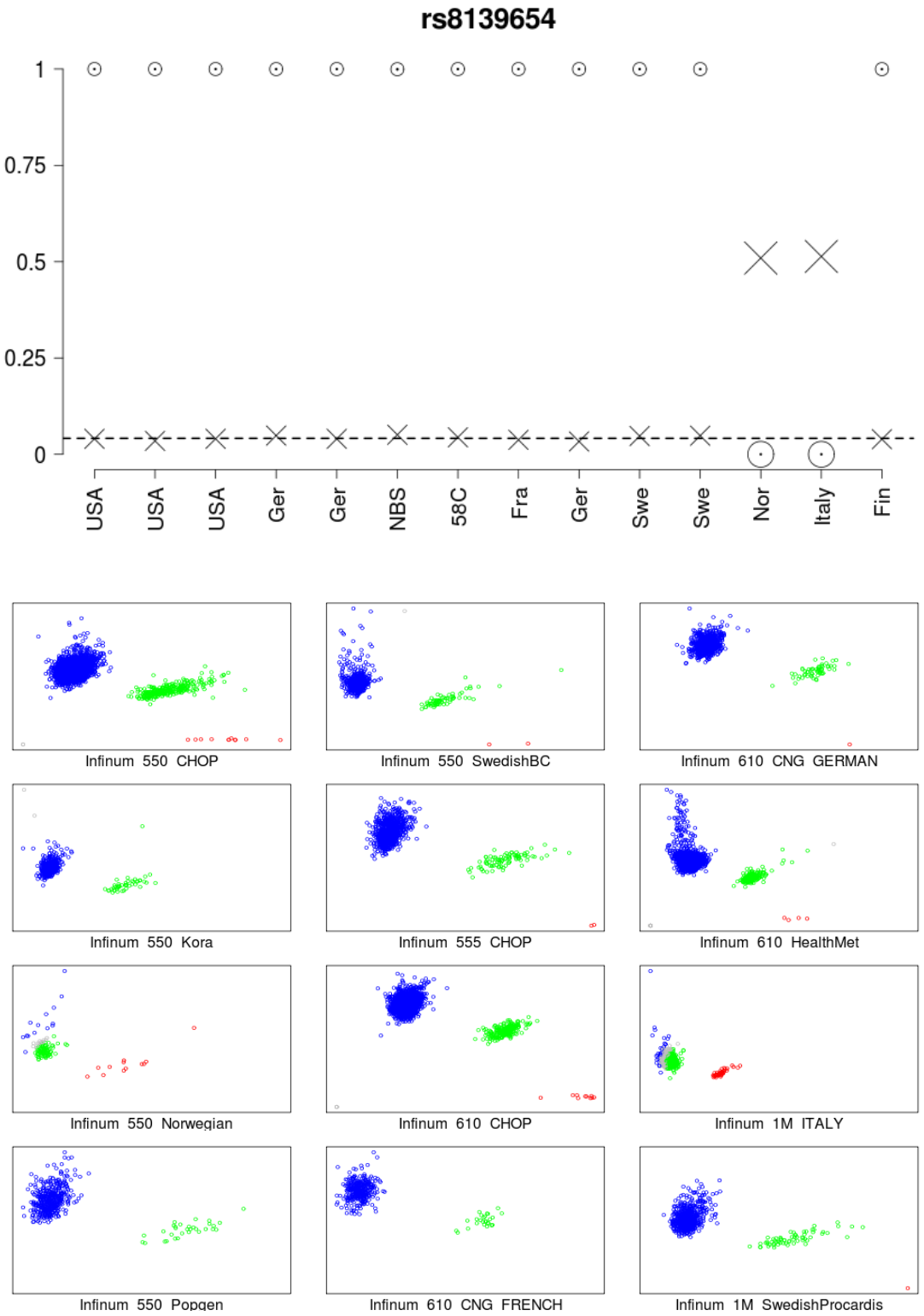

Figure S14. (top) Example of SNP rs8139654 (see legend above). Here the Norwegian and Italian populations, corresponding to the Infinum_550_Norwegian and Infinum_1M_ITALY datasets respectively, have outlying sample allele frequencies and are flagged by the model as "errors". (bottom) Visual inspection of the intensity cluster plots at this SNP suggests that these two datasets have questionable calls relative to the other datasets.

Results

Controlling for population structure

Acknowledging that it is probably impossible to completely eliminate stratification artefacts while still maintaining adequate power, we tried several approaches to cope with this issue and used estimates of λ, the genomic inflation factor,[36,37] as the primary quantity for judging the extent to which the confounding effects of structure had been removed. This parameter is the ratio between the median observed test statistic and the median expected under the null. The parameter thus estimates the factor by which test statistics are inflated in the majority of SNPs.[38] Two main reasons for an elevated λ are population structure between cases and controls and the polygenic architecture of the phenotype under which very many of the tested SNPs are truly associated but each only exerts a very modest individual effect.[39,40] In line with our previous observations[22] we saw little evidence for inflation when analysis was restricted to the UK alone. However, substantial inflation was apparent when the rest of the data were included in the analysis (see Figure S15). Since, on the one hand, there are obvious sources for spurious population structure effects in our non-UK part of the data set and, on the other hand, we have previously observed evidence for polygenic architecture underlying susceptibility to multiple sclerosis[41], it is likely that the observed genomic inflation reflects both of these components. But we are not able to convincingly separate these two sources of inflation from each other by any statistical approach. In Figure S15 and the rest of this section where SNPTESTv2 (www.stats.ox.ac.uk/~marchini/software/gwas/snptest.html) was used, we tested each SNP for association using the frequentist model which is additive for log-odds, incorporating uncertainty in individuals' genotype calls and using a score test to calculate p-values.

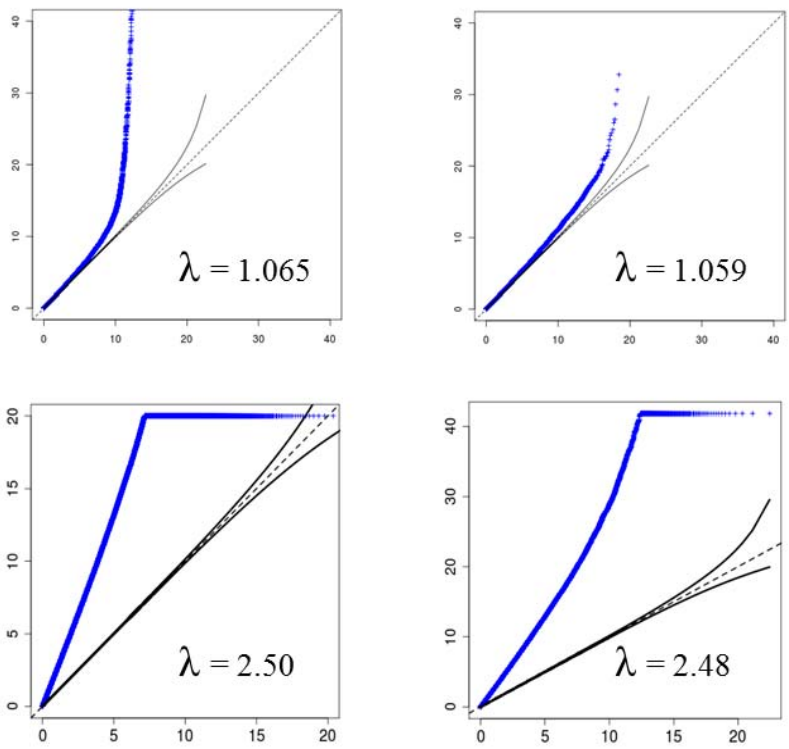

Figure S15. Q-Q plots without any correction for structure. Plots based on the UK data alone are shown on the top row and those based on the frequentist fixed effect meta-analysis of UK and non-UK data sets are shown on the bottom row. In each row the plot for the whole genome is shown on the left and that obtained after excluding the MHC is shown on the right.

Each panel shows the expected distribution under the null (thin black dotted line) and its 95% confidence limits (thin black solid lines). Each panel also shows the observed results for that analysis (blue dots) and the corresponding genomic inflation factor, λ. Note the x-axis scale is twice as long in the panels on the top row.

Principal Components As Covariates

In one attempt to address population stratification in our dataset, we performed a principal components analysis (PCA) based solely on the data from the samples we had genotyped ourselves, the "internal data," i.e. the data from the cases, the specific Swedish controls and the 58BC and NBS cohorts. This PCA was performed using the SHELLFISH program and was based on a subset of SNPs (n=205,688) selected to have minimal inter-SNP LD, as described above. We then projected each of the remaining samples (the "external data" - the data from the control samples generated at other sites as part of other experiments) onto the top 100 of these principal components. Visual inspection indicated that the first seven principal components were capturing genome-wide structure (ancestry) in the genotypes, while subsequent components were dominated by local genome effects (LD). In view of these findings we used the first seven principal components as covariates in the analysis of the non-UK data and repeated the analysis using SNPTESTv2. The results from this first pass attempt to correct for structure using principal components are shown in Figure S16. We also analyzed each case population individually against all controls, and stepwise removed case populations with the highest λ in these individual analyses. However, λ was reduced only modestly when the more outlying case populations (Finland, Poland and Ireland) were excluded and could not be reduced below 1.11 even when less extreme populations such as Italy, the USA, Germany and Sweden were excluded.

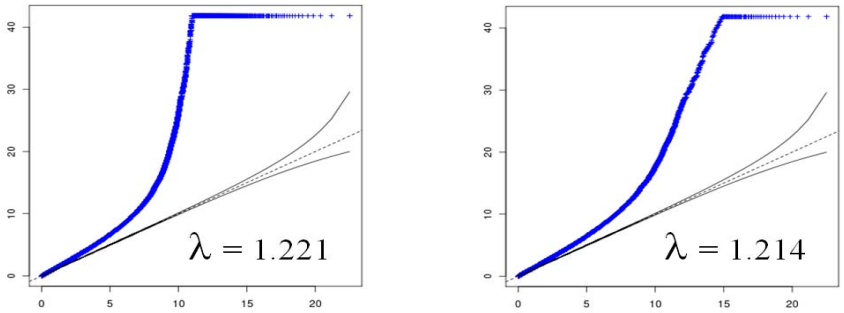

Figure S16. Q-Q plots demonstrating the impact of PCA correction on the frequentist fixed effect meta-analysis of UK and non-UK data sets. The plot for the whole genome is shown on the left and that obtained after excluding the MHC is shown on the right. In each panel the expected distribution under the null (thin black dotted line) and its 95% confidence limits (thin black solid lines). Each panel also shows the observed results for that analysis (blue dots) and the corresponding genomic inflation factor, λ.

Clustering into Subgroups Based on Ancestry

A second technique we implemented to control for structure was to cluster case and control subjects into subgroups, with the property that within a subgroup cases and controls are well-matched for ancestry. More specifically, for each subject we used a beta-binomial model to estimate the proportion of SNPs from that individual that were ancestrally related to each of the 10 HapMap Phase 3 populations[42] (using the same subset of LD-free SNPs as were used for PCA). We then applied a Markov Chain Monte Carlo (MCMC) clustering algorithm similar to that employed in STRUCTURE version 1[43] to cluster individuals into a fixed number of subgroups K based on similarities among their vectors of HapMap copying proportions. We then tested for association in each sub-group separately using SNPTESTv2. We then combined scores across the K subgroups using a fixed effects meta-analysis approach that weighted each subgroup's log-odds estimate by the inverse of its estimated variance. Plots of the results are given below (Figure S17) for K=7, where individuals were assigned to clusters based on their posterior probabilities of cluster membership after running the MCMC for 20,000 iterations. The genomic inflation factor λ within each of our seven clusters in this example ranged from 1.13 to 1.65, and λ resulting from a fixed-effect meta-analysis across clusters was 1.44.

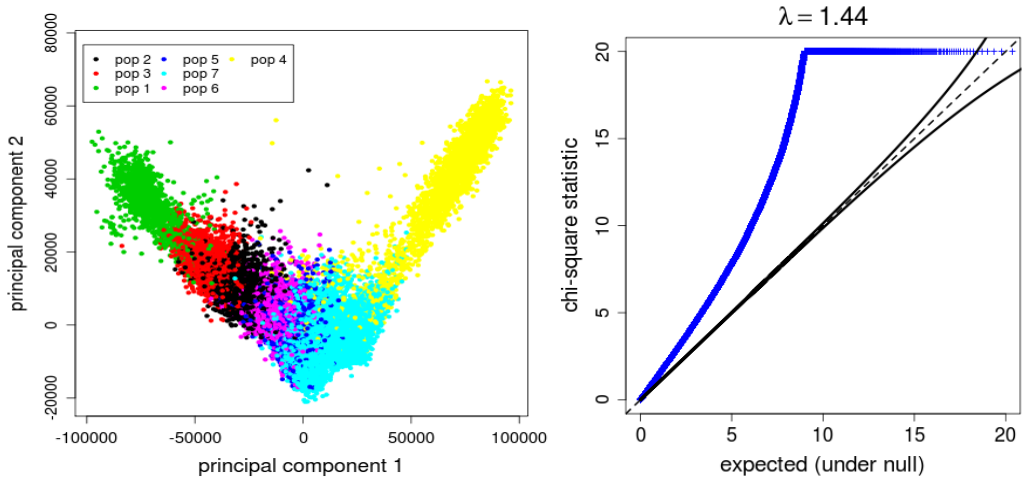

Figure S17. (left) All post-QC samples projected onto the first two components of a PCA applied to the internal samples, color-coded by which population they have been clustered into using the method described above. (right) Despite this apparently sensible clustering, the resulting meta-analysis Q-Q plot gives an over-inflated lambda of 1.44.

Linear Mixed Model

Our third approach was to use a linear mixed model that explicitly accounts for correlations in individuals' phenotypes due to their relatedness. One major advantage of this approach is that it accounts for structure due to relatedness on multiple time scales, from close relatives to distant ancestral structure. We generated a covariance matrix R by calculating for every pair of individuals the genome-wide averaged correlation among their genotypes. This corresponds to a method of moments estimate of the proportion of genome related identical-by-descent between two individuals sampled from the population.[44] Linear mixed models that incorporate this type of measure of relatedness in a GWAS setting have been used before.[44-49] In this study we use a novel implementation described below.

Let Y denote case/control status across n individuals, X be an n by k matrix with columns containing individuals' information across k covariates, and β a vector containing the coefficients corresponding to the k covariates. As in standard linear regression, we assume

$$Y = X\beta + \varepsilon$$

but in contrast to standard linear regression, we incorporate the estimated relatedness among individuals as a component of the phenotypic variance:

$$E(\varepsilon) = 0 \quad \text{and} \quad Var(\varepsilon) = h\sigma^2 R + (1-h)\sigma^2 I$$

Here R is a symmetric n by n matrix with each entry the relatedness estimate for a pair of individuals, σ^2 is the remaining phenotypic variance after accounting for the covariate effects, h is the proportion of this variance explained by R, and I is the identity matrix. In basic scans without extra covariates, for each SNP, X is an n by 2 matrix with the first column consisting of 1s and the second column consisting of each individual's genotype (determined as the expected genotype given by the genotype calling method). Since our phenotype is binary, the linear model corresponds to an additive model on the probability scale. We have verified that the use of a standard linear model for our case-control ratios and effects sizes in non-MHC SNPs (OR<1.3) gives an excellent approximation to the additive model on log-odds scale. We have also established a transformation of the parameter estimates and standard errors from the linear model to the log-odds scale using a Taylor series approximation. The reason for applying a linear mixed-model, rather than generalized linear mixed-model, to case-control data set is computational. Assuming normally distributed errors we use a conditional maximization procedure to find the maximum likelihood estimates (MLEs) of σ^2, h, and β under this full model and to find the MLEs of σ^2 and h under a null model where β is fixed to 0. This allows us to implement the likelihood-ratio test for SNP effects. In contrast to several previously published implementations of linear mixed models for large GWAS data sets,[46,48,49] we maximise both of the variance parameters at each SNP. This is expected to lead to a gain of statistical power[49] although this gain is typically small because the variance parameters do not vary much across SNPs when the effect sizes of individual SNPs are small. The computation is challenging when the covariance matrix R is large, and for this reason we applied the linear mixed model to the "UK cohort" (7,029 individuals) and "non-UK cohort" (20,119 individuals) separately and then combined scores using a fixed-effect meta-analysis as described below. The matrix R for the "UK cohort" was estimated using 199,761 SNPs and the matrix R for the "non-UK cohort" was estimated using 191,166 SNPs. Q-Q plots obtained using this method are shown in Figure S18. This gave λ values suggesting that the overall genome-wide structure is well accounted for under this approach. We note that in addition to the population structure effects, the linear mixed model also accounts for the possible polygenic component of the genetic susceptibility to MS. This may lead to a slight loss of power to see associations at those loci which have been used in computing the R matrix. On the other hand, by including the polygenic component in the model we are explaining some of

the small effects of SNPs genome-wide and this ability to more accurately model the phenotype may also gain us power to see individual associations at some of the SNPs.

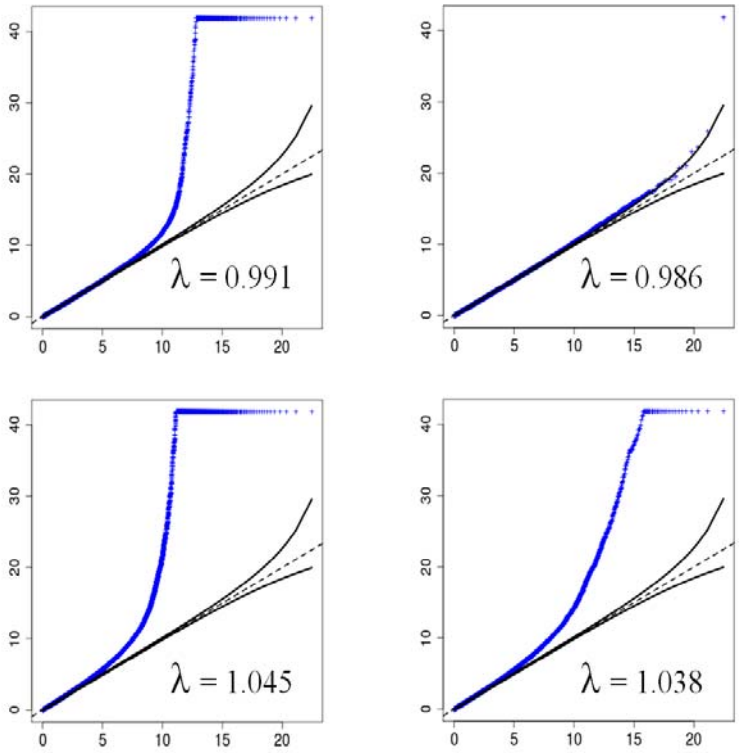

Figure S18. Q-Q plots using linear mixed model. Plots are equivalent to those shown in Figure S16 but using the linear mixed model. Top row UK alone, bottom row fixed effects meta-analysis of UK and non-UK data, left hand including the MHC and right hand excluding the MHC.

Validation of the Linear Mixed Model Approach

Even though the overall genome-wide distribution of the test statistic in the linear mixed model scan is well controlled for population structure as measured by λ, there could still exist some SNPs that are highly differentiated between European populations and that could produce spurious association signals. To investigate this we considered the impact of including the seven primary PCs as covariates in the linear mixed model scan. Figure S19 shows that the results of the linear mixed model at our 102 lead SNPs in the non-UK data set are not affected by adding seven PCs as covariates in the linear mixed model, but that the results between logistic regression with seven PCs and the linear mixed model (without PCs) are different. These results are in accordance with the genomic-inflation factors (λ=1.015 for linear mixed model in non-UK and λ=1.22 for logistic regression with 7 PCs in non-UK) and suggest that for our lead SNPs the structure captured by the leading PCs is well accounted for by the linear mixed model, but not vice-versa. We only considered the non-UK data set here because in the UK data the effects of the structure corrections are very modest.

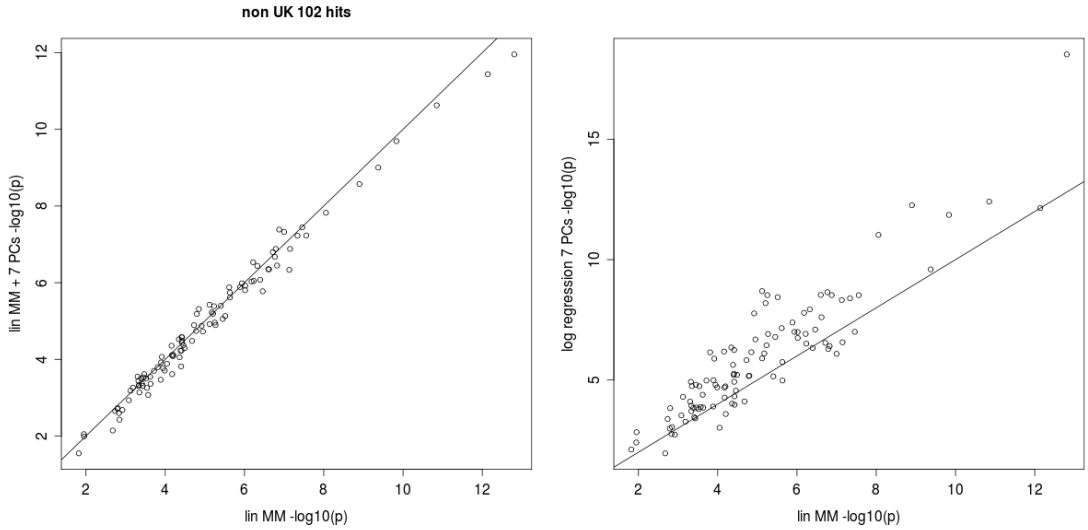

Figure S19. Left panel shows $-\log_{10}(p)$ for the 102 lead SNPs in the non-UK data set calculated using the linear mixed model (MM) with and without the seven primary principal components (PC) as covariates. The y-axis on the right hand panel shows the same data analysed using a logistic model with seven PCs as covariates.

Because matrix decompositions were by far the most demanding part of the computations, we were not able to perform SNP-wise exclusions of individuals according to the SNP-specific quality of the genotype data. Our approach was to use the expected allele counts from the genotype calling algorithm for those individuals whose probability of the NULL class was below 0.90, and to set the remaining genotypes to the average genotype of the population. Table S12 lists quality statistics for the 102 SNPs that we took to replication, and shows that the calls were of excellent quality with negligible amount of uncertainty. Our inability to take the genotyping uncertainty into account does not have any practical consequences at these SNPs.

Table S12. Quality statistics in our 27,148 discovery samples (UK and non-UK together) at the 102 SNPs taken to replication.

	min	**1st quartile**	**median**	**3rd quartile**	**max**
Avg call prob	0.9992	0.9997	0.9998	0.9999	1.0
Avg NULL prob	4.0E-06	1.0E-04	1.8E-04	2.8E-04	7.8E-04
NULL>0.90	0	1	2	4	15
MAF	0.049	0.230	0.284	0.384	0.493

Rows: (1) Average genotype calling probability. (2) Average probability of NULL class (i.e. 1-calling probabilities of the three genotypes). (3) Number of individuals whose NULL class probability is > 0.90. These individuals were set to have population average genotype. (4) MAF = Minor allele frequency in the whole sample.

All reported p-values and effect size estimates for the non-MHC SNPs in the main paper and, unless otherwise stated, also in this supplementary material were calculated using the linear mixed model approach.

Summary of approaches for protecting against population structure

While we acknowledge that completely accounting for any structural bias induced by our sampling protocol is a challenging problem, we have implemented several means of minimising or evaluating the extent to which population stratification is influencing our results. These include:

- using a linear mixed model (with and without including the top principal components as covariates) to account for correlations in individuals' phenotypes that can be explained by their level of genome-wide relatedness

- using a beta-binomial model to test if population allele frequencies differ among control datasets according to frequencies expected under a simple population genetics model

- for each SNP showing strong evidence of association, calculating the proportion of non-QC SNPs genome-wide that have an "allele variability" score greater than that of the lead SNP, where the "allele variability" score is a Pearson's chi-squared statistic testing for allele frequency differences among all control datasets (13 degrees of freedom) and case datasets (14 degrees of freedom); these empirical quantiles are provided in the Supplementary Data

- investigating whether associated SNPs tag known differentiated SNPs from the 1000 Genomes project (see section on 1000 Genomes analysis below)

- assessing population heterogeneity in the effect size estimates (see section on population homogeneity below)

A possible consequence of applying these criteria is to exclude regions of the genome that may harbour variation which influences MS susceptibility.

Meta Analysis

In all our scans where several data sets were analysed separately, we combined the results using a fixed-effects meta-analysis. All of these meta-analyses were performed by combining parameter estimates weighted by the inverses of their estimated variances. The combined parameter estimate (b) and its standard error(s) were calculated according to the following formulae

$$b = s^2\left(\sum_i \frac{b_i}{s_i^2}\right) \qquad\qquad s = \sqrt{1\Big/\left(\sum_i \frac{1}{s_i^2}\right)}$$

where b_i and s_i are the parameter estimates and standard errors of the individual studies. We found that the p-values obtained using this approach were highly correlated (see Figure S20) with those obtained from weighted z-scores $z = \sum_i w_i z_i$, where weights $w_i = \sqrt{\left(n_i \big/ N\right)}$ are determined by the effective sample sizes n_i and $N = \sum_i n_i$.

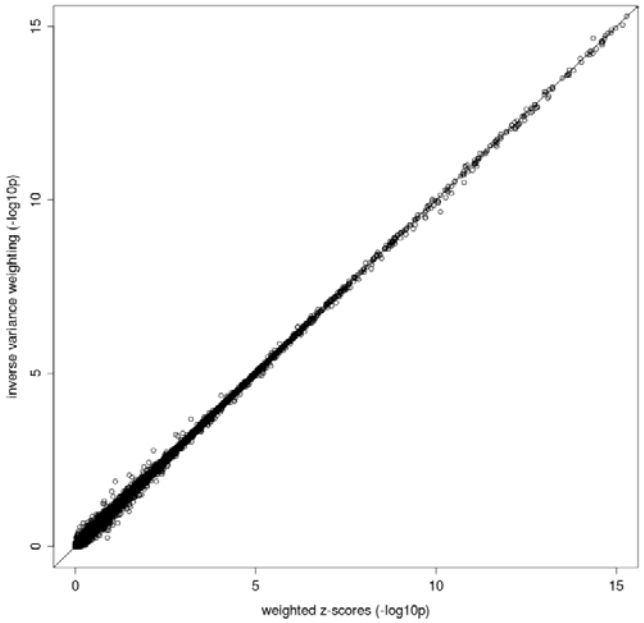

Figure S20. UK and non-UK susceptibility meta-analysis p-values obtained by combining parameter estimates weighted by their inverse-variance (y-axis) compared with those obtained by combining weighted z-scores (x-axis).

Combined Bayes factors under the fixed-effects model were calculated using the approximate Bayes factor.[50] These can be found in Supplementary Data.

Meta-analysis in the non-UK data set using sub-populations

In attempting to correct for stratification we also tested the approach of simply dividing the non-UK data into the seven population specific groups where we had population appropriate controls (Table S10). We ran a logistic regression with seven PCs as covariates separately for each of these populations and combined the results using fixed-effects meta-analysis.

Genomic inflation factors (λ) for each country are shown in Table S13 for the meta-analysis λ=1.114 and when Finland was excluded from the meta-analysis, λ=1.077. 17 out of 23 previously established associations with MS had lower p-values in the linear mixed model scan than in the population-based meta-analysis when genomic control was applied to make inflation factors equal in both methods (see Figure S21). Both methods used the same set of controls but the linear mixed model made use of 1,993 additional cases, which were not collected from any of these seven countries.

Table S13. Non-UK countries included in the subpopulation meta-analysis.

	Finland	**France**	**Germany**	**Italy**	**Norway**	**Sweden**	**USA**
Cases	581	479	1100	745	953	685	1382
Controls	2165	347	1699	571	121	1928	5370
λ	1.228	1.045	1.049	1.028	1.088	1.018	1.033

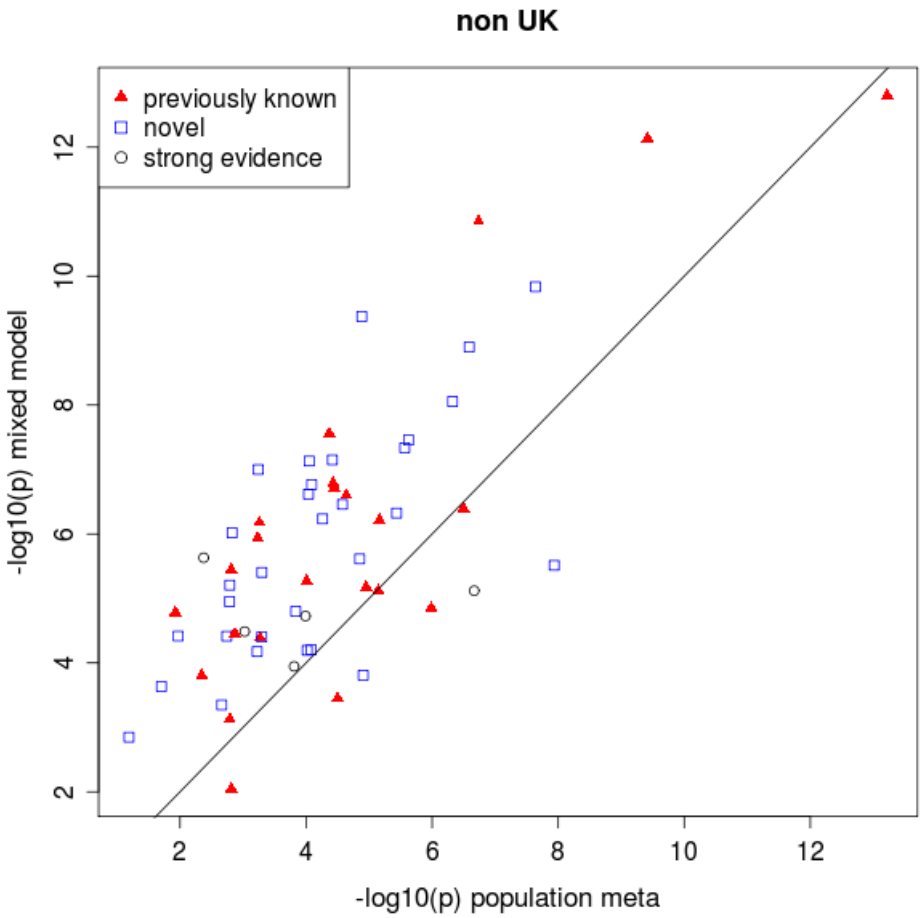

Figure S21. P-values ($-\log_{10}$ transformed) from meta-analysis using seven non-UK populations (x-axis) against p-values from linear mixed model on all non-UK data (y-axis). Values on the x-axis have been corrected to have the same inflation factor (1.015) that is present in linear mixed model results. 23 previously known SNPs for MS susceptibility are marked by red triangles, 31 novel SNPs are marked by blue squares and five SNPs with strong evidence are marked with black circles.

Evidence at Previously Suggested Loci

Table S14 gives the p-value of our highest scoring SNP in the previously identified regions listed in Table S5, as well as its correlation with the previously identified SNP.

Table S14. Outcome for previously identified or strongly suspected loci

Original	New	r^2	D'	Gene	$-\log_{10}$(p)
rs6897932_C	rs6897932_C	1.00	1.00	*IL7Rα*	5.6
rs2104286_T	rs3118470_G	0.13	1.00	*IL2Rα*	8.7
rs12708716_A	rs7200786_A	0.48	1.00	*CLEC16A*	13.2
rs2300747_A	rs1335532_A	0.87	1.00	*CD58*	8.7
rs12122721_G	rs7522462_G	0.79	0.96	*KIF21B*	6.0
rs1132200_C	rs2293370_G	0.63	0.90	*TMEM39A*	9.0
rs10735781_G	rs11810217_A	0.57	1.00	*EVI5*	11.2
rs2587156_G	rs1520333_G	0.02	0.00	*IL7*	6.2
rs34536443_G	rs8112449_G	-	-	*TYK2*	5.8
rs3748816_T	rs4648356_C	0.93	1.00	*MMEL1*	13.5
rs9523762_A	rs9523762_A	1.00	1.00	***GPC5***	0.02
rs1800693_G	rs1800693_G	1.00	1.00	*TNFRSF1A*	9.7
rs17445836_G	rs13333054_A	0.10	1.00	*IRF8*	7.2
rs17824933_G	rs650258_G	0.04	0.47	*CD6*	8.8
rs744166_G	rs9891119_C	0.65	1.00	*STAT3*	6.3
rs1790100_G	rs949143_G	0.47	0.94	***MPHOSPH9***	3.8
rs4680534_C	rs2243123_G	0.11	0.28	*IL12A*	5.4
rs2760524_G	rs1323292_A	0.86	1.00	*RGS1*	6.1
rs6896969_C	rs4613763_G	0.14	1.00	*PTGER4*	13.2
rs882300_C	rs7371043_A	0.03	0.58	***CXCR4***	0.8
rs1250540_G	rs1250550_A	0.45	0.74	*ZMIZ1*	5.9
rs9321619_A	rs13192841_A	0.02	0.60	*OLIG3*	6.2
rs703842_A	rs12368653_A	0.44	1.00	*CYP27B1*	6.7
rs6074022_G	rs2425752_A	0.70	0.86	*CD40*	5.8
rs9657904_A	rs2028597_G	0.23	1.00	***CBLB***	3.7
rs763361_A	rs763361_A	1.00	1.00	***CD226***	0.8

Original = the SNP and risk allele previously identified as listed in Table S5. New = the most strongly associated SNP and risk allele in the current study at the previously identified locus. Linkage disequilibrium between these two markers is shown in terms of r^2 and D'. Gene = the nearest gene to the originally identified SNP (it is not necessarily established that this is the relevant gene). $-\log_{10}$(p-value) for the most strongly associated marker in our new GWAS from the region encompassing the original signal. Genes in bold were not identified in the new data at the cut-off used for inclusion in the replication phase.

As anticipated, for most of these loci HapMap data showed positive LD between the original risk allele and the most significantly associated risk allele from the same region identified in our new study. In some areas the interpretation was less straightforward:
1) TYK2 region. Since the original SNP implicating TYK2 (rs34536443) was identified in a screen of non-synonymous SNPs[3] and this SNP was not included on the Illumina Human660-Quad chip or on HapMap it was not possible to directly calculate LD between this SNP and the association seen with rs8112449. However, these SNPs are only 60kb apart and both lie within the same LD block making it likely that these are the same rather than independent associations.
2) IL7 region. The new screen does not include any good proxies for the original SNP (rs2587156) from the IL7 region[51] suggesting that this signal is likely to be independent of that we have identified in this new study.
3) CXCR4 region. The Illumina Human660-Quad chip SNPs from this region that were in LD with the original SNP implicating CXCR4 (rs882300)[5] all failed QC in our new study. As a result we had no power to detect the presence or absence of this association. This suggests that our failure to observe association in the region of CXCR4 is possibly a false negative.
4) GPC5 and CD226 regions. In both cases several SNPs in strong LD with the originally implicated SNPs were successfully typed in this new screen but we saw no evidence for association in this screen in either region.

Only *CXCR4*, *GPC5* and *CD226* failed to show nominally significant evidence for association in the new study (*CXCR4* had little power). In considering the concordance between these new results and the previously established/suggested loci, it should be noted that since most of the previous multiple sclerosis GWAS used the WTCCC1 controls as part of their screen and many of the samples used in the replication and follow up studies identifying these 26 loci are now included in this screen, these studies are not fully independent.

In addition to our top-scoring SNP in each previously reported region, we report in the Supplementary Data the score at the SNP in our dataset that had the highest correlation coefficient with the previously reported SNP, according to the phased HapMap Phase 2 CEPH haplotypes (if more than one SNP had the same highest correlation with the previously reported SNP, we report the SNP with the lowest p-value in our data). Scores are given for these SNPs both with and without the WTCCC1 controls included in the analysis.

Analysis of signals of association

Independent signals

To identify association signals we used an iterative process in which we ranked all non-MHC autosomal SNPs on the basis of the p-value from linear mixed model scan, and then directly inspected the cluster plot for the most associated SNP. If the clustering was considered to be suspect, this SNP was ignored and the cluster plot for the next most associated was inspected. Once a SNP with satisfactory clustering was identified, we declared this the lead SNP for the region and excluded all SNPs within 1Mb of this SNP. The process was then repeated for each successive SNP until we had no SNPs with $-\log_{10}(p) > 4.5$. This identified a total of 85 regions each characterised by a lead SNP with $-\log_{10}(p) > 4.5$ and satisfactory clustering. To identify potentially independent associations within the 2Mb interval containing each of the lead SNPs, we repeated the analysis for all SNPs in each interval after conditioning on the corresponding lead SNP. In those intervals with at least one SNP with a conditional $-\log_{10}(p) > 4.0$, we ranked the SNPs on the basis of the conditional p-values and inspected the cluster plot for the most associated SNP. If the cluster plot was satisfactory, the SNP was defined as a secondary lead SNP. If the clustering was suspect, then that SNP was ignored and the cluster plots for next most associated SNP was inspected. This process was repeated until a SNP with adequate cluster plots and $-\log_{10}(p) > 4.0$ was identified, or there were no further SNPs with p-values exceeding this threshold. Through this process we identified secondary signals in 16

regions. The SNPs in these 16 intervals were then re-analysed after conditioning on both the original lead and secondary lead SNPs, and in one region a third association was identified (with reliable cluster plots and $-\log_{10}(p) > 4.0$). We thereby identified 102 SNPs that were taken to replication. Association plots illustrating each signal are available on line (see below) and the details of each SNP are available in Supplementary Data

In ten of 16 regions containing a secondary SNP, we deemed the secondary SNPs as being independent from the lead SNP according to the following criteria:

- The association regions (defined below) for the secondary SNP and the lead SNP did not substantially overlap.
- The p-value and effect size estimates of the secondary SNP did not vary substantially between the original unconditioned scan and after conditioning on the lead SNP.
- The r^2 between the lead and secondary SNPs was <0.01.

In three regions the secondary SNP in the region showed a substantial increase in association signal after conditioning on the lead SNP (see "Haplotype Analysis" below for details of these regions). As a result we identified 95 independent regions of association with five containing an additional secondary signal and one containing two secondary signals (95 + 1 x 5 + 2 x 1 = 102).

Defining association regions

For each of the 102 SNPs chosen for replication, each SNP with a combined p-value < 1E-03 in the discovery cohort (used in the pathway analysis described below), we defined an association region to be an interval of 0.25cM centred on the SNP using the HapMap phase II recombination map[52]. We defined the flanking region to be the association region plus a margin of 25kb at either end. For each SNP we then identified a list of proximal genes, defined as those having at least one transcript intersecting the flanking region, and noted the nearest gene to the SNP among the list of proximal genes. Gene transcripts were identified using the `refGene.txt` file available from UCSC Genome Bioinformatics.[53]

Regional association plots

Based on the analysis of our GWAS data we generated a regional association plot for each of the 102 lead SNPs, available at http://www.well.ox.ac.uk/wtccc2/ms. In each plot there are six panels. The two panels on the left depict the association region surrounding the lead SNP listed in the plot title, plus 100kb to the left and right of the association region boundaries. The top left plot shows the -log10(p-value) for all SNPs within this interval, with the SNPs' positions in megabases given on the x-axis. SNPs are coloured by their squared correlation coefficient (estimated from the 58C control genotypes) with the lead SNP according to the legend in the top left corner; SNPs represented with a black dot have $r^2 < 0.01$. The bottom left plot gives the recombination rate in the region in cM/Mb and lists all genes found in the region, with horizontal solid red lines indicating the start and end of the gene and arrows denoting the direction of transcription. Vertical red dotted lines denote the boundaries of the LD region, and the horizontal and vertical black dotted lines intersect at the location of the lead SNP. On the right, allele intensity cluster plots for the lead SNP are shown for each of the MS internal ("MSCCC2"), 58C ("58C"), UK National Blood Service ("UKBS"), and MS external ("MS_ext") datasets. For those plots generated after conditional analysis, the SNP conditioned on is also indicated in the title.

Replication analysis

Replication of the 102 SNPs that reached our pre-specified statistical significance criteria was performed *in silico* using data from previously published GWAS (Table S15). These data were considered in six strata roughly corresponding to those used in the original studies, but amended so as to increase matching of cases and controls and to avoid any overlap with the cases and controls used in our discovery screen. Three of the strata (GeneMSA CH, GeneMSA NL, GeneMSA US) were the three component studies previously published by the GeneMSA group.[4] These three had already gone through QC and imputation (with HapMap phase II release 21 as the reference panel) and were used in our previously published meta-analysis of multiple sclerosis GWAS.[5] For the other three strata we performed equivalent QC (see below) and imputation (using HapMap phase II release 22 as the reference panel). These strata consisted of:

1) The ANZgene study[6] (without the 1,425 WTCCC1 controls).

2) 971 cases and 271 matched controls form the Brigham & Women's Hospital (BWH) GWAS, enriched with 2,681 controls from a myocardial infarction study (MIGEN).[54] Part of this dataset was used in the previous meta-analysis of GWAS.[5]

3) A dataset including the cases from our previous IMSGC GWAS[2] along with US control data but not the WTCCC1 controls. This strata thus included US and UK cases and US controls. As with the GeneMSA and BWH GWAS, these data were previously included in our meta-analysis of multiple sclerosis GWAS.[5]

Replication p-values were calculated from imputed data using a fixed effect meta-analysis as previously described.[5] In brief, for all six datasets the same QC criteria were applied for sample exclusion (genotype call rate >95%, gender discordance, excess heterozygosity) and for SNP exclusion (Hardy-Weinberg equilibrium $p<10\text{-}6$; minor allele frequency (MAF) <1%, genotype call rate >95%). We used EIGENSOFT[55] to calculate the dominant 10 eigenvectors within each stratum, and to remove outliers in terms of genetic ancestry. All six datasets were imputed with the MACH software.[56] Post-imputation, SNPs with a MAF less than 0.01 or imputation quality score (ratio of the observed vs. the expected variance) equal or less than 0.10 were excluded. The imputed allelic dosage data were analysed per dataset in a logistic regression model using the 10 first eigenvectors of the principal components analysis as covariates in PLINK.[57] For the SNPs that were included in the list of variants to replicate after the conditional analyses, we analysed the datasets also by adjusting with respect to the lead SNP(s) per locus. For each of the six datasets the genomic inflation factor (λ) was calculated[36] (see Table S15). The results from the replication and combined analysis are available in Supplementary Data.

Table S15. GWAS data used in replication and the strata considered.

Dataset	GeneMSA CH	GeneMSA NL	GeneMSA US	ANZ	BWH	IMSGC
Cases	253	230	486	1618	973	795
Controls	208	232	431	1988	2952	1679
Clinical						
F/M	2.8	2.9	3.1	2.6	2.6	3.1
Duration/Years	12	13	15	NA	14	13
AAO/Years	33	33	33	34	33	28
Analysis						
Platform	Illumina 550	Illumina 550	Illumina 550	Illumina[a]	Affy 6.0	Affy 500K
Cases[b]	251	225	477	1616	860	789
Controls[b]	208	228	425	1987	2772	1676
Lambda	1.040	1.026	1.029	1.061	1.050	1.032

F/M = the female to male ratio, Duration is the mean duration and AAO the mean age at onset, NA = not available.

[a] The cases were typed with Illumina 370CNV and the controls with Illumina Infinium

[b] These rows indicate the number of samples passing QC and included in the analysis

Further Analysis

1000 Genomes analysis

Haplotype data available through the 1000 Genomes population resequencing project[58] allowed us to extensively catalogue variants correlated with SNPs implicated in this study. For the most associated SNP in each of the association regions we used these data, in conjunction with other publically available annotations, to flag SNPs which are in LD with variants in the following three categories:

- Putatively functional SNP: $r^2 > 0.8$ with a 1000 Genomes SNP labelled as either generating a stop codon or amino acid change, or lying within an essential splice site or miRNA. These functional categories were assigned using the Ensembl variation api (http://www.ensembl.org/info/docs/api/variation/index.html).

- Highly differentiated SNP: $r^2 > 0.1$ with any of the 292 highly differentiated SNPs identified in the analysis of the 1000 Genomes pilot paper. A list of these SNPs can be found in Supplementary Tables 7 and 8 of [58].

- Previous GWAS SNP: $r^2 > 0.1$ with a SNP listed in the NHGRI GWAS catalogue[59] as downloaded in December 2010. Only SNPs associated with autoimmune phenotypes are used.

The above annotations are related to the 1000 Genomes data using rsIDs. Therefore it is possible that associations could be missed if either SNPs are not contained with the 1000 Genomes data used (taken from haplotypes provided at http://mathgen.stats.ox.ac.uk/impute/impute_v2.html) or if rsIDs are inconsistent with the annotations. For computational efficiency LD was calculated only for SNPs within 0.5Mb of the most associated SNP within the region, assuming r^2 to be less than 0.1 outside this interval. Note that none of the SNPs identified from the analysis of the discovery data tagged any highly differentiated SNPs using the criteria defined above.

Gene Ontology analysis

For each term in the Gene Ontology (GO) hierarchy,[60] we performed a simple overrepresentation analysis using the genes annotated to MS-associated SNPs as follows. Analysis was restricted to a list of human protein-coding genes obtained from UniProtKB.[61] We used the GO term gene annotations available in the assocdb database downloaded from the Gene Ontology website (http://archive.geneontology.org/lite/2011-01-01/). For each of the three SNP categories (i. SNPs in Table S1; ii. SNPs in the top tier of Table S2 or with $P<1x10^{-4.5}$ in discovery and the same direction of effect in replication; iii. SNPs in either of the above category), we performed a Fisher's exact test on the 2x2 table of gene counts categorized by gene status (nearest gene, as defined above, to one of the selected SNPs) and term membership. In this context, Fisher's exact test tests the null hypothesis that a gene being nearest to one of the selected SNPs is independent of membership of a specific GO term.

To show that results were not an artefact of the choice of nearest gene, we also repeated the analysis using all proximal genes (as defined above) to each selected SNP. These analyses gave similar results, with all of the most significantly overrepresented terms being immune-related terms. This remained true whichever of the three SNP categories was used. Full results are available in the Supplementary Data.

In principle, the above analysis might be confounded by gene size, since larger genes would be more likely to occur as nearest or proximal to a given SNP even under the null hypothesis. However, we found that immune system process genes (those annotated to the "Immune system process" GO term) were shorter on average (mean 47.7kb, 0.062cM) than non-immune system process genes (mean 60.3kb, 0.07cM).

Sibling recurrence risk and variance explained on the liability scale

We estimated that the non-HLA SNPs listed in tables S1 to S3 together explain sibling recurrence risk (λ_s) of 1.148 (95% interval 1.142 - 1.153). Using the effect size estimates from the replication data only, the corresponding values are 1.153 (1.127 - 1.183). When combined with the estimated λ_s of 1.38 for the four HLA-alleles (see below), we explain λ_s of about 1.58 by marginal effects of the strongly implicated genetic variants in this study.

In a large study in the Swedish population, Hemminki et al. (2009) report a sibling recurrence risk estimate of 6.3 (3.7 – 10.6) for multiple sclerosis.[62] This estimate also includes possible environmental risk factors that are shared between siblings. The genetic variants strongly implicated in our study (57 SNPs and 4 HLA-alleles) explain about 25% (19% - 35%) of this total sibling risk estimate on the logarithmic scale.

For heritability calculations we used a liability threshold model according to which the total variance on the liability scale is 1 in the population. By assuming that the prevalence of MS is K=0.001 this model identifies MS-cases as the individuals whose liability is larger than T=3.09, which is the point that separates the right-hand tail-area of K=0.001 from the standard normal distribution. By using the above mentioned sibling risk estimate for MS as if it were all due to genetic effects, we get an estimate for the heritability of MS on the liability scale of 38% (26% - 51%) (see formula 3 in the paper by Reich et al.[63])

For the chosen 57 SNPs and 4 HLA alleles we estimated the variance that they explain on the liability scale by defining, for each of them, an appropriate displacement t between the two homozygote genotypes in such a way that the mean liabilities for the non-risk homozygote, heterozygote and high-risk homozygote are –pt, 0.5t-pt and t-pt, respectively, where p is the risk-allele frequency in the population. In this situation the mean liability in the population is 0, the variance explained by the variant is $0.5p(1-p)t^2$, and the proportion of the genetic variance that the variant explains is $0.5p(1-p)t^2/h^2$, where h^2 is the heritability estimate. To find a displacement t that approximately matches our estimated odds ratio (OR) of the variant under an additive model on a log-odds scale, we minimised the quantity

$$\left(\frac{1-\Phi(T+pt-t)}{1-\Phi(T+pt-0.5t)}-OR\right)^2+\left(\frac{1-\Phi(T+pt-0.5t)}{1-\Phi(T+pt)}-OR\right)^2$$

with respect to t, where Φ is the cumulative distribution function of the standard normal distribution. As a result the 57 SNPs together explain 6.5% and the 4 HLA-alleles (with frequencies and effect sizes from UK-analysis) together explain 10.5% of the genetic variance on the liability scale. Thus the proportion of the genetic variance explained by the implicated variants (57 SNPs and 4 HLA-alleles) is 17% (13% - 25%). The 95%-interval is derived only from the uncertainty in the sibling risk estimate whereas the uncertainty in the prevalence of MS, the possible environmental contribution to the sibling risk-estimate and the dependencies between different HLA-alleles have not been taken into account. As a consequence these results should be taken only as rough estimates for the underlying quantities.

Homogeneity of effects

To assess possible heterogeneity among the 102 SNPs taken to replication, we separately analysed each of the eight populations with population specific controls in our discovery data set (Finland, France, Germany, Italy, Norway, Sweden, UK, USA) using seven PCs as covariates in the logistic regression models. Heterogeneity was assessed in two ways. Firstly, we computed the I^2 heterogeneity index[64] and secondly, we computed Bayes factor (BF) between a hierarchical random-effects model and a fixed-effect model. More specifically, the fixed-effect model assumes that there is a common effect β with prior distribution $N(0,0.2^2)$ (on log-odds scale) and the random-effects model assumes that each study draws its own effect from a t-distribution with a mean of β, a scale of σ and 3 degrees of freedom, where the prior on β is $N(0,0.2^2)$ and the prior on σ is Gamma(shape=2,scale=0.04). Values of I^2 and the heterogeneity Bayes factor for each SNP taken to replication are given in Supplementary Data.

Eight SNPs had I^2 estimate >50% (Figure S22) and sixteen of the SNPs had BF>1 with two of the SNPs having BF>3 (rs11984075 BF=7.7 and rs281783 BF=4.9, also in Figure S22). To empirically assess significance of the heterogeneity measure, we simulated 1,000 replicates for each SNP of meta-analysis case-control data sets by assuming that the effect in each population was equal to the effect that we had estimated from the fixed-effect meta-analysis for that SNP. For each replication, the control allele frequencies were sampled from a $Beta(40f_i,40(1-f_i))$ distribution for population i, where f_i was the observed risk allele frequency in our data for that population at that SNP. Control genotype frequencies were assumed to be in Hardy-Weinberg equilibrium and case genotype frequencies were then derived from the effect size estimate and the control genotype frequencies assuming the additive model on log-odds scale. For each of the simulated replicates we computed the I^2 heterogeneity index. We then calculated an empirical p-value as the proportion of the replicates, where the computed I^2 index was higher than the I^2 index in our original data set for that SNP. None of the 102 lead SNPs had an empirical p-value less than 0.01.

We also divided individuals into Northern (Finland, Sweden, Norway) and Southern (UK, USA, Germany, France, Italy) groups and estimated the effects using logistic regression with seven PCs as covariates separately for the two groups. There were no general tendencies for larger effect sizes or higher risk allele frequencies in controls in either of the groups compared to the other at the 102 lead SNPs.

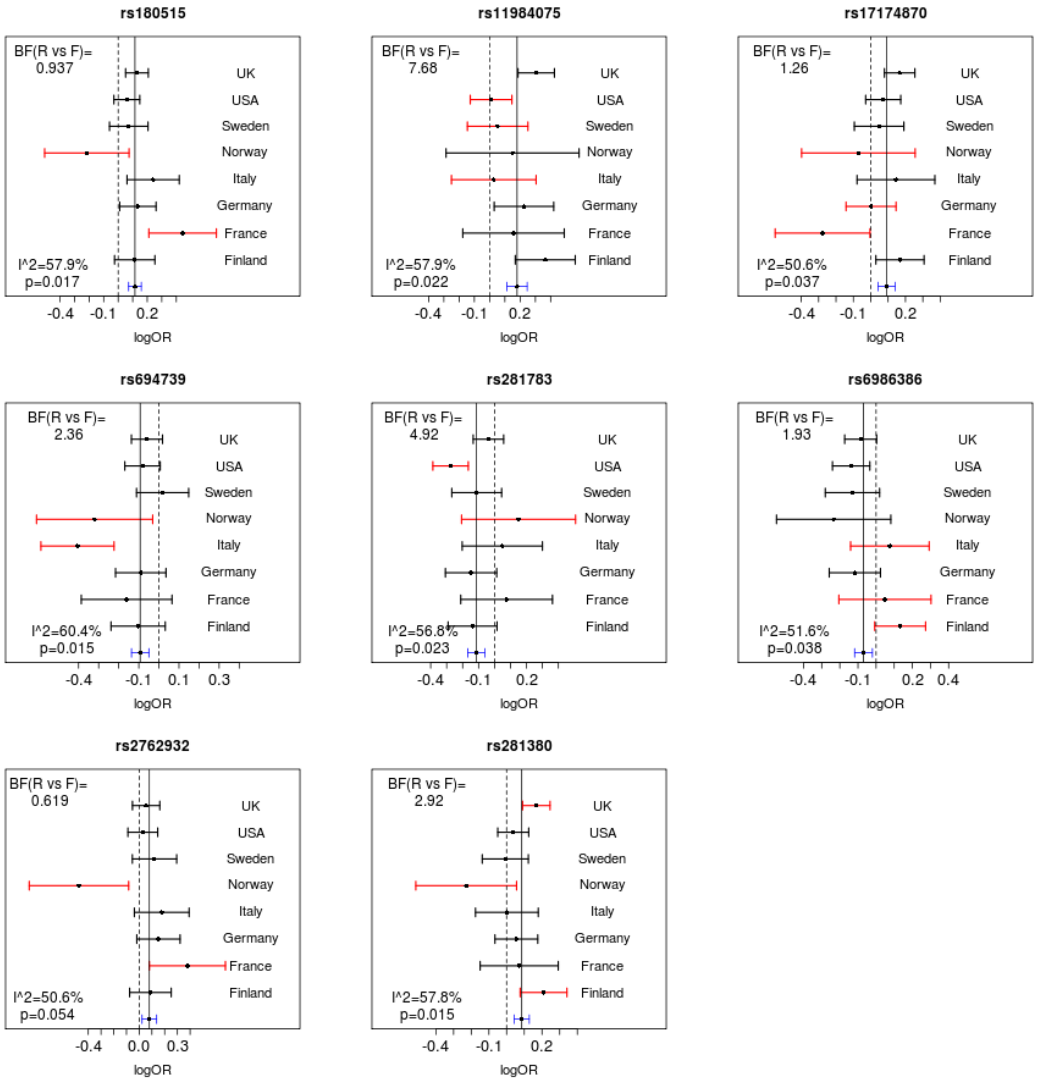

Figure S22. Forest plots with 95% CIs for the eight lead SNPs with I^2 index > 50%. All possible divisions of the populations into a fixed-effects group and an independent-effects group (outlier populations) were considered and the one with the largest marginal likelihood determined the colours of the populations (black ones belong to the fixed-effects group, red ones to the independent-effects group). Top-left corners give Bayes factors between random-effects model and the fixed-effects model. Bottom-left corner gives I^2 index and its empirical p-value. Blue line at the bottom corresponds to the fixed-effects meta-analysis effect.

Interactions

We tested all pair-wise interactions between the 102 lead SNPs (5151 pairs) using a linear mixed model, $y = x_1\beta_1 + x_2\beta_2 + x_1x_2\gamma + \varepsilon$, where y is the case-control status, x_1 and x_2 are the mean-centred SNP genotypes and γ is the interaction parameter. The five pairs with p-values < 5×10^{-4} for the interaction term are listed in Table S16.

Table S16. Pairs of lead SNPs with pair-wise interaction p-values < 5×10^{-4}.

Chr1	**SNP1**	**Chr2**	**SNP2**	**Sign of γ**	**p-value**
7	rs354033_G	7	rs2066992_C	+	1.4×10^{-4}
16	rs7200786_G	22	rs2072711_G	+	1.7×10^{-4}
10	rs3118470_G	14	rs2119704_C	+	1.9×10^{-4}
6	rs17066096_G	18	rs7238078_C	-	2.3×10^{-4}
12	rs12368653_G	2	rs281783_G	+	2.6×10^{-4}

Haplotype analysis

In our discovery analysis we identified three regions where conditioning on the lead SNP from the region revealed a second effect in the region with considerably larger effect than was seen at that SNP initially. In two cases the phenomenon replicated (Table S17), whereas the third SNP, rs2762932 on chromosome 20, did not replicate (p-values after conditioning on rs2248359 are 6×10^{-8} (discovery) and 0.66 (replication)). The 1000 Genomes database (www.1000genomes.org; accessed December 2010) suggests that only three two-SNP haplotypes segregate in the CEU population in the two successfully replicated regions.

Table S17. Marginal and conditional results for two regions with haplotype effects.
First column reports marginal effects of the lead SNP. Column "cond" reports results after conditioning on the lead SNP in the first column. Column "uncond" reports the marginal results (without conditioning on the lead SNP).

Chr 10 *IL2RA*	rs3118470_G		rs7090512_G cond		rs7090512_G uncond	
	OR	p-value	OR	p-value	OR	p-value
discovery	1.12	2.0×10^{-9}	1.19	2.6×10^{-14}	1.09	2.2×10^{-5}
replication	1.10	4.7×10^{-3}	1.21	5.0×10^{-7}	1.11	1.5×10^{-3}

Chr 3 *CD86*	rs9282641_G		rs4308217_C cond		rs4308217_C uncond	
	OR	p-value	OR	p-value	OR	p-value
discovery	1.21	1.5×10^{-9}	1.11	3.3×10^{-7}	1.08	1.3×10^{-4}
replication	1.20	2.3×10^{-3}	1.10	5.5×10^{-3}	1.08	2.5×10^{-2}

Under the assumption that only three haplotypes exist in these regions, we inferred the haplotypes for the individuals in our discovery data set and applied the linear mixed model $y = \mu + \alpha x_1 + \beta x_2 + \varepsilon$, where x_1 and x_2 are the number of copies of the two risk haplotypes that an individual carries (Table S18).

Table S18. Haplotype effects. Each cell gives the OR and 95%-CI with respect to the most protective haplotype (which by definition is set to have OR=1) as well as the haplotype frequency calculated from controls. Proportions of individuals with missing haplotype data were 0.0039 and 0.00062 for chromosome 10 and chromosome 3 regions, respectively.

Chr 10 *IL2RA* Haplotype effects		rs7090512 A	G
rs3118470	A	1 37%	1.20 (1.14-1.25) 30%
	G	1.22 (1.16-1.27) 33%	-----

Chr 3 *CD86* Haplotype effects		rs4308217 C	A
rs9282641	A	1 9%	-----
	G	1.25 (1.17-1.34) 58%	1.14 (1.06-1.23) 33%

Gender effects

We divided the discovery data set into four parts in order to estimate gender-specific effects: UK females (1293 cases, 2564 controls), UK males (561 cases, 1122 controls), non-UK females (5683 cases, 6320 controls) and non-UK males (2235 cases, 5881 controls). To balance the case-control ratio in order to justify the linear mixed model, we have dropped some UK male controls from this analysis. The four data sets were analysed using the linear mixed model, and UK and non-UK results were combined by fixed-effects meta-analysis to get the overall results for both males and females. To compare males and females we used statistic

$\frac{(b_M - b_F)^2}{(se_M^2 + se_F^2)}$, where b_M and b_F are estimated effects in males and females, and se's are their standard errors. P-values were computed from chi-square distribution with 1df and the SNPs with $p<0.05$ are shown in Table S19. We did not find any SNPs with estimated effects in different directions between males and females.

Table S19. The lead SNPs which show a difference in effect sizes between males and females at p<0.05.

Chr	SNP_Allele	OR (M)	P (M)	OR (F)	P (F)	P_{diff}
16	rs13333054_A	1.24	$2.1x10^{-9}$	1.06	0.0415	0.00029
12	rs1800693_G	1.05	0.14	1.16	$8.9x10^{-11}$	0.0078
12	rs12368653_A	1.18	$2.6x10^{-7}$	1.07	0.0072	0.012
3	rs2293370_G	1.26	$1.4x10^{-8}$	1.11	0.00076	0.012
10	rs1250550_A	1.16	$3.8x10^{-6}$	1.06	0.0083	0.032
8	rs6986386_A	1.02	0.48	1.12	$6.5x10^{-6}$	0.037
5	rs756699_A	1.20	$2.9x10^{-5}$	1.07	0.035	0.038
5	rs6897932_G	1.18	$6.4x10^{-6}$	1.07	0.0075	0.044

M=males, F=females, OR=Odds ratio, P=p-value for association, P_{diff}=p-value for difference.

X chromosome analysis

For X-chromosome analyses we used the same grouping as in the analysis of gender effects (UK males, UK females, non-UK males, non-UK females). We analysed the four data sets separately using the linear mixed model and then combined all results using fixed-effects meta-analysis. Male genotypes and homozygous females were coded as 0 and 2 and heterozygous females were coded as 1. This coding assumes that the difference in log-odds ratio is the same between the two homozygous female genotypes as it is between the two possible male genotypes.

After QC there were 10,372 SNPs on the X-chromosome with usable data. The genomic inflation factor (λ) computed from X-chromosome SNPs was 1.116 for males, 1.080 for females and 1.130 for combined analysis. The expected 95% confidence interval for λ based on 10,372 independent samples from the chi-square distribution with 1df is 0.956 to 1.046. In addition to dependence between the observed statistics due to LD between SNPs, another reason for the apparent inflation with the linear mixed model is that the relatedness matrix computed from autosomal markers does not accurately capture the population structure that is present at the X-chromosome. Despite the apparent inflation, only one X-chromosomal SNP had p-value below 10^{-5}(rs7052934_C, $p=2.5x10^{-24}$, OR 1.40 (1.32 - 1.50)). However, the cluster plot for this SNP is suspect (see Figure S23) and the replication data (for males only) showed the effect in the opposite direction with OR=0.75 (95% CI=0.57 – 0.98) and p-value=0.038.

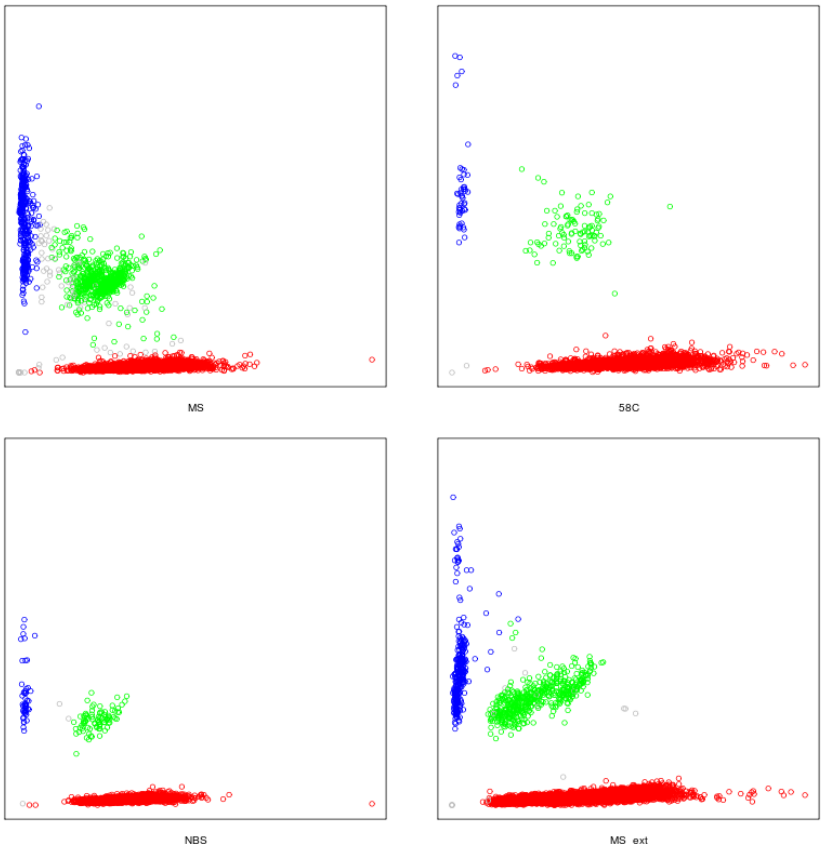

Figure S23. The cluster plots for rs7052934 in the internally generated MS data, the 58BC, the NBS and the externally generated data.

Secondary phenotypes

Age at onset (AAO)

We ran a genome-wide scan with the linear mixed model considering age at onset (AAO) as the phenotype and treating gender as a covariate. AAO was available for 8,715 MS cases (mean AAO = 32.3 +/- 9.8). We applied the linear mixed model to the raw phenotypes and to the log-transformed phenotypes, but as the results were very similar only the results with the raw phenotypes are shown. Across the genome (465,508 SNPs) the genomic inflation factor (λ) was 1.005 with the linear mixed model. For comparison, λ=1.104 with the standard linear model. A Q-Q plot of the test statistics (Figure S24) revealed several SNPs with more extreme values than expected under the null, all from the MHC region.

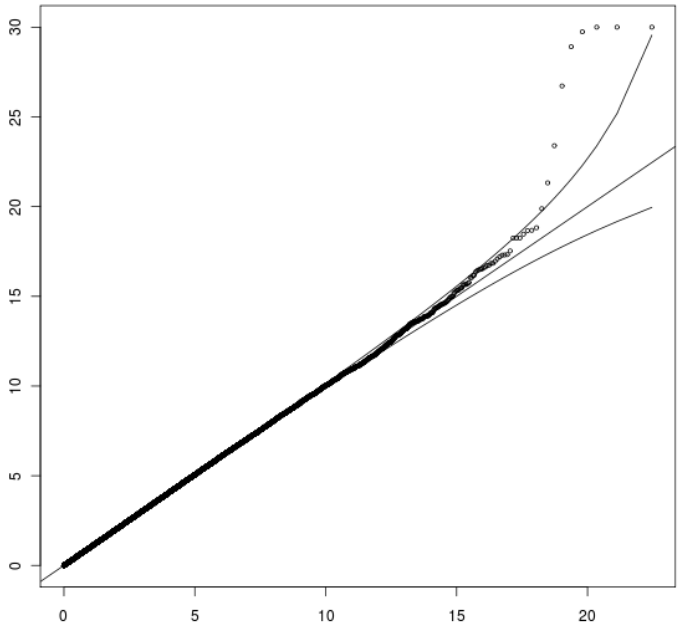

Figure S24. Q-Q plot for the AAO scan employing the linear mixed model and raw phenotypes. Expected chi^2 is given on the x-axis and observed statistics on the y-axis. The null (y=x) line and the 95% confidence bands around this are marked by thin lines. Each circle is a single SNP from the whole genome scan.

The strongest signal is seen with rs3129934 ($p=9.7x10^{-9}$), see Figure S25. Adding geographical origin and the seven primary PCs to the linear mixed model as fixed-effect covariates had only minimal effect on the strength of the association ($p=1.1x10^{-8}$). Each copy of the minor allele A at rs3129934 decreases age at onset by 10.6 months (+/-1.9 months). Allele A has a high positive correlation with our imputed DRB1*15:01 allele (correlation from genotype data = 0.86) and hence we see a very similar effect by using DRB1*15:01 genotypes instead of rs3129934. No other regions contained p-values below $1.0x10^{-5}$.

In principle, the association we have observed between AAO and DRB1*15:01 could result from ascertainment bias if diagnostic accuracy were to be inversely correlated with age. However, although the differential diagnosis for neurological dysfunction increases after middle life (age >50), and therefore the diagnostic accuracy is likely to be lower in older patients, it is unlikely that such a bias would generate the observed effect since only 10% of our cases were diagnosed after the age of 50.

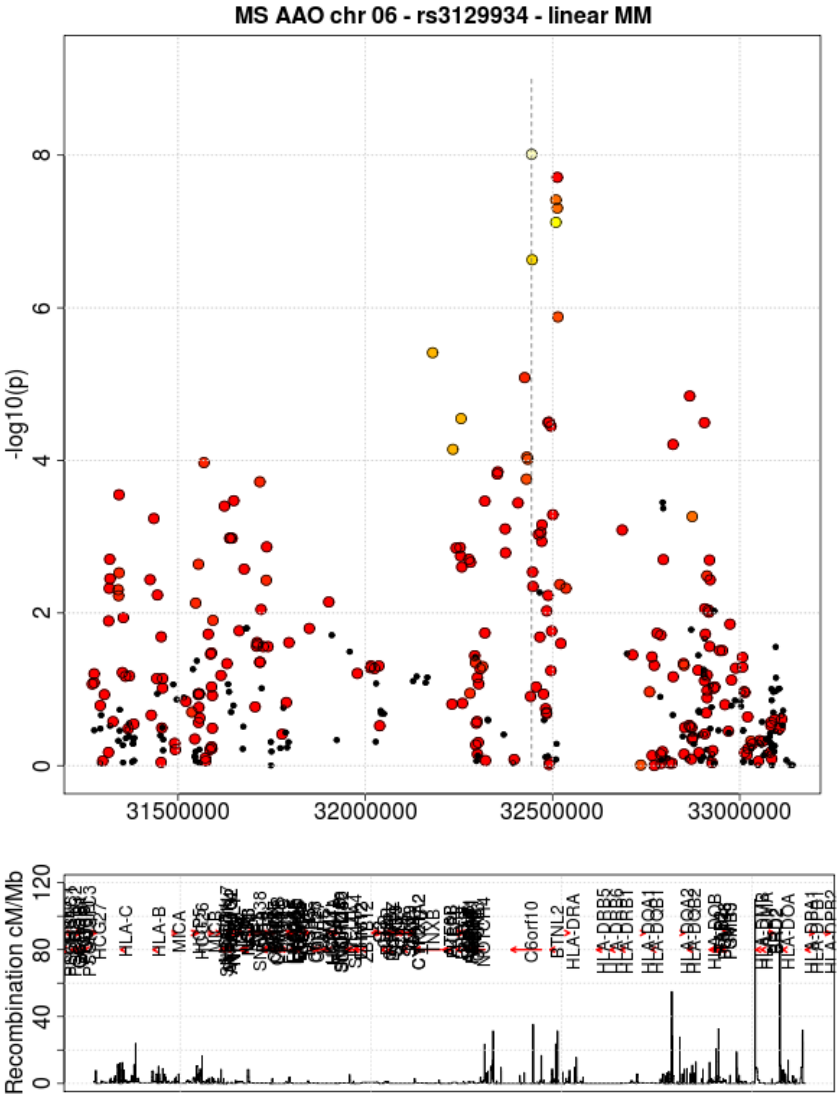

Figure S25. Hit plot for the AAO scan employing the linear mixed model showing the region containing rs3129934. Each circle represents a SNP from the region colour coded according to the level of LD with the lead SNP (using the same legend as in the "regional association plots"). The y-axis indicates the -$\log_{10}$(P) for the SNPs and the x-axis their physical positions on chromosome 6. The bottom panel shows the recombination map and positions of the known genes.

We also noticed that the identified multiple sclerosis susceptibility loci tend to have smaller p-values in the AAO scan than expected by chance (Table S20), and that the direction of the effects between the susceptibility scan and the AAO scan at those SNPs tend to be more often consistent (i.e. multiple sclerosis risk allele decreases AAO) than expected by chance (Table S21).

Table S20. AAO p-values at the 59 SNPs with strong evidence for association with MS.

Threshold	#Below Threshold	#Total	Prop below	p-value
0.5	35	59	0.59	0.10
0.2	20	59	0.34	0.0087
0.1	12	59	0.20	0.013
0.05	8	59	0.14	0.0089

Columns: (1) p-value threshold in AAO scan. (2) Number of susceptibility SNPs below threshold in AAO scan. (3) Number of susceptibility SNPs. (4) Proportion below threshold. (5) One-sided P-value for the null hypothesis that each SNP is below the given threshold with probability=threshold.

Table S21. Consistency of the directions of the effects between susceptibility scan and AAO scan in our discovery data set (UK + non-UK)

Threshold	#Consistent	#Total	Prop cons	p-value
$5x10^{-8}$	18	21	0.86	0.00075
$5x10^{-7}$	26	32	0.81	0.00027
$5x10^{-6}$	39	56	0.70	0.0023
$1x10^{-5}$	45	69	0.65	0.0077

Columns: (1) p-value threshold in susceptibility scan. (2) number of SNPs that are below threshold in susceptibility scan and have "consistent" effects on AAO, where "consistent" means that the risk allele for MS decreases AAO. (3) Total number of SNPs below threshold in susceptibility scan. (4) Proportion of consistent SNPs. (5) One-sided P-value for the null hypothesis that each SNP is consistent with probability 0.5.

Clinical course

The clinical course of multiple sclerosis is characterised by self-limiting episodes of neurological dysfunction (relapses) and the progressive accumulation of disability. Relapses are generally more common in women than in men and tend to decline in frequency with age.[65] For most patients relapses are the earliest manifestations of the disease (Bout Onset multiple sclerosis, BOMS) and often occur for several years before the development of progression. Only a minority of patients never have a relapse and present exclusively with progressive disease (Primary Progressive multiple sclerosis, PPMS). In our data, as expected, PPMS was more common in males (17%) than in females (9%) and had a significantly older mean age at onset (AAO): 40.5 years for PPMS compared with 31.6 years for BOMS. The extent to which the variation in clinical course might reflect underlying genetic heterogeneity is unclear.

We ran a genome-wide scan with the linear mixed model comparing PPMS and BOMS. Because BOMS (8041 cases) massively outnumbers PPMS (999 cases) it was not possible to include all the available data as it was unlikely that the linear approximation to the logistic model would hold in this setting. We therefore considered a subset of the data with 723 PPMS individuals and 2,209 BOMS individuals, who were matched with respect to gender and geographical origin to PPMS individuals. Because (as anticipated) AAO, and to a lesser extent age, were correlated with PPMS status (Figure S26) we included AAO and age as covariates.

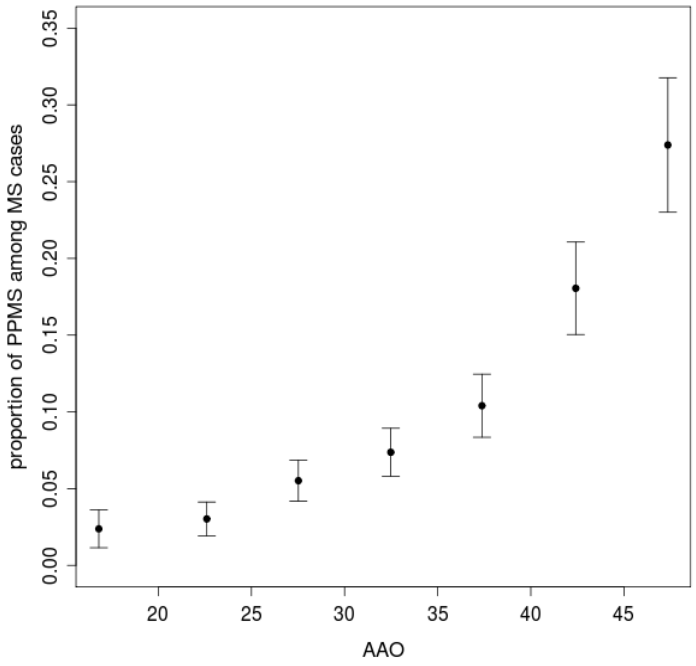

Figure S26. Proportion of PPMS by AAO.

In the PPMS vs BOMS scan the genomic inflation factor was 1.01 with the linear mixed model and 1.07 with the standard linear regression. Figure S27 shows that the distribution of the test statistic matches with its expectation under the null. Table S22 shows the results for the only four SNPs with $p < 1x10^{-5}$.

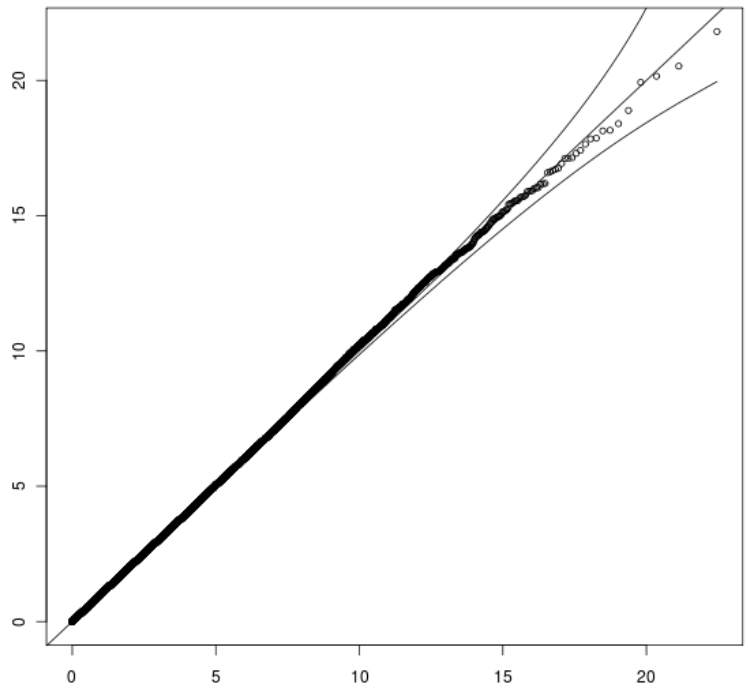

Figure S27. Q-Q plot for the PPMS vs. BOMS employing the linear mixed model and raw phenotypes. Expected chi^2 is given on the x-axis and observed statistics on the y-axis. The null (y=x) line and the 95% confidence bands around this are marked by thin lines. Each circle is a single SNP from the whole genome scan.

Table S22. Top results for PPMS vs. BOMS scan, where PPMS individuals were coded as 1 ("cases") and BOMS as 0 ("controls").

Chr	SNP_Allele	Position/bp	OR	p-value	$log_{10}BF$	Gene
9	rs1757948_C*	80500500	1.32	3.0E-06	3.81	PSAT1
9	rs1634352_G*	80503640	1.30	8.0E-06	3.43	PSAT1
13	rs9550637_G	19810527	1.31	5.9E-06	3.56	CRYL1
14	rs1125221_G	73982583	1.29	7.1E-06	3.48	TMEM90A

* These two alleles are in virtually complete LD.

Five of the 102 lead SNPs of the MS susceptibility scan had p-values<0.05 in PPMS vs. BOMS analysis - rs7200786 (*CLEC16A*), rs2425752 (*CD40*), rs140522 (*ODF3B*), rs1843938 (*CARD11*) and rs2066992 (*IL6*). Generally, we did not find evidence for smaller than expected p-values at the susceptibility lead SNPs in the PPMS vs. BOMS scan.

Rate of progression (severity)

The rate at which individuals with multiple sclerosis accumulate disability is highly variable, with some patients only having minimal disability after decades of disease (benign disease) and others developing profound disability within a few years (severe disease). Since the Expanded Disability Status Scale (EDSS) score used to quantify disability inevitably increases with the passage of time, we measured severity using the Multiple Sclerosis Severity Scale (MSSS), which provides a decile score for each patient by comparing their EDSS with the distribution of EDSS scores seen in individuals with the same duration of disease.

To identify genetic factors that might influence severity, we ran a genome-wide scan with the linear mixed model considering the MSSS as the phenotype, with gender and AAO as covariates. Raw phenotype values for 7,069 cases were fairly uniformly distributed between 0 and 10 as shown in Figure S28.

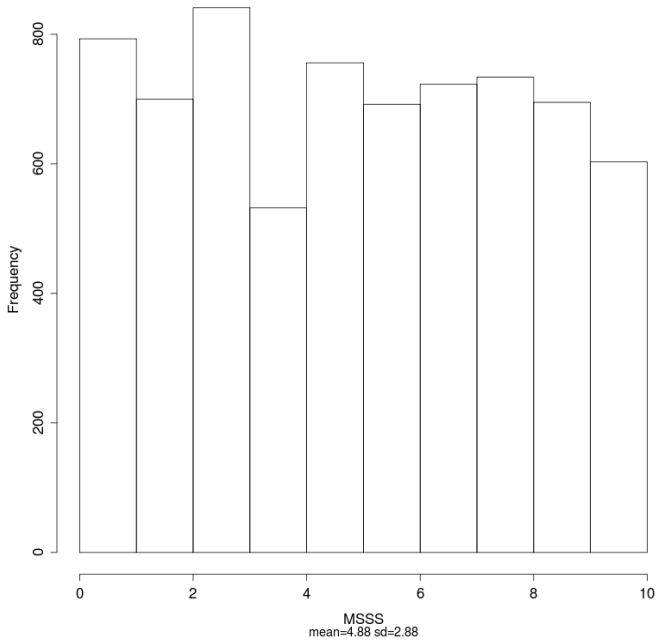

Figure S28. Distribution of MSSS in the MS cases with available scores.

We applied the linear mixed model to the raw phenotype values as well as to the quantile normalised values. In both cases the genomic inflation factor (λ) was 1.00 with the linear mixed model and 1.06 with the standard linear regression. Figure S29 shows a comparison of the results obtained using the two versions of phenotype data (465,506 SNPs).

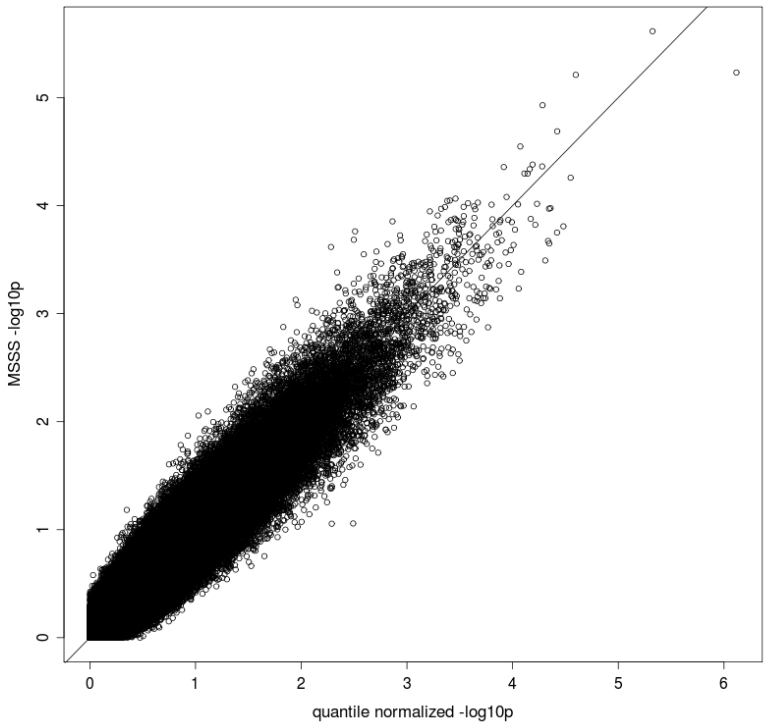

Figure S29. Plot comparing MSSS scan results ($-\log_{10}(p)$) based on raw data (y-axis) and quantile normalised data (x-axis) employing the linear mixed model.

There were no SNPs with strong evidence for association. The three SNPs with $p < 1x10^{-5}$ are listed in Table S23. Four of the 102 susceptibility lead SNPs had p-values<0.05 in the MSSS analysis: rs4285028 (*SLC15A2*), rs2762932(*CYP24A1*), rs1373089 (*WNT9B*) and rs1843938 (*CARD11*). In general, we did not find evidence for smaller than expected p-values at the MS-susceptibility SNPs in the MSSS scan, nor did we see evidence for consistency between direction of effects in the susceptibility scan and MSSS scan.

Table S23. Top results for MSSS scan

Chr	**SNP_Allele**	**Position/bp**	**ΔMSSS**	**p-value**	**$\log_{10}$BF**	**Gene**
3	rs6798831_A	109204824	0.22	2.4E-06	3.78	CD47
3	rs10937486_A	192722265	0.35	5.9E-06	3.55	CCDC50
8	rs6998423_G	134058472	0.22	6.2E-06	3.39	TG

ΔMSSS indicates the average increase in MSSS per allele.

DRB1*15:01 stratified analysis

Given the predominant effect of the DRB1*15:01 allele, we divided our data set into DRB1*15:01 carriers and non-carriers, and did separate genome-wide scans using the linear mixed model within each group to assess whether effects at some SNPs might depend on the DRB1*15:01 status. In the UK cohort we had 2,012 individuals who carried at least one copy of DRB*15:01 (916 cases and 1,096 controls) and 4,373 individuals with no copies of DRB*15:01 (850 cases and 3,525 controls). In the non-UK cohort there were 6,405 carriers (3,735 cases and 2,670 controls) and 13,094 non-carriers (3,824 cases and 9,270 controls). Some of the individuals from our primary analysis were excluded from this analysis because the QC-measures implicated that HLA-imputation was not reliable. Genomic inflation factors (λ) for the fixed-effects combined UK and non-UK scans were 1.034 for the DRB1*15:01 carriers and 1.038 for the non-carriers.

To test the difference of the effects in carriers (i=1) versus non-carriers (i=0) we used the statistic

$$\frac{(b_1 - b_0)^2}{\left(se_1^{\,2} + se_0^{\,2} - 2se_0 se_1 r\right)}$$

where b_i is the effect size estimate and se_i its standard error in group i=0,1, and r=0.066 is the empirical correlation coefficient between b_0 and b_1 calculated from the whole genome (excluding MHC).

After excluding the MHC, the genome-wide distribution of this statistic does not show any deviation from the chi-square distribution with one degree of freedom (Figure S30).

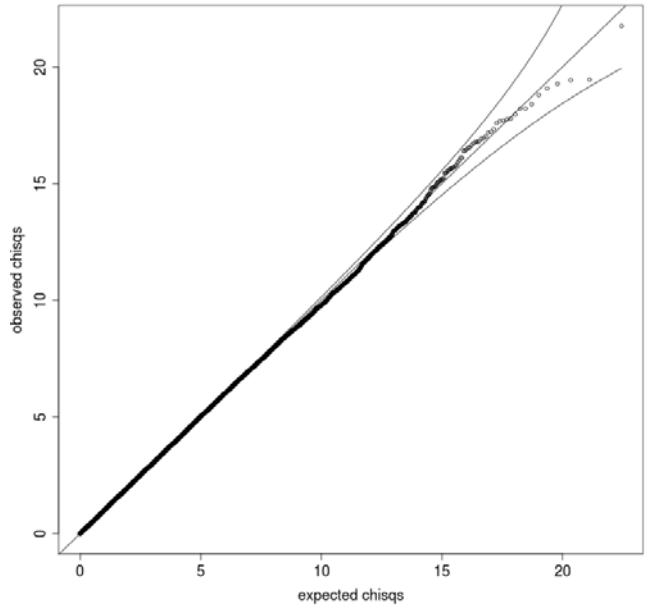

Figure S30. Q-Q plot for the scan based on effect size difference between carriers vs. non-carriers. Expected chi^2 is given on the x-axis and observed statistics on the y-axis. The null (y=x) line and the 95% confidence bands around this are marked by thin lines. Each circle is a single SNP from the whole genome scan (excluding MHC).

Only one SNP (rs7195761) outside of the MHC showed evidence of association with a p-value < 10^{-5} ($p=3.1x10^{-6}$, *ANKS4B*). Five of the 102 susceptibility lead SNPs showed nominally significant evidence ($p<0.05$) for a difference in effect between the two groups as shown in Table S24. In general, we did not find evidence for smaller than expected p-values when testing for the differences in effect sizes between DRB1*15:01 carriers and non-carriers at the MS susceptibility SNPs.

Table S24. Results for susceptibility lead SNPs showing nominally significant evidence for a difference of effect in the comparison of DRB1*15:01 carriers and non-carriers.

Chr	**SNP_Allele**	**Gene**	**OR(+)**	**p(+)**	**OR(-)**	**p(-)**	**pΔ**	**log_{10}BF**
3	rs2293370_G	TMEM39A	1.09	0.040	1.23	1.4E-10	0.014	0.516
9	rs290986_A	SYK	1.04	0.36	1.16	1.2E-06	0.021	0.409
5	rs4613763_G	PTGER4	1.14	0.0029	1.26	2.3E-11	0.049	0.0425
20	rs6062314_A	ZBTB46	1.33	3.6E-07	1.12	0.0074	0.014	0.439
11	rs650258_G	CD6	1.04	0.23	1.14	9.6E-08	0.018	0.396

OR = Odds Ratio, p = p-value, + indicates the result in the carriers, - indicates the results in the non-carriers. pΔ indicates the significance of the difference and log10BF the log_{10} of the Bayes factor for that difference.

Month of Birth

Given that month of birth (MOB) has been shown to influence the risk of developing multiple sclerosis[66], we explored this issue in our samples. Since birth rate varies between populations and over time, as well as during the year, we established population and year specific control monthly birth rates using publicly available data sources.

Australian Bureau of Statistics (ABS) http://www.abs.gov.au/
Centers for Disease Control and Prevention (CDC) http://www.cdc.gov/nchs/nvss.htm
Eurostat http://epp.eurostat.ec.europa.eu/portal/page/portal/eurostat/home/
FPS Economie Belgium http://economie.fgov.be/
Institut national de la statistique et des études économiques (INSEE) www.insee.fr/
Instituto Nacional de Estadística www.ine.es/
Istituto Nazionale di Statistica (ISTAT) www.istat.it/
Northern Ireland Statistics and Research Agency (NISRA) www.nisra.gov.uk/
Statistisches Bundesamt Deutchland (DESTATIS) www.destatis.de/
Statistics Finland (STAT) http://www.stat.fi/index.html
Statistics Norway (SSB) www.ssb.no/
UK National Statistics www.statistics.gov.uk

We did not include Poland in this analysis as year of birth (YOB) and MOB data were only available for 17 Polish individuals and no population specific control data could be located. Excluding Poland we had MOB and YOB data for 17,875 of the cases from our study (counting each twin pair only once). Corresponding population and YOB specific control data were available for 86% of these individuals. For the remainder, control data were estimated using the closest available population and YOB specific monthly birth rate data. Considering the Northern and Southern hemispheres separately, data were combined across populations and each month was tested for association using a normal approximation to the binomial distribution. Data are shown in Table S25 (Northern hemisphere) and Table S26 (Southern hemisphere). In concordance with the earlier report [66], we saw nominally significant evidence for a MOB effect in our Northern hemisphere data with increased risk of multiple sclerosis in May and August, and reduced risk in November (restricting the analysis to just those cases which were born in a year with full control information did not significantly change the result). Simulating 50,000 replicate studies, where the observed birth months were assigned according to expected proportions, indicates that the probability of seeing concordant data by chance (i.e. significant in both May and November) is 0.002. There was no significant evidence for a MOB effect in the Southern hemisphere populations, but the considerably smaller sample size in this group limits the power of the test. Figure S31 and Figure S32 show the ratio of observed and expected monthly birth rates in the Northern and Southern hemisphere groups, respectively. We found no evidence for any effect of MOB on disease course (as has previously been suggested[67]), severity or age at onset.

Table S25. Number of observed and expected cases by MOB across the Northern hemisphere populations (Belgium, Denmark, Finland, France, Germany, Ireland, Italy, Norway, Spain, Sweden, UK and US). P-values are two-tailed.

Month	Observed	Expected	Z-score	p-value
January	1397	1393.3	0.104	0.92
February	1295	1329.6	-0.989	0.32
March	1462	1491.4	-0.798	0.42
April	1467	1450.5	0.453	0.65
May	1548	1469.2	2.153	0.031
June	1400	1393.6	0.179	0.86
July	1426	1418.0	0.222	0.82
August	1462	1380.9	2.279	0.023
September	1388	1391.4	-0.0952	0.92
October	1302	1349.9	-1.360	0.17
November	1199	1274.8	-2.209	0.027
December	1320	1323.3	-0.095	0.92

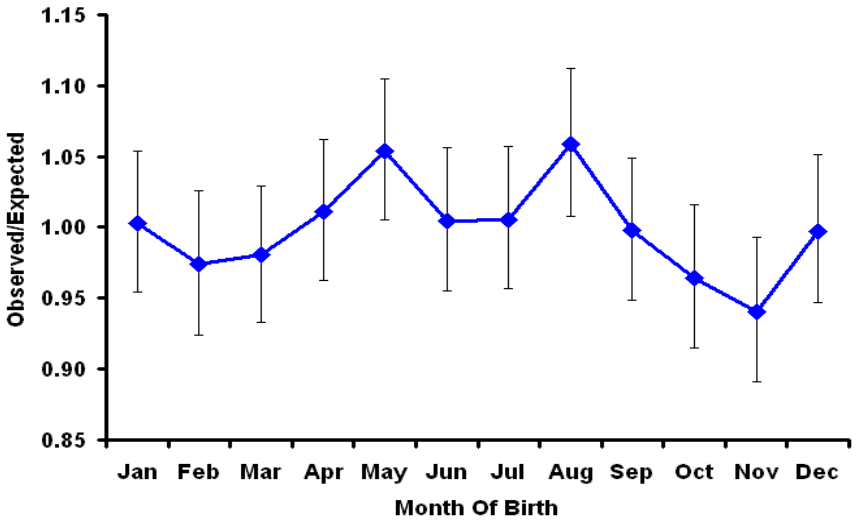

Figure S31. Ratio of observed to expected number of cases by MOB in Northern hemisphere populations, with 95% confidence intervals.

Table S26. Number of observed and expected cases by MOB across the Southern hemisphere populations (Australia and New Zealand). P-values are two-tailed.

Month	Observed	Expected	Z-score	p-value
January	110	102.2	0.806	0.42
February	102	95.6	0.682	0.50
March	112	103.6	0.863	0.39
April	96	98.0	-0.211	0.83
May	106	103.7	0.236	0.81
June	91	99.4	-0.879	0.38
July	96	103.4	-0.761	0.45
August	89	103.1	-1.452	0.15
September	112	102.4	0.991	0.32
October	97	106.8	-0.993	0.32
November	106	99.1	0.723	0.47
December	96	95.7	0.0319	0.97

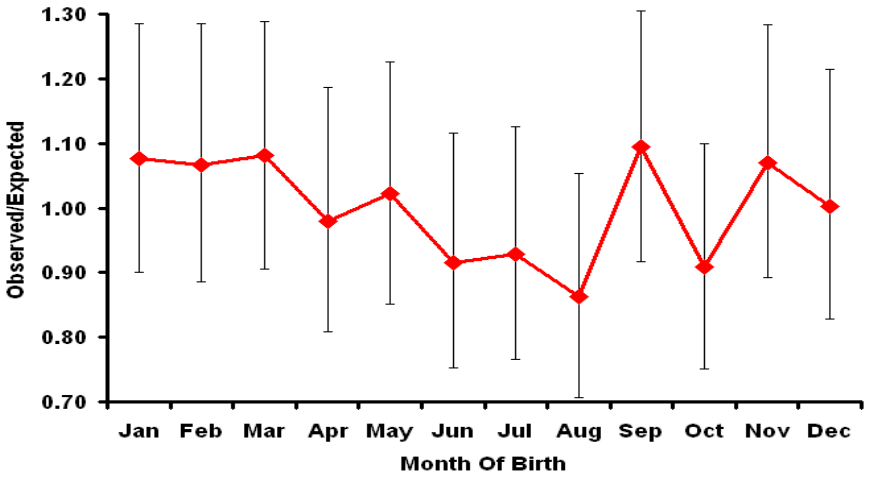

Figure S32. Ratio of observed to expected number of cases by MOB in Southern hemisphere populations, with 95% confidence intervals (note the different scale on the y-axis compared to the Northern hemisphere figure).

Comparing the high risk “season” (April, May and June) with the low risk “season” (October, November and December) in the Northern hemisphere we find a relative risk of 1.057 (1.012 - 1.105). This is smaller than any of the genetic effects thus far described. Because seasons were picked on the basis of the months with the highest deviation from expected, we would necessarily expect to see an apparent relative risk even if there were no actual MOB effect. In other words, the calculated value is likely to overestimate any real effect size (unless the relevant MOB varies considerably between populations).

We then tested for evidence of association between case allele counts and MOB for all disease associated markers (with $p < 0.01$) using a Pearson's chi-squared test with 11 df. Figure S33 shows the Q-Q plot for this analysis. All disease associated markers lie within the 95% confidence intervals, showing no evidence for any statistically significant variation in allele frequency with MOB at any of these markers. The SNP tagging DRB1*15:01 showed no evidence for association with MOB (p=0.6).

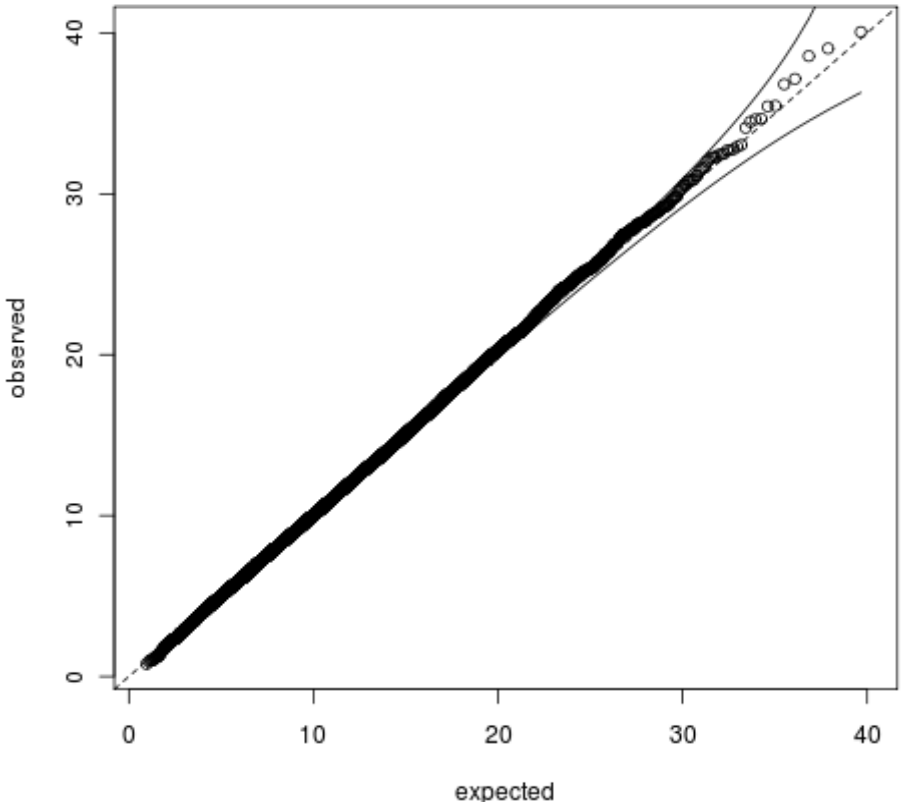

Figure S33. Q-Q plot for association with MOB in all disease associated SNPs (i.e. those showing evidence of association with disease with p<0.01). Dotted line indicates the null and the solid curved lines the 95% confidence interval on the null.

In our data the influence of MOB on the risk of developing multiple sclerosis appears small. Furthermore, none of our disease associated markers show any evidence of variation in allele frequency by MOB, suggesting this small but fascinating observation from the epidemiology of multiple sclerosis seems unlikely to have a strong genetic basis.

Imputation-based analysis of HLA

Overview

Genotypes at six classical HLA loci (*HLA-A*, *B*, *C*, *DQA1*, *DQB1* and *DRB1*), where not available for samples, were imputed using the method of Leslie et al.[68] with a reference panel consisting of over 3000 samples from the 1958 birth cohort and the extended HapMap CEU panel.[69] Thresholding calls at a posterior probability of 0.7 gives call rates between 95% (*HLA-DRB1*) and 99% (*HLA-DQB1*) and an accuracy (posterior predictive value: PPV), estimated from 2/3 cross-validation and independent experiments, of over 97% for all loci at the two-digit level and between 97% (*HLA-C*) and 99% (*HLA-DQB1*) at the four-digit level. Validation results for all alleles mentioned in the text are given below. Previous unpublished work has established that matching genetic ancestry is important when imputing HLA alleles, hence we focused discovery on the UK samples, which also have the advantages of well-matched controls and availability of SNP cluster plots to enable QC. The uncertainty associated with imputation (quantified by the posterior probability of the call) was incorporated into the logistic regression framework, with numerical optimisation used to find maximum likelihood estimates. Only cohorts with both cases and controls were analysed to reduce effects of population stratification. These were analysed independently and then combined through fixed-effect meta-analysis with the variance of parameter estimates being obtained by bootstrap resampling, maintaining the proportions of cases and controls. To calculate the sibling recurrence risk predicted by the results, we simulated 10,000 pseudo-sibships without recombination within the HLA from the phased 1958BC samples, and predicted their disease risk from the coefficients estimated by the logistic regression except for the base-line risk, which was modified so as to achieve an average disease risk of 1 in 1000.

Detailed methods for classical HLA allele imputation

HLA*IMP[68,70] uses a set of reference data in order to produce HLA type imputations for an imputation dataset. Both sets require careful quality control and data preparation. Here, we describe creation, assembly and quality control measures for the datasets we used in the present study.

Reference Set
The reference set, subsequently referred to as "Golden Set" (GS), was created by combining HLA- and SNP-genotyped samples from three cohorts:
1. The 1958 Birth Cohort (http://www.b58cgene.sgul.ac.uk/), typed on the Illumina 1.2M (2589 samples) and the Affymetrix Genome-Wide Human SNP Array 6.0. (2711 samples).
2. The HapMap CEU samples (60 samples)[52]
3. The CEPH CEU+ additional samples (32 samples)[69]

Step 1: Cohort-specific protocols

1958 BC. We removed all SNPs not present in HapMap r27 and those outside the extended MHC region (xMHC). The region considered was that defined by Horton et al.[71] with 50Kb flanks at the two ends. We removed all samples and SNPs which were not typed on both the Affymetrix and Illumina chip in order to be able to compare Affymetrix and Illumina typing data for each genotype in the remaining set (overlap 2462 samples).

We applied an EM-based procedure to align SNP strandedness to HapMap (cohort 2) separately for the Illumina and Affymetrix data. First, non-complementary (i.e not A/T or G/C alleles) SNPs' strandedness was adjusted to HapMap. Then, for each complementary SNP, we selected the two nearest non-complementary neighbors (with the complementary SNP in the middle) and calculated the likelihood of the observed SNP triplet genotypes under

two hypotheses and under the observed HapMap haplotypes. H0: the complementary SNP's strand is not inverted compared to HapMap. H1: the complementary SNP's strand is inverted compared to HapMap. We selected the hypothesis with the higher likelihood, set the SNP strand accordingly and used an EM algorithm to estimate haplotype frequencies in the target dataset. Finally, we compared the likelihood of the observed SNP triplet genotypes under the EM-estimated haplotype frequencies and under the HapMap-observed haplotypes and flagged SNPs for removal from both datasets if the two likelihoods showed gross deviations. To merge data from the Affymetrix and Illumina datasets, we applied the following procedure: call each SNP genotype based on a call threshold of T = 0.9 on the posterior probability. Non-called SNP genotypes were marked as 'missing data'. Compare each called SNP genotype between the two datasets and mark them as 'missing data' if they do not agree. Finally, calculate the percentage of missing data for all SNPs and all samples and remove each SNP and each individual with missing data > 5% from both sets. For the final step of merging, average the posterior genotype probabilities for each genotype and call, employing a threshold of T = 0.9. All genotypes below this threshold are marked as 'missing data'.
The resulting consensus dataset (2420 samples, 7733 SNPs) was phased using IMPUTE v2,[72] including phased HapMap samples as haplotype templates. Missing SNP data was imputed as part of this process.

HapMap. SNPs outside the xMHC region were removed. Missing data thresholds on the SNP genotype and individual level as described for cohort 1 were applied to the HapMap datasets. No data had to be removed. Finally, we removed all SNPs which were not present in the merged version of cohort 1.

***CEPH CEU+*.** SNPs outside the xMHC region were removed. Missing data thresholds on the SNP genotype and individual level as described for cohort 1 were applied. No data had to be removed. IMPUTE v2 was used for phasing, including phased HapMap samples. Missing SNP genotypes for SNPs present in the merged version of cohort 1 were imputed as part of the phasing process.

The described quality control and data preparation measures led to a set of 5024 high-quality SNP haplotypes in 7733 SNPs in the xMHC region.

Step 2: Combining classically typed HLA data and SNP haplotypes
In order to obtain full SNP + HLA haplotypes, we had to merge classically typed HLA genotypes and the SNP haplotypes created in step 1. We applied the following procedure: for each cohort, remove individuals without HLA typing. Use PHASE[73,74] to phase HLA alleles into the SNP haplotypes inferred in step 1, employing standard settings for multiallelic loci. To do so, input the SNP haplotypes from step 1 as invariable, so that only the phase of the HLA alleles, determined by the surrounding SNP context, is determined.

Step 3: Final merging procedure & Summary
Finally, we merged SNP and HLA data from all cohorts to obtain the Golden Set, comprising 2474 (HLA-A), 3090 (HLA-B), 2022 (HLA-C), 175 (HLA-DQA1), 2629 (HLA-DQB1), 2665 (HLA-DRB1) HLA- and SNP-genotyped chromosomes.

Step 4: MS-specific protocols
The imputation approach of HLA*IMP requires a pre-imputation model building stage, during which informative SNPs from the intersection of the reference and imputation SNP datasets are selected. Therefore, as a last step, the Golden Set was reduced to the intersection SNP set between the Golden Set and the quality-controlled imputation datasets (see next section), resulting in 5024 haplotypes in 2038 SNPs.

MS case and control cohorts
To prepare the MS case and control cohorts for imputation, we generally followed the procedures described under "Step 1" of the previous section:

1. Application of sample ID exclusion lists
2. Removal of SNPs outside the xMHC
3. Application of missing data thresholds (T = 0.05) for individuals then SNPs
4. SNP strand adjustment
5. Phasing with IMPUTE v2, including phased HapMap haplotype templates. Prior to phasing, we ensure that the cohort only includes SNPs which are also present in HapMap (this is generally the case).
6. Reduction to SNPs which are also in the Golden Set.

Note that "control cohorts" includes the MS country-specific controls and the NBS cohort. In a subsequent step, we also imputed missing 4-digit HLA types in the 1958BC, but this did not involve additional quality control measures. See Table S27 for a summary of the numbers involved.

Table S27. Summary of pre- and post-QC SNPs, samples and haplotypes for the imputed cohorts.

	Pre QC		**Post QC / Phasing**	
	Samples	**SNPs**	**Haplotypes**	**SNPs**
NBS	2737	6284	5474	6205
MS cases	11376	2879	20592	2307
MS controls	13203	2083	23348	2069

Validation of classical allele imputation for reported alleles

We assessed expected imputation accuracy by a 2/3 (training) – 1/3 (validation) cross validation experiment, using the same statistical model (including an identical set of informative SNPs) also employed for producing the case and control cohort imputations. At 4-digit HLA type resolution and applying a posterior probability call threshold of T = 0.7, accuracy ranged from 0.94 to 1, at call rates between 0.94 and 0.99 (see Table S28). We also examined sensitivity, specificity and positive predictive value (PPV) for alleles found to be associated with MS that are mentioned in the text (see Table S29). For DRB1*15:01, DRB1*03:01 and A*68:01, these values ranged from 0.92 to 1.00. DRB1*13:03 exhibited slightly decreased sensitivity (88%), but a high PPV (100%). We found no systematic patterns in mis-imputation (which have the potential to lead to spurious associations). In addition, for some of the MS cases from the UK, experimental typing was available for a number of loci. These comparisons indicated discordance between imputation and direct typing of 3.9% for HLA-A, 1.6% for HLA-B, 1.2% for HLA-C, 1.2% for HLA-DQB and 4.2% for DRB1. Errors in imputation will influence both our ability to identify association and also to detect interactions or departures from additivity.

These analyses provide an upper limit on the inaccuracies of classical HLA allele imputation. It is worth noting that experimental typing methods also carry errors. Although anecdotal, a number of samples for which imputation and direct methods disagreed, were shown to be correctly imputed following further experimental analysis.

Table S28. Imputation accuracy and call rate at 4-digit type resolution in a 2/3 – 1/3 cross-validation experiment with a threshold for calling on the posterior probabilities of 0.7.

Locus	Call Rate	Accuracy
HLA-A	0.98	0.97
HLA-B	0.97	0.97
HLA-C	0.99	0.97
HLA-DRB1	0.95	0.93
HLA-DQA1	0.98	0.98
HLA-DQB1	0.99	0.98

Table S29. Allele specific sensitivity, positive predictive value (PPV) and specificity for alleles discussed in the text in a 2/3 – 1/3 cross-validation experiment at 4-digit HLA type resolution with a threshold on the posterior probability of 0.7

Allele	Sensitivity	PPV	Specificity
DRB1*15:01	0.98	0.97	1.00
DRB1*13:03	0.88	1.00	1.00
DRB1*03:01	0.98	0.99	0.99
DRB1*08:01	1.00	0.92	1.00
A*02:01	1.00	0.82	1.00
A*68:01	0.92	1.00	0.99

Details of classical HLA allele analysis

As described in the main text, our analysis of association within the HLA was to focus discovery on the UK cohort, considering possible risk factors in a stepwise fashion to construct a coherent risk model. Factors were considered if the strength of association in the relevant conditional analysis within the UK cohort had $p<10^{-4}$ (assuming additivity on the log-odds-ratio). Such factors were then analysed in the other cohorts for which both cases and controls were available, using fixed effect meta-analysis to combined evidence. Only effects that had a combined $p<10^{-9}$ are reported. Where appropriate, alleles included within the model were analysed for departures from additivity (on the log-odds-ratio), interactions with gender and interactions with other loci and alleles. We included sex as a covariate in all analyses ($p=3.7x10^{-49}$; OR = 2.4 in the UK cohort). To choose among competing models we used likelihood ratio tests, where models are nested, and AIC otherwise.

Analysis of DRB1*15:01

Among both imputed classical HLA alleles and SNP variation, the strongest signal of association within the HLA is for the allele DRB1*15:01 ($p_{UK}=2.0x10^{-113}$; OR = 3.0). Similar results are seen in all cohorts giving $p_{combined}<10^{-320}$ and OR =3.1. Other alleles in the extended haplotype (DQB*06:02 and DQA*01:02) show similar association, but in six of the eight cohorts, the strongest signal is observed for DRB1*15:01. We therefore focus all subsequent analyses on DRB1*15:01 as the primary risk allele.

Within the UK, we find no evidence for a departure from additivity on the log odds ratio for DRB1*15:01 ($p_{UK}=0.30$), nor any evidence for sex-specific risk for DRB1*15:01 ($p_{UK}=0.46$ for the interaction term). However, we note that while the DRB1*15:01 allele has very similar frequencies in males and females (0.32 in females, 0.30 in males, p=0.25), a slightly higher

fraction of female cases are DRB1*15:01 positive (0.55 versus 0.50, p=0.06) and there is evidence for a departure from Hardy-Weinberg equilibrium (HWE) in females (p=0.005, with a dearth of 15:01 homozygotes), which is not observed in males (p=0.65). Departures from HWE are observed in female cases ($p<0.05$) from six out of the eight cohorts where there are both cases and controls (FIN, FRA, NOR, SWE, UK, GER), but in only one such cohort (ITA) for males.
Further analysis of the UK cohort using a retrospective likelihood rather than a prospective one (i.e. treating the genotypes as random variables, rather than the disease outcome), provides some evidence (p=0.005) for a differential risk profile for DRB1*15:01 in males and females, in which the allele acts in a purely additive manner in males (OR = 1.07), but is slightly dominant in females (OR = 1.18/2.14 for female heterozygotes and homozygotes respectively). However, it is worth noting that any departure from additivity is, at best, small. For all subsequent analyses the effects of DRB1*15:01 were assumed to be additive and independent of gender.

The protective class I signal is driven by HLA-A*02:01
Once HLA-DRB1*15:01 is included in the risk model, the strongest signal within the UK cohort comes from HLA-A*02:01 ($p_{UK} = 7.9x10^{-17}$; OR = 0.66), which is, again, stronger than any other SNP signal across the HLA. Similar results are found across all cohorts, giving $p_{combined} = 9.1x10^{-23}$ (OR = 0.73). Again, we find no evidence within the UK cohort for sex-specific effects ($p_{UK} = 0.31$) or a departure from additivity ($p > 0.1$). We also find no evidence for interactions with DRB1*15:01 ($p_{UK} = 0.57$).

Additional risk associated with the DRB1*03:01/DQB*02:01 haplotype
After conditioning on both DRB1*15:01 and A*02:01, the next strongest signal in the UK cohort is DRB1*03:01 ($p_{UK} = 7.8x10^{-10}$; OR = 1.43), which is only slightly stronger than the highly-correlated allele ($r^2>0.95$) DQB*02:01. A similarly strong signal is observed in the USA cohort ($p_{USA} = 2.1x10^{-6}$) and in the other cohorts combined ($p_{combined} = 3.6x10^{-10}$; OR = 1.26). In these other cohorts the individually estimated coefficients are consistent, except for FIN and SWE, where the allele has lower frequency. In the combined analysis, DRB1*03:01 has a more significant effect than DQB*02:01, and hence we include this allele within the risk model. Because of its rarity, we do not have power to detect a departure from additivity. We see no significant sex-specific effect or interaction with other alleles at HLA-A or HLA-DRB1.

Additional risk associated with DRB1*13:03
Including DRB1 alleles 15:01 and 03:01 and the protective effect of A*02:01 reveals a further candidate for risk associated with DRB1*13:03 in the UK cohort ($p_{UK} = 2.5x10^{-5}$; OR = 2.2). Similar results are found in the other cohorts ($p_{combined} = 1.3x10^{-11}$; OR = 2.4). After conditioning on all classical alleles mentioned so far, no other allele meets the criteria for inclusion. One additional allele achieves the strength of association for candidacy (HLA-B*38:01, $p_{UK} < 10^{-4}$). However, apart from the GER cohort, there was no additional support for the allele from other cohorts and the allele did not achieve $p_{combined} < 10^{-9}$.

Evidence for risk associated with alleles at the HLA-DPB1 locus
The above analysis has focused on classical HLA alleles. In addition, we have analysed patterns of associated SNPs genotyped across the region. Most patterns of association at SNPs can be explained by association to one of the alleles described above. However, we see an additional, independent signal around the HLA-DPB1 locus, for which we do not have classical HLA data for imputation. The signal is strongest at rs9277535 ($p_{UK} = 10^{-6}$; OR = 1.25) and this replicates across cohorts ($p_{combined} = 4.2x10^{-27}$; OR = 1.26). As discussed in the text, previous work has suggested that this association is driven by LD with DPB1*03:01 ($r^2 = 0.37$).[75]

In order to assess whether conclusions regarding classical HLA alleles other than DRB1*15:01 might be driven by slight (but non-significant) departures from

additivity at 15:01, we repeated our model fitting separately at each of A*02:01, DRB*13:03, and DRB*03:01 where now in each case DRB1*15:01 was included with a general (2-paramater) model. The results, shown in Table S39 below, indicate that both the model fit and the effect size estimate at the other three alleles are very similar whether DRB1*15:01 is fitted additively or with the general model.

Genecluster analysis of secondary signals at HLA-DRB1 and HLA-A

The analysis described above considers each classical allele independently. However, because of the biological similarity of alleles, risk may be shared among closely-related alleles. The GENECLUSTER method is effectively a haplotype-based method for identifying groups of haplotypes carrying the same risk.[76] This is achieved by identifying strong similarity between the haplotypes in the experimental sample and a reference set, here from the CEU population in the HapMap Project,[52] for which a genealogical tree has been estimated previously at a given locus. The algorithm then places mutations on the underlying tree, considering models with a single risk allele initially, but then expanding to consider models with additional risk alleles. By using this method it is therefore possible to explore risk signals in the data that do not correspond to one of the typed or imputed variants.
The method was applied to both the HLA-DRB1 and HLA-A loci. At HLA-DRB1, the method identifies three clusters of risk alleles (Figure S34). Of these, within the 120 CEU haplotypes, one is nearly perfectly correlated with the presence of DRB1*15:01, one is perfectly correlated with DRB1*03:01 and one includes DRB1*13:03 and DRB1*08:01, thus in near-perfect agreement with the imputation-based analysis. It is worth noting that the imputation-based analysis did indicate a strong signal for DRB1*08:01 in the Finnish cohort (OR = 1.88, $p=6.7\times10^{-9}$). However, the signal in other cohorts is weak ($p>0.01$). Alleles DRB1*08:01 and DRB1*13:03 are closely related both in terms of protein sequence (5 amino acid differences and one 8 amino-acid insertion in 258 aligned residues) and haplotype background, lending support to the notion of shared risk. Independent data support this interpretation.[77]

At HLA-A, the method identifies two variants (Figure S35). In the HapMap CEU panel, one of these jointly tags the A*02 alleles present (in the UK cohort 95% of these are A*02:01, with A*02:05 and A*02:06 comprising 3.5% and 1.5% respectively) and the closely-related allele A*68:01 (13 amino acid differences in 365 aligned residues). In the conditional analysis, A*68:01 shows some association with MS risk ($p_{UK} = 1.1\times10^{-3}$), but while a protective effect is found in seven out of eight cohorts, the effect is not significant ($p_{combined} = 0.61$). Neither A*02:05 nor A*02:06 show a consistent protective effect, but their frequencies are very low (typically c. 1% and <1% respectively). The estimated ORs and p-values for HLA-DRB1*08:01 and HLA-A alleles A*02:05, A*02:06 and A*68:01 are shown below along with cohort-specific (and combined) estimates for each cohort for the alleles described in the main text.

In addition, a second signal is identified that partially tags A*03:01. The tagged A*03:01 haplotypes carry a DRB1*15:01 allele indicating that this signal is likely to reflect LD from 15:01. Weak LD between HLA-A and HLA-DRB1 is well recognised; for A*03:01 and DRB1*15:01 the r^2 =0.2 in the 1958 Birth Cohort data. In the imputation analyses, after conditioning on DRB*15:01, we find no evidence for association between A*03:01 and disease risk ($p_{UK}>0.1$).

Figure S34. DRB1 genealogical tree as in Figure 4 in the main text, but with expanded terminal branches showing individual haplotypes.

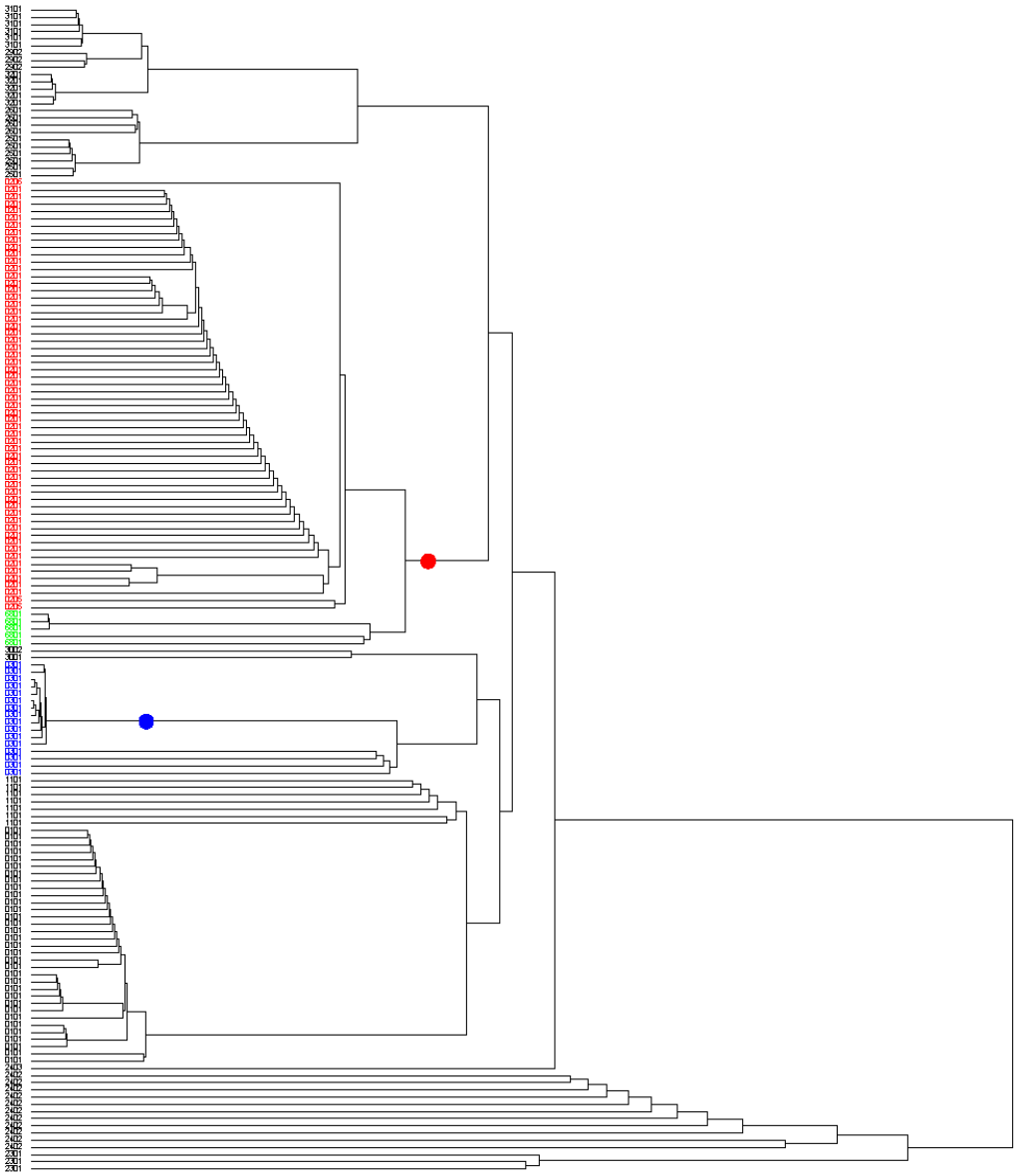

Figure S35. HLA-A genealogical tree as in Figure 4 in the main text with expanded terminal branches showing individual haplotypes.

Estimated coefficients for alleles in each cohort

The following tables (Table S30- Table S38) show the p-values and estimated effect sizes for each of the risk factors (both established and discussed) in each of the cohorts for which we have both case and control data. In each cohort we have fitted the model

$$\log\left(\frac{p}{1-p}\right) = \beta + \beta_{\text{male}}\text{I}_{\text{male}} + \gamma_1\text{G}_1 + \gamma_2\text{G}_2 + \gamma_3\text{G}_3 + \gamma_4\text{G}_4 + \gamma_5\text{G}_5$$

where p is the probability (prospective) of an individual having the disease, β is the baseline coefficient, β_{male} is a gender coefficient for male samples, $\text{I}_{\text{male}} \in \{0,1\}$ is an indicator for gender (1 being male), and γ_1-γ_5 are the coefficients for the genotype effects of each of the five HLA alleles included in our model, denoted here as G_1 - G_5 , where $\text{G}_x \in \{0,1,2\}$ for each of them. Here, G_1 – G_4 are the genotypes for the four risk factors for which there is convincing evidence of association with MS, namely DRB*15:01, DRB*13:03, DRB*03:01 and A*02:01. G_5 denotes HLA alleles for which there is some evidence of co-clustering with A*02:01 and DRB*13:03 in the GENECLUSTER analysis, namely A*68:01 and DRB*08:01.

Table S30. Association of key alleles in defined risk model for UK cohort

Locus/allele	OR	p-value	Freq (cases)	Freq (controls)
DRB*15:01	3.22	3.7E-115	0.310	0.133
DRB*13:03	2.2	3.7E-05	0.015	0.009
DRB*03:01	1.47	2.2E-10	0.159	0.146
A*02:01	0.71	3.1E-12	0.184	0.259
DRB*08:01	1.4	2.5E-02	0.020	0.019
A*02:05	0.69	1.1E-01	0.007	0.010
A*02:06	0.73	4.1E-01	0.004	0.005
A*68:01	0.88	1.1E-03	0.025	0.035

Table S31. Association of key alleles in defined risk model for Italian cohort

Locus/allele	OR	p-value	Freq (cases)	Freq (controls)
DRB*15:01	2.66	4.0E-10	0.121	0.049
DRB*13:03	3.09	4.1E-04	0.028	0.011
DRB*03:01	1.22	1.4E-01	0.113	0.102
A*02:01	0.76	1.4E-02	0.142	0.182
DRB*08:01	1.43	1.7E-01	0.028	0.023
A*02:05	0.78	4.2E-01	0.001	0.009
A*02:06	1.60	7.4E-01	0.001	0.001
A*68:01	0.88	5.9E-01	0.029	0.032

Table S32. Association of key alleles in defined risk model for Norwegian cohort

Locus/allele	OR	p-value	Freq (cases)	Freq (controls)
DRB*15:01	3.33	4.7E-11	0.322	0.132
DRB*13:03	1.53	7.3E-01	0.006	0.004
DRB*03:01	1.27	2.3E-01	0.151	0.132
A*02:01	0.68	6.0E-03	0.237	0.322
DRB*08:01	0.99	9.7E-01	0.041	0.054
A*02:05	>1	1.1E-01	0.005	0
A*02:06	0.42	3.3E-01	0.007	0.008
A*68:01	0.43	4.5E-02	0.018	0.037

Table S33. Association of key alleles in defined risk model for Swedish cohort

Locus/allele	OR	p-value	Freq (cases)	Freq (controls)
DRB*15:01	2.94	1.4E-36	0.329	0.151
DRB*13:03	2.76	3.0E-03	0.015	0.006
DRB*03:01	0.99	7.9E-01	0.106	0.127
A*02:01	0.62	1.0E-09	0.216	0.317
DRB*08:01	1.27	1.7E-01	0.043	0.044
A*02:05	1.09	8.7E-01	0.004	0.004
A*02:06	1.47	3.7E-01	0.011	0.010
A*68:01	0.84	2.9E-01	0.044	0.046

Table S34. Association of key alleles in defined risk model for USA cohort

Locus/allele	OR	p-value	Freq (cases)	Freq (controls)
DRB*15:01	3.25	1.5E-93	0.301	0.120
DRB*13:03	2.35	1.3E-06	0.023	0.013
DRB*03:01	1.39	4.4E-06	0.126	0.115
A*02:01	0.77	9.0E-06	0.179	0.227
DRB*08:01	1.25	1.5E-01	0.023	0.024
A*02:05	0.55	2.6E-02	0.006	0.012
A*02:06	1.48	4.8E-01	0.004	0.003
A*68:01	1.08	5.3E-01	0.039	0.036

Table S35. Association of key alleles in defined risk model for German cohort

Locus/allele	OR	p-value	Freq (cases)	Freq (controls)
DRB*15:01	3.07	1.4E-48	0.302	0.134
DRB*13:03	2.72	4.8E-06	0.027	0.014
DRB*03:01	1.33	5.2E-03	0.113	0.104
A*02:01	0.8	2.1E-03	0.193	0.235
DRB*08:01	1.49	2.3E-02	0.031	0.029
A*02:05	0.96	9.2E-01	0.006	0.006
A*02:06	0.58	4.3E-01	0.003	0.003
A*68:01	0.88	4.1E-01	0.036	0.043

Table S36. Association of key alleles in defined risk model for French cohort

Locus/allele	OR	p-value	Freq (cases)	Freq (controls)
DRB*15:01	4.49	7.4E-22	0.281	0.091
DRB*13:03	1.84	1.5E-01	0.022	0.016
DRB*03:01	1.11	7.3E-01	0.104	0.115
A*02:01	0.74	2.2E-02	0.168	0.226
DRB*08:01	2.26	1.4E-02	0.035	0.023
A*02:05	0.21	8.4E-02	0.001	0.009
A*02:06	0.94	9.7E-01	0.001	0.001
A*68:01	0.81	5.6E-01	0.018	0.025

Table S37. Association of key alleles in defined risk model for Finnish cohort

Locus/allele	OR	p-value	Freq (cases)	Freq (controls)
DRB*15:01	3.03	4.2E-32	0.295	0.133
DRB*13:03	1.77	3.2E-01	0.005	0.005
DRB*03:01	1.12	9.0E-01	0.086	0.101
A*02:01	0.78	1.4E-03	0.214	0.271
DRB*08:01	1.87	6.7E-09	0.142	0.101
A*02:05	0.02	1.6E-01	0	0.001
A*02:06	1.43	1.9E-01	0.030	0.025
A*68:01	0.91	4.6E-01	0.070	0.069

Table S38. Association of key alleles in defined risk model for combined cohorts

Locus/allele	OR	p-value
DRB*15:01	3.08	<1E-312
DRB*13:03	2.43	1.3E-11
DRB*03:01	1.26	3.6E-10
A*02:01	0.73	9.1E-23
DRB*08:01	1.18	1.6E-07
A*02:05	0.76	1.5E-01
A*02:06	1.23	5.1E-01
A*68:01	0.97	6.1E-01

Table S39. Association with MS in each cohort for each of A*02:01, DRB*13:03, and DRB*03:01 under an additive model, after including DRB*15:01 as an independent covariate in the risk model. For the leftmost -$\log_{10}$ p-value and OR, we have assumed a general (2-parameter) model for the effect of DRB*15:01 that allows for departures from additivity. For the rightmost -$\log_{10}$p-value and OR, we have assumed the effect of DRB*15:01 to be additive.

a) A*02:01.

Cohort	-$\log_{10}$P	OR	-$\log_{10}$P	OR
SWE	9.75	0.60	9.23	0.62
NOR	2.60	0.63	2.41	0.65
FIN	3.05	0.75	2.73	0.78
FRA	1.80	0.71	1.72	0.73
ITA	1.77	0.76	1.67	0.81
USA	6.39	0.74	6.01	0.76
GER	3.23	0.77	3.16	0.78
UK	15.44	0.66	14.48	0.68

b) DRB*13:03.

Cohort	-$\log_{10}$P	OR	-$\log_{10}$P	OR
SWE	2.95	3.07	2.87	2.98
NOR	0.29	1.88	0.28	1.69
FIN	0.39	1.50	0.36	1.45
FRA	0.90	1.79	0.88	1.77
ITA	3.28	2.98	3.22	2.92
USA	5.49	2.27	5.36	2.23
GER	5.29	2.63	5.11	2.56
UK	4.11	2.11	4.00	2.07

c) DRB*03:01.

Cohort	$-\log_{10}P$	OR	$-\log_{10}P$	OR
SWE	0.26	1.07	0.22	1.06
NOR	1.21	1.42	1.11	1.39
FIN	0.20	1.06	0.19	1.06
FRA	0.24	1.10	0.20	1.09
ITA	0.99	1.24	0.94	1.22
USA	5.86	1.41	5.44	1.38
GER	2.82	1.36	2.59	1.33
UK	13.61	1.56	12.61	1.52

References

1 Maier, L. M. *et al.* IL2RA genetic heterogeneity in multiple sclerosis and type 1 diabetes susceptibility and soluble interleukin-2 receptor production. *PLoS Genet* **5**, e1000322 (2009).

2 The International Multiple Sclerosis Genetics Consortium (IMSGC). Risk Alleles for Multiple Sclerosis Identified by a Genomewide Study. *N Engl J Med* **357**, 851-862 (2007).

3 The Wellcome Trust Case Control Consortium. Association scan of 14,500 nonsynonymous SNPs in four diseases identifies autoimmunity variants. *Nat Genet* **39**, 1329-1337 (2007).

4 Baranzini, S. E. *et al.* Genome-wide association analysis of susceptibility and clinical phenotype in multiple sclerosis. *Hum Mol Genet* **18**, 767-778 (2009).

5 De Jager, P. L. *et al.* Meta-analysis of genome scans and replication identify CD6, IRF8 and TNFRSF1A as new multiple sclerosis susceptibility loci. *Nat Genet* **41**, 776-782 (2009).

6 The ANZgene Consortium. Genome-wide association study identifies new multiple sclerosis susceptibility loci on chromosomes 12 and 20. *Nat Genet* **41**, 824-828 (2009).

7 Sanna, S. *et al.* Variants within the immunoregulatory CBLB gene are associated with multiple sclerosis. *Nat Genet* **42**, 495-497 (2010).

8 Aulchenko, Y. S. *et al.* Genetic variation in the KIF1B locus influences susceptibility to multiple sclerosis. *Nat Genet* **40**, 1402-1403 (2008).

9 Jakkula, E. *et al.* Genome-wide association study in a high-risk isolate for multiple sclerosis reveals associated variants in STAT3 gene. *Am J Hum Genet* **86**, 285-291 (2010).

10 Nischwitz, S. *et al.* Evidence for VAV2 and ZNF433 as susceptibility genes for multiple sclerosis. *J Neuroimmunol* **227**, 162-166 (2010).

11 Poser, C. M. *et al.* New diagnostic criteria for multiple sclerosis: guidelines for research protocols. *Ann Neurol* **13**, 227-231 (1983).

12 McDonald, W. I. *et al.* Recommended diagnostic criteria for multiple sclerosis: guidelines from the International Panel on the diagnosis of multiple sclerosis. *Ann Neurol* **50**, 121-127 (2001).

13 Polman, C. H. *et al.* Diagnostic criteria for multiple sclerosis: 2005 revisions to the "McDonald Criteria". *Ann Neurol* **58**, 840-846 (2005).

14 Kurtzke, J. F. Rating neurologic impairment in multiple sclerosis: an expanded disability status scale (EDSS). *Neurology* **33**, 1444-1452 (1983).

15 Roxburgh, R. H. *et al.* Multiple Sclerosis Severity Score: using disability and disease duration to rate disease severity. *Neurology* **64**, 1144-1151 (2005).

16 Schumacker, G. A. *et al.* Problems of Experimental Trials of Therapy in Multiple Sclerosis: Report by the Panel on the Evaluation of Experimental Trials of Therapy in Multiple Sclerosis. *Ann N Y Acad Sci* **122**, 552-568 (1965).

17 Confavreux, C., Compston, D. A., Hommes, O. R., McDonald, W. I. & Thompson, A. J. EDMUS, a European database for multiple sclerosis. *J Neurol Neurosurg Psychiatry* **55**, 671-676 (1992).

18 Lublin, F. D. & Reingold, S. C. Defining the clinical course of multiple sclerosis: results of an international survey. National Multiple Sclerosis Society (USA) Advisory Committee on Clinical Trials of New Agents in Multiple Sclerosis. *Neurology* **46**, 907-911 (1996).

19 Hedstrom, A. K., Baarnhielm, M., Olsson, T. & Alfredsson, L. Tobacco smoking, but not Swedish snuff use, increases the risk of multiple sclerosis. *Neurology* **73**, 696-701 (2009).
20 Mack, T. M., Deapen, D. & Hamilton, A. S. Representativeness of a roster of volunteer North American twins with chronic disease. *Twin Res* **3**, 33-42 (2000).
21 Islam, T. *et al.* Differential twin concordance for multiple sclerosis by latitude of birthplace. *Ann Neurol* **60**, 56-64 (2006).
22 The Wellcome Trust Case Control Consortium. Genome-wide association study of 14,000 cases of seven common diseases and 3,000 shared controls. *Nature* **447**, 661-678 (2007).
23 Wedren, S. *et al.* Oestrogen receptor alpha gene haplotype and postmenopausal breast cancer risk: a case control study. *Breast Cancer Res* **6**, R437-449 (2004).
24 Kauffmann, F. *et al.* Epidemiological study of the genetics and environment of asthma, bronchial hyperresponsiveness, and atopy: phenotype issues. *Am J Respir Crit Care Med* **156**, S123-129 (1997).
25 Kauffmann, F. *et al.* EGEA (Epidemiological study on the Genetics and Environment of Asthma, bronchial hyperresponsiveness and atopy)--descriptive characteristics. *Clin Exp Allergy* **29 Suppl 4**, 17-21 (1999).
26 Wichmann, H. E., Gieger, C. & Illig, T. KORA-gen--resource for population genetics, controls and a broad spectrum of disease phenotypes. *Gesundheitswesen* **67 Suppl 1**, S26-30 (2005).
27 Krawczak, M. *et al.* PopGen: population-based recruitment of patients and controls for the analysis of complex genotype-phenotype relationships. *Community Genet* **9**, 55-61 (2006).
28 Farrall, M. *et al.* Genome-wide mapping of susceptibility to coronary artery disease identifies a novel replicated locus on chromosome 17. *PLoS Genet* **2**, e72 (2006).
29 Broadbent, H. M. *et al.* Susceptibility to coronary artery disease and diabetes is encoded by distinct, tightly linked SNPs in the ANRIL locus on chromosome 9p. *Hum Mol Genet* **17**, 806-814 (2008).
30 Conrad, D. F. *et al.* Origins and functional impact of copy number variation in the human genome. *Nature* **464**, 704-712 (2009).
31 Teo, Y. Y. *et al.* A genotype calling algorithm for the Illumina BeadArray platform. *Bioinformatics* **23**, 2741-2746 (2007).
32 Barrett, J. C. *et al.* Genome-wide association study of ulcerative colitis identifies three new susceptibility loci, including the HNF4A region. *Nat Genet* **41**, 1330-1334 (2009).
33 Marchini, J. & Howie, B. Genotype imputation for genome-wide association studies. *Nat Rev Genet* **11**, 499-511 (2010).
34 Balding, D. J. & Nichols, R. A. DNA profile match probability calculation: how to allow for population stratification, relatedness, database selection and single bands. *Forensic Sci Int* **64**, 125-140 (1994).
35 Falush, D., Stephens, M. & Pritchard, J. K. Inference of population structure using multilocus genotype data: linked loci and correlated allele frequencies. *Genetics* **164**, 1567-1587 (2003).
36 Devlin, B. & Roeder, K. Genomic control for association studies. *Biometrics* **55**, 997-1004 (1999).
37 Bacanu, S. A., Devlin, B. & Roeder, K. The power of genomic control. *Am J Hum Genet* **66**, 1933-1944 (2000).

38 Clayton, D. G. *et al.* Population structure, differential bias and genomic control in a large-scale, case-control association study. *Nat Genet* **37**, 1243-1246 (2005).
39 Purcell, S. M. *et al.* Common polygenic variation contributes to risk of schizophrenia and bipolar disorder. *Nature* **460**, 748-752 (2009).
40 Yang, J. *et al.* Genomic inflation factors under polygenic inheritance. *Eur J Hum Genet* (2011).
41 The International Multiple Sclerosis Genetics Consortium (IMSGC). Evidence for polygenic susceptibility to multiple sclerosis--the shape of things to come. *Am J Hum Genet* **86**, 621-625 (2010).
42 Consortium, T. I. H. Integrating common and rare genetic variation in dicerse human populations. *Nature* **467**, 52-58 (2010).
43 Pritchard, J. K., Stephens, M. & Donnelly, P. Inference of population structure using multilocus genotype data. *Genetics* **155**, 945-959 (2000).
44 Astle, W. & Balding, D. J. Population Structure and Cryptic Relatedness in Genetic Association Studies. *Statistical Science* **24**, 451-471 (2009).
45 Yu, J. *et al.* A unified mixed-model method for association mapping that accounts for multiple levels of relatedness. *Nat Genet* **38**, 203-208 (2006).
46 Aulchenko, Y. S., de Koning, D. J. & Haley, C. Genomewide rapid association using mixed model and regression: a fast and simple method for genomewide pedigree-based quantitative trait loci association analysis. *Genetics* **177**, 577-585 (2007).
47 Kang, H. M. *et al.* Efficient control of population structure in model organism association mapping. *Genetics* **178**, 1709-1723 (2008).
48 Zhang, Z. *et al.* Mixed linear model approach adapted for genome-wide association studies. *Nat Genet* **42**, 355-360 (2010).
49 Kang, H. M. *et al.* Variance component model to account for sample structure in genome-wide association studies. *Nat Genet* **42**, 348-354 (2010).
50 Wakefield, J. Bayes factors for genome-wide association studies: comparison with P-values. *Genet Epidemiol* **33**, 79-86 (2009).
51 Zuvich, R. L. *et al.* Genetic variation in the IL7RA/IL7 pathway increases multiple sclerosis susceptibility. *Hum Genet* **127**, 525-535 (2010).
52 Frazer, K. A. *et al.* A second generation human haplotype map of over 3.1 million SNPs. *Nature* **449**, 851-861 (2007).
53 Fujita, P. A. *et al.* The UCSC Genome Browser database: update 2011. *Nucleic Acids Res* **39**, D876-882 (2011).
54 Kathiresan, S. *et al.* Genome-wide association of early-onset myocardial infarction with single nucleotide polymorphisms and copy number variants. *Nat Genet* **41**, 334-341 (2009).
55 Price, A. L. *et al.* Principal components analysis corrects for stratification in genome-wide association studies. *Nat Genet* **38**, 904-909 (2006).
56 Li, Y. Rapid haplotype reconstruction and missing genotype inference. *Am J Hum Genet* **S79**, 2290 (2006).
57 Purcell, S. *et al.* PLINK: a tool set for whole-genome association and population-based linkage analyses. *Am J Hum Genet* **81**, 559-575 (2007).
58 The 1000 Genomes Project Consortium. A map of human genome variation from population-scale sequencing. *Nature* **467**, 1061-1073 (2010).
59 Hindorff LA, J. H., Hall PN, Mehta JP, and Manolio TA. *A Catalog of Published Genome-Wide Association Studies*, <www.genome.gov/gwastudies> (2010).
60 Ashburner, M. *et al.* Gene ontology: tool for the unification of biology. The Gene Ontology Consortium. *Nat Genet* **25**, 25-29 (2000).

61 The Universal Protein Resource (UniProt) in 2010. *Nucleic Acids Res* **38**, D142-148 (2010).
62 Hemminki, K., Li, X., Sundquist, J., Hillert, J. & Sundquist, K. Risk for multiple sclerosis in relatives and spouses of patients diagnosed with autoimmune and related conditions. *Neurogenetics* **10**, 5-11 (2009).
63 Reich, T., James, J. W. & Morris, C. A. The use of multiple thresholds in determining the mode of transmission of semi-continuous traits. *Ann Hum Genet* **36**, 163-184 (1972).
64 Higgins, J. P., Thompson, S. G., Deeks, J. J. & Altman, D. G. Measuring inconsistency in meta-analyses. *Bmj* **327**, 557-560 (2003).
65 Compston, A. *et al. McAlpine's Multiple Sclerosis*. Fourth edn, (Churchill Livingstone, 2006).
66 Willer, C. J. *et al.* Timing of birth and risk of multiple sclerosis: population based study. *BMJ* **330**, 120 (2005).
67 Sadovnick, A. D., Duquette, P., Herrera, B., Yee, I. M. & Ebers, G. C. A timing-of-birth effect on multiple sclerosis clinical phenotype. *Neurology* **69**, 60-62 (2007).
68 Leslie, S., Donnelly, P. & McVean, G. A statistical method for predicting classical HLA alleles from SNP data. *Am J Hum Genet* **82**, 48-56 (2008).
69 de Bakker, P. I. *et al.* A high-resolution HLA and SNP haplotype map for disease association studies in the extended human MHC. *Nat Genet* **38**, 1166-1172 (2006).
70 Dilthey, A., Moutsianas, L., Leslie, S. & McVean, G. HLA*IMP - an integrated framework for imputing classical HLA alleles from SNP genotypes. *Bioinformatics* **00**, 1-5 (2011).
71 Horton, R. *et al.* Gene map of the extended human MHC. *Nat Rev Genet* **5**, 889-899 (2004).
72 Howie, B. N., Donnelly, P. & Marchini, J. A flexible and accurate genotype imputation method for the next generation of genome-wide association studies. *PLoS Genet* **5**, e1000529 (2009).
73 Stephens, M., Smith, N. J. & Donnelly, P. A new statistical method for haplotype reconstruction from population data. *Am J Hum Genet* **68**, 978-989 (2001).
74 Scheet, P. & Stephens, M. A fast and flexible statistical model for large-scale population genotype data: applications to inferring missing genotypes and haplotypic phase. *Am J Hum Genet* **78**, 629-644 (2006).
75 Field, J. *et al.* A polymorphism in the HLA-DPB1 gene is associated with susceptibility to multiple sclerosis. *PLoS One* **5**, e13454 (2010).
76 Su, Z., Cardin, N., Donnelly, P. & Marchini, J. A Bayesian method for detecting and characterizing allelic heterogeneity and boosting signals in genome-wide association studies. *Statistical Science* **24**, 430-450 (2009).
77 Dyment, D. A. *et al.* Complex interactions among MHC haplotypes in multiple sclerosis: susceptibility and resistance. *Hum Mol Genet* **14**, 2019-2026 (2005).

Individual contributions

Sample acquisition

Stephen Sawcer[1], Annette Bang Oturai[10], Janna Saarela[11], Bertrand Fontaine[12], Bernhard Hemmer[13], Frauke Zipp[14,15], Roland Martin[16], Stanley Hawkins[18], Sandra D'alfonso[19], Filippo Martinelli Boneschi[20], Hanne F. Harbo[21,22], Anne Spurkland[23], Marcin P. Mycko[24], Manuel Comabella[25], Clive Hawkins[27], John Zajicek[28], Neil Robertson[29], Lisa F. Barcellos[30,31], Roby Abraham[27], Lars Alfredsson[32], Katharine Baker[29], Laura Bergamaschi[19], Roberto Bergamaschi[34], Allan Bernstein[31], Achim Berthele[13], Mike Boggild[35], David Brassat[37], Simon A. Broadley[38], Dorothea Buck[13], Helmut Butzkueven[39-42], Ruggero Capra[43], William M. Carroll[44], Paola Cavalla[45], Elisabeth G. Celius[21], Sabine Cepok[13], Rosetta Chiavacci[36], Katleen Clysters[9], Giancarlo Comi[20], Mark Cossburn[29], Mathew B. Cox[47], Wendy Cozen[48], Bruce A.C. Cree[33], Anne H. Cross[49], Marc Debouverie[56], Marie Beatrice D'hooghe[57], Bénédicte Dubois[9], Irina Elovaara[59,60], Federica Esposito[20], Simon Foote[61], Daniela Galimberti[62], Angelo Ghezzi[63], Refujia Gomez[33], Olivier Gout[64], Franca Rosa Guerini[68], Per Hall[69], Anders Hamsten[70], Hans-Peter Hartung[71], Rob N. Heard[8], Jeremy Hobart[28], Muna Hoshi[13], Carmen Infante-Duarte[73], Gillian Ingram[29], Wendy Ingram[28], Talat Islam[48], Allan G. Kermode[44], Trevor J. Kilpatrick[39,40,75], Keijo Koivisto[77], Jeannette S. Lechner-Scott[47,78], Maurizio A. Leone[79], Åslaug R. Lorentzen[22,83], Thomas Mack[48], Mark Marriott[39,40], Vittorio Martinelli[20], Deborah Mason[86], Tania Mihalova[27], Xavier Montalban[25], John Mottershead[88,89], Kjell-Morten Myhr[90,91], Paola Naldi[79], Alison Page[92], Jean Pelletier[95], Laura Piccio[49], Trevor Pickersgill[29], Fredrik Piehl[26], Susan Pobywajlo[5], Hong L. Quach[30], Patricia P. Ramsay[30], Mauri Reunanen[96], Richard Reynolds[97], Mariaemma Rodegher[20], Sabine Roesner[16], Justin P. Rubio[39], Marco Salvetti[99], Catherine A. Schaefer[31], Rodney J. Scott[47], Finn Sellebjerg[10], Krzysztof W. Selmaj[24], Ling Shen[31], Brigid Simms-Acuna[31], Sheila Skidmore[1], Cathrine Smestad[21], Per Soelberg Sørensen[10], Jim Stankovich[61], Richard C. Strange[27], Bruce Taylor[61], Pentti Tienari[106], Ayman Tourbah[108], Niall Tubridy[40,111], Jane Vickery[28], Pablo Villoslada[114], Ernest Willoughby[122], Juliane Winkelmann[13,123,124], Jacqueline Yaouanq[126], Jorge R. Oksenberg[33], Tomas Olsson[26], Jan Hillert[26], Adrian J. Ivinson[51,130], Philip L. De Jager[4,5,51], Leena Peltonen[7,11,80,93,94], Graeme J. Stewart[8], David A. Hafler[4,131], Stephen L. Hauser[33], Alastair Compston[1]

DNA processing

Sarah Edkins[7], Emma Gray[7], Emma Davis[53], Katherine Dixon[53], David R. Booth[8], An Goris[9], Annette Bang Oturai[10], Janna Saarela[11], Rhian Gwilliam[7], Sandra D'alfonso[19], Filippo Martinelli Boneschi[20], Jennifer Liddle[7], Hanne F. Harbo[21,22], Marc L. Perez[7], Anne Spurkland[23], Matthew J Waller[7], Marcin P. Mycko[24], Michelle Ricketts[7], Manuel Comabella[25], Ingrid Kockum[26], Owen T. McCann[7], Maria Ban[1], Pamela Whittaker[7], Anu Kemppinen[1], Paul Weston[7], Clive Hawkins[27], Sara Widaa[7], Neil Robertson[29], Lisa F. Barcellos[30,31], Roby Abraham[27], Kristin Ardlie[4], Cristin Aubin[4], Amie Baker[1], Laura Bergamaschi[19], Simon A. Broadley[38], Sabine Cepok[13], Françoise Clerget-Darpoux [46], Isabelle Cournu-Rebeix[12], Mathew B. Cox[47], Anne H. Cross[49], Rita Dobosi[9], Federica Esposito[20], Claire Fontenille[12], Simon Foote[61], Colin Graham[65], Anders Hamsten[70], Carmen Infante-Duarte[73], Gillian Ingram[29], Maja Jagodic[26], Norman Klopp[76], Jeannette S. Lechner-Scott[47,78], Virpi Leppä[11,80], Izaura Lima Bomfim[26], Robin R. Lincoln[33], Jenny Link[26], Jianjun Liu[82], Åslaug R. Lorentzen[22,83], Sara Lupoli[50,84], Jacob L. McCauley[87], Inger-Lise Mero[21,83], Tania Mihalova[27], William Ollier[53], Laura Piccio[49], Hong L. Quach[30], Patricia P. Ramsay[30], Richard Reynolds[97], Justin P. Rubio[39], Adam Santaniello[33], Christian Schulze[102], Rodney J. Scott[47], David Sexton[103], Helle Bach Søndergaard[10], Richard C. Strange[27], Anna-Maija Sulonen[11,80], Emilie Sundqvist[26], Bruce Taylor[61], Ewa Tronczynska[24], Pablo Villoslada[114], Rebecca Zuvich[103], Philip L. De Jager[4,5,51], Panos Deloukas[7], Cordelia Langford[7]

Genotyping

Sarah E. Hunt[7], Sarah Edkins[7], Emma Gray[7], Rhian Gwilliam[7], Rathi Ravindrarajah[7], Hannah Blackburn[7], Suzannah J. Bumpstead[7], Serge Dronov[7], Matthew Gillman[7], Naomi Hammond[7],

Alagurevathi Jayakumar[7], Jennifer Liddle[7], Marc L. Perez[7], Simon C. Potter[7], Matthew J Waller[7], Michelle Ricketts[7], Owen T. McCann[7], Pamela Whittaker[7], Paul Weston[7], Sara Widaa[7], Panos Deloukas[7] Cordelia Langford[7]

Analysis of Primary Data
Garrett Hellenthal[2], Matti Pirinen[2], Loukas Moutsianas[6], Alexander Dilthey[6], Zhan Su[2], Stephen Sawcer[1], Colin Freeman[2], Gavin Band[2], Amy Strange[2], Céline Bellenguez[2], James Wason[117], Stephen Leslie[17], Eleni Giannoulatou[2], Gil McVean[2], Peter Donnelly[2,6], Chris C.A. Spencer[2]

Analysis of Replication Data
Nikolaos A. Patsopoulos[3-5], Paul I.W. de Bakker[3,4,54,55], Philip L. De Jager[4,5,51]

Data handling (clinical, demographic or genotypic)
Stephen Sawcer[1], Garrett Hellenthal[2], Matti Pirinen[2], Chris C.A. Spencer[2], Nikolaos A. Patsopoulos[3-5], Loukas Moutsianas[6], Alexander Dilthey[6], Zhan Su[2], Colin Freeman[2], Sarah E. Hunt[7], Sarah Edkins[7], Emma Gray[7], David R. Booth[8], Simon C. Potter[7], An Goris[9], Gavin Band[2], Annette Bang Oturai[10], Amy Strange[2], Janna Saarela[11], Céline Bellenguez[2], Bertrand Fontaine[12], Matthew Gillman[7], Bernhard Hemmer[13], Rhian Gwilliam[7], Frauke Zipp[14,15], Roland Martin[16], Stephen Leslie[17], Stanley Hawkins[18], Eleni Giannoulatou[2], Sandra D'alfonso[19], Filippo Martinelli Boneschi[20], Jennifer Liddle[7], Hanne F. Harbo[21,22], Marc L. Perez[7], Matthew J Waller[7], Marcin P. Mycko[24], Michelle Ricketts[7], Manuel Comabella[25], Ingrid Kockum[26], Owen T. McCann[7], Maria Ban[1], Pamela Whittaker[7], Anu Kemppinen[1], Paul Weston[7], Clive Hawkins[27], Sara Widaa[7], John Zajicek[28], Neil Robertson[29], Lisa F. Barcellos[30,31], Rathi Ravindrarajah[7], Roby Abraham[27], Lars Alfredsson[32], Kristin Ardlie[4], Cristin Aubin[4], Amie Baker[1], Katharine Baker[29], Sergio E. Baranzini[33], Laura Bergamaschi[19], Roberto Bergamaschi[34], Allan Bernstein[31], Achim Berthele[13], Mike Boggild[35], Jonathan P. Bradfield[36], David Brassat[37], Simon A. Broadley[38], Dorothea Buck[13], Helmut Butzkueven[39-42], Ruggero Capra[43], William M. Carroll[44], Paola Cavalla[45], Elisabeth G. Celius[21], Sabine Cepok[13], Rosetta Chiavacci[36], Françoise Clerget-Darpoux [46], Katleen Clysters[9], Giancarlo Comi[20], Mark Cossburn[29], Isabelle Cournu-Rebeix[12], Mathew B. Cox[47], Bruce A.C. Cree[33], Daniele Cusi[50], Mark J. Daly[4,51,52], Emma Davis[53], Paul I.W. de Bakker[3,4,54,55], Marc Debouverie[56], Marie Beatrice D'hooghe[57], Katherine Dixon[53], Rita Dobosi[9], Bénédicte Dubois[9], David Ellinghaus[58], Irina Elovaara[59,60], Federica Esposito[20], Claire Fontenille[12], Andre Franke[58], Daniela Galimberti[62], Angelo Ghezzi[63], Joseph Glessner[36], Refujia Gomez[33], Olivier Gout[64], Colin Graham[65], Struan F.A. Grant[36,66,67], Franca Rosa Guerini[68], Hakon Hakonarson[36,66,67], Anders Hamsten[70], Hans-Peter Hartung[71], Rob N. Heard[8], Simon Heath[72], Jeremy Hobart[28], Muna Hoshi[13], Carmen Infante-Duarte[73], Gillian Ingram[29], Wendy Ingram[28], Maja Jagodic[26], Michael Kabesch[74], Allan G. Kermode[44], Trevor J. Kilpatrick[39,40,75], Cecilia Kim[36], Keijo Koivisto[77], Malin Larsson[70], Mark Lathrop[72], Jeannette S. Lechner-Scott[47,78], Maurizio A. Leone[79], Virpi Leppä[11,80], Ulrika Liljedahl[81], Izaura Lima Bomfim[26], Robin R. Lincoln[33], Jenny Link[26], Åslaug R. Lorentzen[22,83], Sara Lupoli[50,84], Fabio Macciardi[50,85], Mark Marriott[39,40], Vittorio Martinelli[20], Deborah Mason[86], Jacob L. McCauley[87], Frank Mentch[36], Inger-Lise Mero[21,83], Tania Mihalova[27], Xavier Montalban[25], John Mottershead[88,89], Kjell-Morten Myhr[90,91], Paola Naldi[79], William Ollier[53], Alison Page[92], Aarno Palotie[7,11,93,94], Jean Pelletier[95], Trevor Pickersgill[29], Fredrik Piehl[26], Susan Pobywajlo[5], Patricia P. Ramsay[30], Mauri Reunanen[96], Richard Reynolds[97], John D. Rioux[98], Mariaemma Rodegher[20], Sabine Roesner[16], Justin P. Rubio[39], Ina-Maria Rückert[76], Marco Salvetti[99], Erika Salvi[50,100], Adam Santaniello[33], Catherine A. Schaefer[31], Stefan Schreiber[58,101], Christian Schulze[102], Rodney J. Scott[47], Finn Sellebjerg[10], Krzysztof W. Selmaj[24], David Sexton[103], Ling Shen[31], Brigid Simms-Acuna[31], Sheila Skidmore[1], Patrick M.A. Sleiman[36,66], Cathrine Smestad[21], Per Soelberg Sørensen[10], Helle Bach Søndergaard[10], Jim Stankovich[61], Richard C. Strange[27], Anna-Maija Sulonen[11,80], Emilie Sundqvist[26], Ann-Christine Syvänen[81], Francesca Taddeo[100], Bruce Taylor[61], Pentti Tienari[106], Ayman Tourbah[108], Ewa Tronczynska[24], Niall Tubridy[40,111], Jane Vickery[28], Pablo Villoslada[114], Kai Wang[36,66], James Wason[117], H-Erich Wichmann[76,119,120], Ernest Willoughby[122], Juliane Winkelmann[13,123,124], Michael Wittig[58,125],

Jacqueline Yaouanq[126], Haitao Zhang[36,66], Rebecca Zuvich[103], Panos Deloukas[7], Cordelia Langford[7], Audrey Duncanson[129], Jorge R. Oksenberg[33], Margaret A. Pericak-Vance[87], Jonathan L. Haines[103], Tomas Olsson[26], Jan Hillert[26], Philip L. De Jager[4,5,51], Leena Peltonen[7,11,80,93,94], Graeme J. Stewart[8], David A. Hafler[4,131], Stephen L. Hauser[33], Alastair Compston[1], Peter Donnelly[2,6]

Provider of control genotypes
Lars Alfredsson[32], Jonathan P. Bradfield[36], Rosetta Chiavacci[36], Daniele Cusi[50], David Ellinghaus[58], Andre Franke[58], Joseph Glessner[36], Struan F.A. Grant[36,66,67], Franca Rosa Guerini[68], Hakon Hakonarson[36,66,67], Per Hall[69], Anders Hamsten[70], Simon Heath[72], Michael Kabesch[74], Cecilia Kim[36], Norman Klopp[76], Malin Larsson[70], Mark Lathrop[72], Ulrika Liljedahl[81], Jianjun Liu[82], Sara Lupoli[50,84], Fabio Macciardi[50,85], Frank Mentch[36], Tomas Olsson[26], Aarno Palotie[7,11,93,94], Leena Peltonen[7,11,80,93,94], Ina-Maria Rückert[76], Erika Salvi[50,100], Stefan Schreiber[58,101], Ann-Christine Syvänen[81], Francesca Taddeo[100], Kai Wang[36,66], H-Erich Wichmann[76,119,120], Michael Wittig[58,125], Haitao Zhang[36,66]

Project Direction
Stephen Sawcer[1], Garrett Hellenthal[2], Matti Pirinen[2], Chris C.A. Spencer[2], Leena Peltonen[7,11,80,93,94], Graeme J. Stewart[8], David A. Hafler[4,131], Stephen L. Hauser[33], Gil McVean[2], Peter Donnelly[2,6], Alastair Compston[1]

Membership of Wellcome Trust Case Control Consortium 2

Management Committee

Peter Donnelly (Chair)[2,6], Ines Barroso (Deputy Chair)[7], Jenefer M. Blackwell[104,105], Elvira Bramon[107], Matthew A. Brown[109], Juan P. Casas[110], Aiden Corvin[112], Panos Deloukas[7], Audrey Duncanson[129], Janusz Jankowski[113], Hugh S. Markus[115], Christopher G. Mathew[116], Colin N.A. Palmer[118], Robert Plomin[121], Anna Rautanen[2], Stephen Sawcer[1], Richard C. Trembath[116], Ananth C. Viswanathan[127], Nicholas W. Wood[128]

Data and Analysis Group

Chris C.A. Spencer[2], Gavin Band[2], Céline Bellenguez[2], Colin Freeman[2], Garrett Hellenthal[2], Eleni Giannoulatou[2], Matti Pirinen[2], Richard Pearson[2], Amy Strange[2], Zhan Su[2], Damjan Vukcevic[2], Peter Donnelly[2,6],

DNA, Genotyping, Data QC and Informatics Group

Cordelia Langford[7], Sarah E. Hunt[7], Sarah Edkins[7], Rhian Gwilliam[7], Hannah Blackburn[7], Suzannah J. Bumpstead[7], Serge Dronov[7], Matthew Gillman[7], Emma Gray[7], Naomi Hammond[7], Alagurevathi Jayakumar[7], Owen T. McCann[7], Jennifer Liddle[7], Simon C. Potter[7], Rathi Ravindrarajah[7], Michelle Ricketts[7], Matthew J Waller[7], Paul Weston[7], Sara Widaa[7], Pamela Whittaker[7], Ines Barroso[7], Panos Deloukas[7]

Associate Members

Alexander Dilthey[6], Stephen Leslie[17], Loukas Moutsianas[6], Marc L. Perez[7], Gil McVean[2]

Publications Committee

Christopher G. Mathew (Chair)[116], Jenefer M. Blackwell[104,105], Matthew A. Brown[109], Aiden Corvin[112], Mark I McCarthy[132], Chris C.A. Spencer[2]

Membership of the International Multiple Sclerosis Genetics Consortium

Strategic Group

Stephen Sawcer[1], Maria Ban[1], Anu Kemppinen[1], David R. Booth[8], An Goris[9], Bénédicte Dubois[9], Annette Bang Oturai[10], Janna Saarela[11], Bertrand Fontaine[12], Bernhard Hemmer[13], Frauke Zipp[14,15], Roland Martin[16], Stanley Hawkins[18], Sandra D'alfonso[19], Filippo Martinelli Boneschi[20], Hanne F. Harbo[21,22], Anne Spurkland[23], Marcin P. Mycko[24], Manuel Comabella[25], Ingrid Kockum[26], Tomas Olsson[26], Jan Hillert[26], John D. Rioux[98], Clive Hawkins[27], Philip L. De Jager[4,5,51], Lisa F. Barcellos[30,31], Sergio E. Baranzini[33], Jorge R. Oksenberg[33], Margaret A. Pericak-Vance[87], Jacob L. McCauley[87], Jonathan L. Haines[103]

Ordinary Members

Roby Abraham[27], Lars Alfredsson[32], Kristin Ardlie[4], Cristin Aubin[4], Amie Baker[1], Katharine Baker[29], Laura Bergamaschi[19], Roberto Bergamaschi[34], Allan Bernstein[31], Achim Berthele[13], Mike Boggild[35], David Brassat[37], Simon A. Broadley[38], Dorothea Buck[13], Helmut Butzkueven[39-42], Ruggero Capra[43], William M. Carroll[44], Paola Cavalla[45], Elisabeth G. Celius[21], Sabine Cepok[13], Françoise Clerget-Darpoux [46], Katleen Clysters[9], Giancarlo Comi[20], Mark Cossburn[29], Isabelle Cournu-Rebeix[12], Mathew B. Cox[47], Wendy Cozen[48], Bruce A.C. Cree[33], Anne H. Cross[49], Mark J. Daly[4,51,52], Emma Davis[53], Paul I.W. de Bakker[3,4,54,55], Marc Debouverie[56], Marie Beatrice D'hooghe[57], Katherine Dixon[53], Rita Dobosi[9], Irina Elovaara[59,60], Federica Esposito[20], Claire Fontenille[12], Simon Foote[61], Daniela Galimberti[62], Angelo Ghezzi[63], Refujia Gomez[33], Olivier Gout[64], Colin Graham[65], Hans-Peter Hartung[71], Rob N. Heard[8], Jeremy Hobart[28], Muna Hoshi[13], Carmen Infante-Duarte[73], Gillian Ingram[29], Wendy Ingram[28], Talat Islam[48], Maja Jagodic[26], Allan G. Kermode[44], Trevor J. Kilpatrick[39,40,75], Keijo Koivisto[77], Jeannette S. Lechner-Scott[47,78], Maurizio A. Leone[79], Virpi Leppä[11,80], Izaura Lima Bomfim[26], Robin R. Lincoln[33], Jenny Link[26], Åslaug R. Lorentzen[22,83], Thomas Mack[48], Mark Marriott[39,40], Vittorio Martinelli[20], Deborah Mason[86], Inger-Lise Mero[21,83], Tania Mihalova[27], Xavier Montalban[25], John Mottershead[88,89], Kjell-Morten Myhr[90,91], Paola Naldi[79], William Ollier[53], Alison Page[92], Aarno Palotie[7,11,93,94], Nikolaos A. Patsopoulos[3-5], Jean Pelletier[95], Laura Piccio[49], Trevor Pickersgill[29], Fredrik Piehl[26], Susan Pobywajlo[5], Hong L. Quach[30], Patricia P. Ramsay[30], Mauri Reunanen[96], Richard Reynolds[97], Neil Robertson[29], Mariaemma Rodegher[20], Sabine Roesner[16], Justin P. Rubio[39], Marco Salvetti[99], Adam Santaniello[33], Catherine A. Schaefer[31], Christian Schulze[102], Rodney J. Scott[47], Finn Sellebjerg[10], Krzysztof W. Selmaj[24], David Sexton[103], Ling Shen[31], Brigid Simms-Acuna[31], Sheila Skidmore[1], Cathrine Smestad[21], Per Soelberg Sørensen[10], Helle Bach Søndergaard[10], Jim Stankovich[61], Richard C. Strange[27], Anna-Maija Sulonen[11,80], Emilie Sundqvist[26], Bruce Taylor[61], Pentti Tienari[106], Ayman Tourbah[108], Ewa Tronczynska[24], Niall Tubridy[40,111], Jane Vickery[28], Pablo Villoslada[114], James Wason[117], Ernest Willoughby[122], Juliane Winkelmann[13,123,124], Jacqueline Yaouanq[126], John Zajicek[28], Rebecca Zuvich[103]

Associate Members

Jonathan P. Bradfield[36], Rosetta Chiavacci[36], Daniele Cusi[50], David Ellinghaus[58], Andre Franke[58], Joseph Glessner[36], Struan F.A. Grant[36,66,67], Franca Rosa Guerini[68], Hakon Hakonarson[36,66,67], Per Hall[69], Anders Hamsten[70], Simon Heath[72], Michael Kabesch[74], Cecilia Kim[36], Norman Klopp[76], Malin Larsson[70], Mark Lathrop[72], Ulrika Liljedahl[81], Jianjun Liu[82], Sara Lupoli[50,84], Fabio Macciardi[50,85], Frank Mentch[36], Ina-Maria Rückert[76], Erika Salvi[50,100], Stefan Schreiber[58,101], Ann-Christine Syvänen[81], Francesca Taddeo[100], Kai Wang[36,66], H-Erich Wichmann[76,119,120], Michael Wittig[58,125], Haitao Zhang[36,66]

Governance Group

Adrian J. Ivinson[51,130], Leena Peltonen[7,11,80,93,94], Graeme J. Stewart[8], David A. Hafler[4,131], Stephen L. Hauser[33], Alastair Compston[1]

Affiliations

1. University of Cambridge, Department of Clinical Neurosciences, Addenbrooke's Hospital, BOX 165, Hills Road, Cambridge, CB2 0QQ, UK.
2. Wellcome Trust Centre for Human Genetics, Roosevelt Drive, Oxford OX3 7BN, UK.
3. Division of Genetics, Department of Medicine, Brigham and Women's Hospital, Harvard Medical School, Boston, MA 02115, USA.
4. Broad Institute of Harvard University and Massachusetts Institute of Technology, Cambridge, MA, USA.
5. Center for Neurologic Diseases, Department of Neurology, Brigham & Women's Hospital, Boston, MA 02115, USA.
6. Dept Statistics, University of Oxford, Oxford OX1 3TG, UK.
7. Wellcome Trust Sanger Institute, Wellcome Trust Genome Campus, Hinxton, Cambridge CB10 1SA, UK.
8. Westmead Millennium Institute, University of Sydney, Australia.
9. Laboratory for Neuroimmunology, Section of Experimental Neurology, Katholieke Universiteit Leuven, 3000 Leuven, Belgium.
10. Danish Multiple Sclerosis Center, Department of Neurology, Copenhagen University Hospital, Rigshospitalet, 2100 Copenhagen, Denmark
11. Institute for Molecular Medicine Finland (FIMM), University of Helsinki, Helsinki, 00290, Finland.
12. INSERM UMR S 975 CRICM, UPMC, Département de neurologie Pitié-Salpêtrière, AP-HP, Paris, France.
13. Department of Neurology, Klinikum Rechts der Isar der Technischen Universität, Ismaninger Strasse 22, 81675 Munich, Germany
14. Department of Neurology, University Medicine Mainz, Johannes Gutenberg University Mainz, Langenbeckstr. 1, 55131 Mainz, Germany.
15. Max Delbrueck Center for Molecular Medicine, Robert-Rössle-Str. 10, 13092 Berlin, Germany.
16. Institute for Neuroimmunology and Clinical MS Research (inims), Centre for Molecular Neurobiology, Falkenried 94, D-20251 Hamburg, Germany
17. Department of Clinical Pharmacology, University of Oxford, Old Road Campus Research Building , Old Road Campus, Oxford, OX3 7DQ, UK.
18. Queen's University Belfast, University Road, Belfast, BT7 1NN, Northern Ireland, UK.
19. Department of Medical Sciences and Interdisciplinary Research Center of Autoimmune Diseases (IRCAD), University of Eastern Piedmont, Novara, Italy.
20. Department of Neurology, Institute of Experimental Neurology (INSPE), Division of Neuroscience, San Raffaele Scientific Institute, Via Olgettina 58, 20132, Milan, Italy.
21. Department of Neurology, Oslo University Hospital, N-0407 Oslo, Norway.
22. Department of Neurology, University of Oslo, N-0318 Oslo, Norway
23. Institute of Basal Medical Sciences, University of Oslo, N-0317 Oslo, Norway.
24. Department of Neurology, Laboratory of Neuroimmunology, Medical University of Lodz, Kopcinskiego 22, 90-153 Lodz, Poland.
25. Clinical Neuroinmunology Unit, Multiple Sclerosis Center of Catalonia (CEM-Cat), Vall d'Hebron University Hospital, Barcelona, Spain.
26. Department of Clinical Neurosciences, Centre for Molecular Medicine CMM, L8:04, Karolinska Institutet, Karolinska Hospital, 171 76 Stockholm, Sweden.
27. Keele University Medical School, Stoke-on-Trent, UK.
28. Peninsula College of Medicine and Dentistry, Universities of Exeter and Plymouth, Clinical Neurology Research Group, Tamar Science Park, Plymouth, PL6 8BX, UK.
29. Department of Neurology, University Hospital of Wales, Heath Park, Cardiff, CF14 4XW, UK.

30. Genetic Epidemiology and Genomics Laboratory, Division of Epidemiology, School of Public Health, University of California, Berkeley, CA 94720-7356, USA.
31. Kaiser Permanente Northern California Division of Research, 2000 Broadway, Oakland, CA, 94612, USA.
32. Institute of Environmental Medicine, Karolinska Institutet, Box 210, 171 77 Stockholm, Sweden.
33. Department of Neurology, University of California San Francisco, 505 Parnassus Avenue, S-256, San Francisco, CA 94143-0435, USA.
34. Neurological Institute C. Mondino, IRCCS, Pavia, Italy.
35. The Walton Centre for Neurology and Neurosurgery, Liverpool, UK.
36. Center for Applied Genomics, The Children's Hospital of Philadelphia, 3615 Civic Center Blvd., Philadelphia, PA, 19104, USA.
37. INSERM U 563 et Pôle Neurosciences, Hopital Purpan, Toulouse, France.
38. School of Medicine, Griffith University, Australia.
39. Florey Neuroscience Institutes, University of Melbourne, Victoria, Australia 3010.
40. Royal Melbourne Hospital, Parkville, Victoria, Australia, 3050.
41. Box Hill Hospital, Box Hill 3128, Australia.
42. Department of Medicine, RMH Cluster, University of Melbourne, Victoria, Australia 3010.
43. Multiple Sclerosis Centre, Department of Neurology, Ospedali Civili di Brescia, Brescia, Italy.
44. Centre for Neuromuscular and Neurological Disorders, University of Western Australia, Perth WA 6009, Australia.
45. Department of Neurosciences, University of Turin, A.O.U. San Giovanni Battista,Turin, Italy.
46. INSERM U535, Univ Paris-Sud, Villejuif, France.
47. University of Newcastle, University Drive, Callaghan NSW 2308, Australia.
48. Department of Preventive Medicine, Keck School of Medicine, University of Southern California, 1540 Alcazar St. NOR 4453, Los Angeles, CA 90033.
49. Department of Neurology, Washington University, St Louis MO, USA.
50. University of Milan, Department of Medicine, Surgery and Dentistry, AO San Paolo, University of Milan, c/o Filarete Foundation - Viale Ortles 22/4 - 20139 Milano, Italy.
51. Harvard Medical School, Boston, MA, USA.
52. Center for Human Genetic Research, Massachusetts General Hospital, USA.
53. The UK DNA Banking Network, Centre for Integrated Genomic Medical Research, University of Manchester, UK.
54. Department of Medical Genetics, Division of Biomedical Genetics, University Medical Center Utrecht, Utrecht, The Netherlands.
55. Julius Center for Health Sciences and Primary Care, University Medical Center Utrecht, Utrecht, The Netherlands.
56. Service de Neurologie, Hôpital Central, Nancy, France.
57. National Multiple Sclerosis Center, 1820 Melsbroek, Belgium.
58. Institute for Clinical Molecular Biology, Christian-Albrechts-University, Kiel, Germany.
59. Department of Neurology, Tampere University Hospital, Tampere, Finland.
60. University of Tampere, Medical School, Tampere, Finland.
61. Menzies Research Institute, Locked Bag 23, Hobart, Tasmania, Australia 7000.
62. Department of Neurological Sciences, Centro Dino Ferrari, University of Milan, Fondazione Cà Granda, Ospedale Maggiore Policlinico, Milan, Italy.
63. Centro Studi Sclerosi Multipla, Ospedale di Gallarate, Gallarate (VA), Italy.
64. Service de Neurologie, Fondation Ophtalmologique Adolphe de Rothschild, Paris, France.
65. Belfast Health and Social Care Trust, City Hospital, Belfast BT9 7AB, Northern Ireland,UK.

66. Division of Genetics, The Children's Hospital of Philadelphia, 3615 Civic Center Blvd., Philadelphia, PA, 19104, USA.
67. Department of Pediatrics, University of Pennsylvania School of Medicine, 3615 Civic Center Blvd., Philadelphia, PA, 19104, USA.
68. Laboratory of Molecular Medicine and Biotechnology, Don C. Gnocchi Foundation IRCCS, S. Maria Nascente, Milan, Italy.
69. Department of Medical Epidemiology and Biostatistics, Karolinska Institute, 17177 Stockholm, Sweden.
70. Atherosclerosis Research Unit, Department of Medicine Solna, Karolinska Institutet, Center for Molecular Medicine, L8:03, Karolinska University Hospital Solna, S-171 76 Stockholm, Sweden.
71. Department of Neurology, Heinrich-Heine-University, Düsseldorf, Germany.
72. Centre National de Genotypage, 2 rue Gaston Cremieux, CO 5721, 91057 Evry Cedex, France.
73. Experimental and Clinical Research Center, Charité – Universitätsmedizin Berlin and Max Delbrueck Center for Molecular Medicine, Berlin, Germany.
74. Clinic for Paediatric Pneumology, Allergology and Neonatology, Hannover Medical School, Germany.
75. Centre for Neuroscience, University of Melbourne, Victoria, Australia 3010.
76. Institute of Epidemiology, Helmholtz Zentrum München, German Research Center for Environmental Health, Ingolstädter Landstrasse 1, 85764 Neuherberg, Munich, Germany.
77. Seinäjoki Central Hospital, Seinäjoki, Finland.
78. Hunter Medical Research Institute, John Hunter Hospital, Lookout Road, New Lambton NSW 2305, Australia.
79. SCDU Neurology, Maggiore della Carità Hospital, Novara, Italy.
80. Unit of Public Health Genomics, National Institute for Health and Welfare, Helsinki, 00290, Finland.
81. Molecular Medicine, Department of Medical Sciences, Uppsala University, Entrance 70, 3rd Floor, Res Dept 2, Univeristy Hospital, S-75185, Uppsala, Sweden.
82. Human Genetics and Cancer Biology, Genome Institute of Singapore, Singapore 138672.
83. Institute of Immunology, Oslo University Hospital, N-0027 Oslo, Norway
84. Institute of Experimental Neurology (INSPE), San Raffaele Scientific Institute, Via Olgettina 58, 20132, Milan, Italy.
85. Dept of Psychiatry and Human Behavior, University of California, Irvine (UCI), 5251 California Av, S.te 240, Irvine CA, 92617 - USA.
86. Christchurch School of Medicine, University of Otago, Christchurch, New Zealand.
87. John P. Hussman Institute for Human Genomics and The Dr. John T Macdonald Foundation Department of Human Genetics, University of Miami, Miller School of Medicine, 1501 NW 10th Avenue, Miami, FL 33136, USA.
88. Greater Manchester Centre for Clinical Neurosciences, Hope Hospital, Salford, UK.
89. The Department of Neurology, Dunedin Public Hospital, Otago, NZ.
90. The Multiple Sclerosis National Competence Centre, Department of Neurology, Haukeland University Hospital, N-5021 Bergen, Norway.
91. Department of Clinical Medicine, University of Bergen, N-5021 Bergen, Norway.
92. Plymouth Hospitals NHS Trust, Department of Neurology, Derriford Hospital, Plymouth, PL6 8DH, UK.
93. Department of Medical Genetics, University of Helsinki and University Central Hospital, Helsinki, Finland.
94. Program in Medical and Population Genetics and Genetic Analysis Platform, The Broad Institute of MIT and Harvard, Cambridge, MA 02142, USA.
95. Pôle Neurosciences Cliniques,Service de Neurologie, Hôpital de la Timone, Marseille, France.
96. Department Neurology, Oulu University Hospital, Oulu, Finland.

97. UK MS Tissue Bank, Wolfson Neuroscience Laboratories, Imperial College London, Hammersmith Hospital, London, W12 0NN.
98. Université de Montréal & Montreal Heart Institute, Research Center, 5000 rue Belanger, Montreal, Quebec H1T 1C8, Canada.
99. Neurology and Center for Experimental Neurological Therapy (CENTERS), Sapienza University of Rome, Italy.
100. KOS Genetic Srl, Via Podgora, 7 - 20123 Milan - Italy.
101. Department of General Internal Medicine, University Hospital, Schleswig-Holstein, Christian-Albrechts-University, Kiel, Germany.
102. Systems Biology and Protein-Protein Interaction, Center for Molecular Neurobiology, Falkenried 94, D-20251 Hamburg, Germany.
103. Center for Human Genetics Research, Vanderbilt University Medical Center, 519 Light Hall, Nashville, TN 37232, USA.
104. Telethon Institute for Child Health Research, Centre for Child Health Research, University of Western Australia, 100 Roberts Road, Subiaco, Western Australia 6008.
105. Cambridge Institute for Medical Research, University of Cambridge School of Clinical Medicine, Cambridge CB2 0XY, UK.
106. Department of Neurology, Helsinki University Central Hospital and Molecular Neurology Programme, Biomedicum, University of Helsinki, Helsinki, Finland.
107. Division of Psychological Medicine and Psychiatry, Biomedical Research Centre for Mental Health at the Institute of Psychiatry, King's College London and The South London and Maudsley NHS Foundation Trust, Denmark Hill, London SE5 8AF, UK.
108. Service de Neurologie et Faculté de Médecine de Reims, Université de Reims Champagne-Ardenne, Reims, France.
109. University of Queensland Diamantina Institute, Princess Alexandra Hospital, Brisbane, Australia.
110. Dept Epidemiology and Population Health, London School of Hygiene and Tropical Medicine, London WC1E 7HT, UK.
111. St. Vincent's University Hospital, Dublin, Ireland.
112. Neuropsychiatric Genetics Research Group, Institute of Molecular Medicine, Trinity College Dublin, Dublin 2, Eire.
113. Centre for Gastroenterology, Bart's and the London School of Medicine and Dentistry, London E1 2AT, UK.
114. Department of Neurosciences, Institute of Biomedical Research August Pi Sunyer (IDIBAPS), Hospital Clinic of Barcelona, Spain.
115. Clinical Neurosciences, St George's University of London, London SW17 0RE.
116. Dept Medical and Molecular Genetics, King's College London School of Medicine, Guy's Hospital, London SE1 9RT, UK.
117. Medical Research Council Biostatistics Unit, Robinson Way, Cambridge, CB2 0SR, UK.
118. Biomedical Research Institute, University of Dundee, Ninewells Hospital and Medical School, Dundee, DD1 9SY.
119. Institute of Medical Informatics, Biometry and Epidemiology, Ludwig-Maximilians-Universität, 81377 Munich, Germany.
120. Klinikum Grosshadern, Munich, Germany.
121. King's College London, Social, Genetic and Developmental Psychiatry Centre, Institute of Psychiatry, Denmark Hill, London SE5 8AF, UK.
122. Department of Neurology, Auckland City Hospital, Grafton Road, Auckland, New Zealand.
123. Institut für Humangenetik, Technische Universität München, Germany.
124. Institut für Humangenetik, Helmholtz Zentrum München, Germany.
125. Popgen Biobank, Christian-Albrechts University Kiel, Kiel, Germany.
126. Pôle Recherche et Santé Publique, CHU Pontchaillou, Rennes, France.

127. NIHR Biomedical Research Centre for Ophthalmology, Moorfields Eye Hospital NHS Foundation Trust and UCL Institute of Ophthalmology, London EC1V 2PD, UK.
128. Dept Molecular Neuroscience, Institute of Neurology, Queen Square, London WC1N 3BG, UK.
129. Molecular and Physiological Sciences, The Wellcome Trust, London NW1 2BE.
130. Harvard NeuroDiscovery Center, Harvard Medical School, Boston, MA, USA.
131. Department of Neurology & Immunology, Yale University Medical School, New Haven, CT, USA.
132. Oxford Centre for Diabetes, Endocrinology and Metabolism (ICDEM), Churchill Hospital, Oxford OX3 7LJ, UK.

Acknowledgements

The principal funding for this study was provided by the Wellcome Trust, as part of the Wellcome Trust Case Control Consortium 2 project (085475/B/08/Z and 085475/Z/08/Z). The Wellcome Trust Case Control Consortium 2 project was funded by the Wellcome Trust (084702/z/07/Z). The International Multiple Sclerosis Genetics Consortium was supported by the National Institutes of Health (AI076544, NS032830, NS049477, NS19142, NS049510, NS26799, NS43559 and NS067305), the US National Multiple Sclerosis Society, the Nancy Davis Foundation, the Cambridge NIHR Biomedical Research Centre, the UK Medical Research Council (G0700061), the Multiple Sclerosis Society of Great Britain and Northern Ireland (898/08), the Australian National Health and Medical Research Council (NHMRC), the Australian Research Council Linkage Program Grant, the JHH Charitable Trust Fund, Multiple Sclerosis Research Australia, the Health Research Council New Zealand, the National MS Society of New Zealand, Wetenschappelijk Onderzoek Multiple Sclerose, the Bayer Chair on Fundamental Genetic Research regarding the Neuroimmunological aspects of Multiple Sclerosis, the Biogen Idec Chair Translational Research in Multiple Sclerosis, the Belgian Neurological Society, the Danish Multiple Sclerosis Society, the Neuropromise EU grant (LSHM-CT-2005-018637), the Center of Excellence for Disease Genetics of the Academy of Finland, the Sigrid Juselius Foundation, Helsinki University Central Hospital Research Foundation, the Bundesministerium für Bildung und Technologie (KKNMS consortium Control MS), Institut National de la Santé et de la Recherche Médicale (INSERM), Association pour la Recherche sur la Sclérose En Plaques (ARSEP), Association Française contre les Myopathies (AFM), the Italian Foundation for Multiple Sclerosis (FISM grants, 2002/R/40, 2005/R/10, 2008/R/11 and 2008/R/15), the Italian Ministry of Health (grant Giovani Ricercatori 2007 - D.lgs 502/92), Regione Piemonte (grants 2003, 2004, 2008, 2009), CRT Foundation, Turin, Moorfields / UCL Institute of Ophthalmology NIHR Biomedical Research Centre, the Norwegian MS Register and Biobank, The Research Council of Norway, South-Eastern and Western Norway regional Health Authories, Ullevål University Hospital Scientific Advisory Council, Haukeland University Hospital, the Amici Centro Sclerosi Multipla del San Raffaele (ACESM), the Association of British Neurologists, Spanish Ministry of Health(FISPI060117), Bibbi and Niels Jensens Foundation, Montel Williams foundation, Hjärnfonden and the Swedish medical research council, the Swedish Council for Working life and Social Research, the Gemeinnützige Hertie Stiftung, Northern California Kaiser Permanente members and the Polpharma Foundation. This research was supported in part by NIH grants CO6 RR020092 and RR024992 (Washington University Institute of Clinical and Translational Sciences - Brain, Behavioral and Performance Unit).

We acknowledge use of the British 1958 Birth Cohort DNA collection, funded by the Medical Research Council grant G0000934 and the Wellcome Trust grant 068545/Z/02, and of the UK National Blood Service controls funded by the Wellcome Trust. This study makes use of data from the popgen biobank. A full list of the investigators who contributed to the generation of the data is available from www.popgen.de. The popgen biobank is supported by the German Ministry of Education and Research (BMBF) through the National Genome Research Network (NGFN) and received infrastructure support through the DFG excellence cluster "Inflammation at Interfaces". The KORA research platform (KORA: Cooperative Research in the Region of Augsburg) and the MONICA Augsburg studies (Monitoring trends and determinants on cardiovascular diseases) were initiated and financed by the Helmholtz Zentrum München–National Research Center for Environmental Health, which is funded by the German Federal Ministry of Education, Science, Research and Technology and by the State of Bavaria. Part of this work was financed by the German National Genome Research Network (NGFN) and within the Munich Center of Health Sciences (MC Health) as part of LMUinnovativ. We gratefully acknowledge the contributions of P. Lichtner, G. Eckstein, Guido Fischer, T. Strom and all other members of the Helmholtz Zentrum München genotyping staff in generating the SNP dataset. We thank the Accelerated Cure Project for its work in collecting samples from subjects with MS and the Brigham & Women's Hospital PhenoGenetic Project for providing DNA samples from healthy subjects. The Swedish CAD control data was funded by the Knut and Alice Wallenberg Foundation, the Swedish Research Council (8691) and the Stockholm County Council (562183) and the genotyping was performed by the SNP Technology Platform in Uppsala (www.genotyping.se). The Norwegian Bone Marrow Donor Registry is acknowledged for collaboration in establishment of the Norwegian control material, and Peter Gregersen's laboratory for genotyping these in collaboration with the Myasthenia Gravis Genetic Consortium (MGGC). We thank all individuals who donated blood samples to Children's Hospital of Philadelphia (CHOP) for genetic research purposes. We thank the technical staff in the Center for Applied Genomics, Children's Hospital of Philadelphia for generating the genotypes used in this study and the medical assistants, nursing and medical staff who recruited the subjects. All CHOP control recruitment, genotyping, and data processing for this study was funded by an Institutional Development Award to the Center for Applied Genomics from the Children's Hospital of Philadelphia. The Swedish Breast Cancer study was supported by funding from the Agency for Science & Technology and Research of Singapore (A*STAR), the Susan G Komen Breast Cancer Foundation, and the National Institute of Health (grant number R01 CA 104021). We acknowledge the collaboration of the BRC-REFGENSEP, Pitié-Salpêtrière Centre d'Investigation Clinique (CIC) and Généthon. The Italian external control data was generated through work supported by the European Commission project HYPERGENES (HEALTH-F4-2007-201550).

AJI and the Harvard NeuroDiscovery Center are supported in part by a number of anonymous donors. JPR is supported by an NHMRC Biomedical Career Development Award. HB is supported by a Peter Doherty Fellowship. BD is a Clinical Investigator of the Research Foundation Flanders (FWO-Vlaanderen). FZ is part of the German Multiple Sclerosis Competence Network. LB is supported by a PhD Lagrange Fellowship. BH is supported by the Deutsche Forschungsgemeinschaft. PLD and SEB are Harry Weaver Neuroscience Scholar of the US National MS Society. JLH, MPV and JLM are supported by NIH grants (NS32830 and NS049477) along with the National Multiple Sclerosis Society (RG 4201-A-1) and its local South Florida chapter. BACC is supported by the National Institute of Health (K23N/S048869). PD was supported in part by a Wolfson Royal Society Merit Award.

We thank S. Bertrand, J. Bryant, S.L. Clark, J.S. Conquer, T. Dibling, J.C. Eldred, S. Gamble, C. Hind, C.R. Stribling, S. Taylor and A. Wilk of the Wellcome Trust Sanger Institute's Sample and Genotyping Facilities, as well as R. Pearson and D. Vukcevic of the Wellcome Trust Centre for Human Genetics for technical assistance. We also thank Dr Bruno Colombo, Dr Lucia Moiola, Dr Gabriella Coniglio, Dr. Laura Collimedaglia, Dr Valentina Pilato, Dr Marta Radaelli and Prof. Elio Scarpini for providing Italian MS patients. MS post-mortem tissue samples were supplied by the UK MS Tissue Bank at Imperial College, funded by the MS Society of Great Britain and Northern Ireland. We thank Hourieh Mousavi and Rosa Guerrero for expert specimen management at UCSF; and Dr Becky J Parks and Dr Robert T Naismith for helping in the collection of blood specimens (Washington). We acknowledge sample management provided by the DNA unit of the National Institute for Health and Welfare (THL), Helsinki, Finland. The Vanderbilt University Center for Human Genetics Research Computational Genomics Core provided software development, computational, and analytical support for this work. We acknowledge DNA sample management undertaken by the UK DNA Banking Network which receives core funding from the Medical Research Council (UK) at the Centre for Integrated Genomic Medical Research, University of Manchester, UK.